ANKARA YILDIRIM BEYAZIT UNIVERSITY

GRADUATE SCHOOL OF NATURAL AND APPLIED SCIENCES

AN INVESTIGATION ON THE INFLUENCE OF DIFFERENT COOLING/LUBRICATION TECHNIQUES ON THE TOOL WEAR AND SURFACE INTEGRITY IN THE HARD TURNING OF AISI 52100 BEARING STEEL

M.Sc. Thesis by

Hüseyin Alp ÇETİNDAĞ

Department of Mechanical Engineering

June, 2019

ANKARA

AN INVESTIGATION ON THE INFLUENCE OF DIFFERENT COOLING/LUBRICATION TECHNIQUES ON THE TOOL WEAR AND SURFACE INTEGRITY IN THE HARD TURNING OF AISI 52100 BEARING STEEL

A Thesis Submitted to

The Graduate School of Natural and Applied Sciences of

Ankara Yıldırım Beyazıt University

In Partial Fulfillment of the Requirements for the Degree of Master of Science in Mechanical Engineering, Department of Mechanical Engineering

by

Hüseyin Alp ÇETINDAĞ

June, 2019

ANKARA

M.Sc. THESIS EXAMINATION RESULT FORM

We have read the thesis entitled **"AN INVESTIGATION ON THE INFLUENCE OF DIFFERENT COOLING/LUBRICATION TECHNIQUES ON THE TOOL WEAR AND SURFACE INTEGRITY IN THE HARD TURNING OF AISI 52100 BEARING STEEL"** completed by **HÜSEYİN ALP ÇETİNDAĞ** under the supervision of **PROF. DR. ADEM ÇİÇEK** and we certify that in our opinion it is fully adequate, in scope and in quality, as a thesis for the degree of Master of Science.

Prof. Dr. Adem ÇİÇEK

Supervisor

Prof. Dr. Kubilay ASLANTAŞ

Jury Member

Assist. Prof. Dr. Yasin SARIKAVAK

Jury Member

Prof. Dr. Ergün ERASLAN

Director

Graduate School of Natural and Applied Sciences

I hereby declare that, in this thesis which has been prepared in accordance with the Thesis Writing Manual of Graduate School of Natural and Applied Sciences,

- All data, information and documents are obtained in the framework of academic and ethical rules,
- All information, documents and assessments are presented in accordance with scientific ethics and morals,
- All the materials that have been utilized are fully cited and referenced,
- No change has been made on the utilized materials,
- All the works presented are original,

and in any contrary case of above statements, I accept to renounce all my legal rights.

10.06.2019 **Hüseyin Alp ÇETİNDAĞ**

ACKNOWLEDGMENTS

Firstly, I would like to express my sincere gratitude to my supervisor, Prof. Dr. Adem ÇİÇEK for his excellent guidance, support and motivation during this study. He always shared his experiences with me and I benefited from his tremendous knowledge throughout my study. In addition to his wisdom, his positive perspective inspired me and gave me confidence while writing this thesis.

Also, I am grateful to Necati UÇAK for their excellent guidance and technical assistance during the tests and measurements. His crucial contributions were one of the most important factor of my ambition to complete these experiments.

This work has been funded by Ankara Yıldırım Beyazıt University Scientific Research Project Division. Because of that I wish to thank for their financial support to the Project No: 4767

Also special thanks should be given to one of the most important bearing manufacturer ORS inc. (Ortadoğu Rulman Sanayi) for their professional and sincere assistance on the workpiece preparation, surface roughness measurement and residual stress quantification. I also would like to thank Gazi University, Technology Faculty, Department of Manufacturing Engineering for their help during the cutting force measurements. Also, many thanks to HİDRONERJİ co. ltd. especially to Yavuz TOPÇU and Mikail YAĞAR for their vital guidance and help during experimental tests. Besides, I am grateful to Özkayalı co. ltd. for their selfless support of providing machining equipment for my experimental setup.

Finally, my deep and sincere gratitude to my family for their continuous love and support. They selflessly encouraged me and helped in whatever way they could during this challenging period. This study would not have been possible without them. Thank you.

2019, 10 June **Hüseyin Alp ÇETİNDAĞ**

AN INVESTIGATION ON THE INFLUENCE OF DIFFERENT COOLING/LUBRICATION TECHNIQUES ON THE TOOL WEAR AND SURFACE INTEGRITY IN THE HARD TURNING OF AISI 52100 BEARING STEEL

ABSTRACT

From the eco-friendly cutting perspective, sustainable manufacturing can be regarded as a solution to improve tool life and product quality. In this context, the studies on different cooling/lubrication techniques employed during hard machining have increasingly become more popular in the literature. This study investigates the performance of eco-friendly cooling/lubrication techniques (MQL, cryogenic and hybrid) in the hard turning of AISI 52100 bearing steel using the wiper and conventional CBN (cubic boron nitride) inserts. The experiments are performed at a cutting speed of 200 m/min, a feed of 0.1 mm/rev and a depth of cut of 0.1 mm. For each machining condition, tool wear, surface roughness (Ra and Rz) and residual stress (axial and hoop) values are measured. On the other hand, the cutting force and subsurface layer thickness measurements are conducted in order to support the obtained results. Experimental results show that MQL+carbon dioxide condition significantly reduces wear formations (flank and crater wear) on conventional and wiper inserts under all test conditions generally. Additionally, lower roughness values ($Ra < 0.15$ μm) are obtained using the wiper inserts whereas the conventional inserts produce higher roughness results ($Ra > 0.26$ μm) under all cooling/lubrication conditions. Besides, MQL+ carbon dioxide and wet conditions provide the best surface roughness results for the wiper and conventional inserts respectively. In addition, it is observed that the magnitudes of residual stresses are significantly affected by cooling/lubrication conditions and tool geometry. The compressive residual stresses are produced at surface and subsurface of the work material up to depth of 30 μm under all test conditions.

Keywords: AISI 52100, hard turning, sustainable manufacturing, MQL, cryogenic cooling, hybrid conditions, CBN, wiper inserts.

AISI 52100 RULMAN ÇELİĞİNİN SERT TORNALANMASINDA FARKLI SOĞUTMA/YAĞLAMA TEKNİKLERİNİN TAKIM AŞINMASI VE YÜZEY BÜTÜNLÜĞÜNE ETKİSİ ÜZERİNE BİR ARAŞTIRMA

ÖZ

Çevre dostu işleme açısından bakıldığında, sürdürülebilir imalat yöntemleri, takım aşınmasını ve ürün kalitesini iyileştirmek için bir çözüm olarak kabul edilebilir. Bu kapsamda, sert talaş kaldırma işlemlerinde çeşitli soğutma/yağlama yöntemlerinin kullanımı üzerine yapılan çalışmalar literatürde giderek daha popüler hale gelmiştir. Bu çalışma, silici (wiper) ve geleneksel kübik bor nitrür (CBN) kesici takımlar kullanarak AISI 52100 rulman çeliğinin sert tornalanmasında, sürdürülebilir soğutma yöntemlerinin (MQL, kriyojenik ve hibrit) performansını incelemektedir. Deneyler, 200 m/dak sabit kesme hızı, 0,1 mm/devir ilerleme ve 0,1 mm kesme derinliğinde gerçekleştirilmiştir. Her kesme koşulu için, takım aşınması, yüzey pürüzlülüğü (Ra ve Rz) ve kalıntı gerilme (eksenel ve çevresel) değerleri ölçülmüştür. Bunun yanı sıra, elde edilen sonuçların desteklenmesi adına, kesme kuvvetleri ve yüzey altı katman kalınlık ölçümleri gerçekleştirilmiştir. Deney sonuçları, genel olarak MQL+karbondioksit şartının hem silici hem de konvansiyonel kesici uçlu takımlarda aşınma oluşumunu (yan yüzey ve krater aşınması) önemli ölçüde azalttığını göstermiştir. Buna ek olarak, silici takımlar kullanıldığında daha düşük pürüzlülük değerleri ($Ra < 0.15$ μm) elde edilirken geleneksel takımlar bütün soğutma/yağlama yöntemleri için daha yüksek pürüzlülük değerleri ($Ra > 0.26$ μm) meydana getirmiştir. Ayrıca MQL+karbondioksit ve geleneksel soğutma şartları, sırasıyla, silici ve geleneksel takımlar için en iyi yüzey pürüzlülüğü değerlerini sağlamıştır. Bununla beraber, kalıntı gerilme büyüklüklerinin soğutma/yağlama şartları ve kesici takım geometrisinden önemli derecede etkilendiği gözlemlenmiştir. Bütün test şartları altında, iş parçası yüzeyinde ve 30 μm derinliğe kadar yüzey altında, basma kalıntı gerilmeleri oluşmuştur.

Anahtar Kelimeler: AISI 52100, sert tornalama, sürdürülebilir imalat, MQL, kriyojenik soğutma, hibrit koşullar, CBN, wiper uçlar

CONTENTS

M.Sc. THESIS EXAMINATION RESULT FORM ii
ETHICAL DECLARATION ..... **Hata! Yer işareti tanımlanmamış.**
ACKNOWLEDGMENTS iv
ABSTRACT v
ÖZ vi
NOMENCLATURE ix
LIST OF TABLES xi
LIST OF FIGURES xii
CHAPTER 1 - INTRODUCTION 1
1.1 Hard Machining 5
1.1.1 Cutting Tool Materials and Geometries 10
1.2 Tool Wear 15
1.3 Surface Integrity 19
1.3.1 Surface Roughness 20
1.3.2 Subsurface phase transformations 23
1.3.2.1 White and dark layer 23
1.3.2.2 Residual Stresses 25
1.4 Sustainable machining 28
1.4.1 MQL (Minimum Quantity Lubrication) system 30
1.4.2 Cryogenic Cooling 31
1.4.3 Hybrid Cooling 33
1.5 Literature Review 34
1.6 Aim of this Study 48
CHAPTER 2 - EXPERIMENTAL SETUP AND PROCEDURE 50
2.1 Workpiece Material 50
2.2 Experimental Setup and Cutting Conditions 52
2.3 Tool Holder and Cutting Inserts 54
2.4 Cooling and/or Lubrication Conditions 55
2.4.1 Conventional Cutting Fluid 56
2.4.2 Minimum Quantity Lubrication 56
2.4.3 Cryogenic Cooling 57

2.4.4 Hybrid Conditions 58
2.5 Measurement Techniques 59
2.5.1 Tool wear 60
2.5.2 Cutting Forces 61
2.5.3 Surface integrity 62
2.5.3.1 Surface Roughness 62
2.5.3.2 White and Dark Layer 63
2.5.3.3 Residual Stress Measurements 64
CHAPTER 3 - RESULTS AND DISCUSSION 66
3.1 Cutting Forces 66
3.2 Surface Roughness 69
3.3 Residual Stresses 74
3.4 Tool Wear 83
CHAPTER 4 - CONCLUSION AND FUTURE WORK 93
4.1 Summary of the Present Study 93
4.2 Future Work 96
REFERENCES 97
CURRICULUM VITAE 108

NOMENCLATURE

Abbreviations

Cryo	Cryogenic
Eff	Effective
Max	Maximum
Min	Minimum

Acronyms

AISI	American iron and steel institute
BUE	Built-up edge
C	Carbon
CBN	Cubic boron nitride
CNC	Computer numerical control
CO_2	Carbon dioxide
Cr	Chrome
EDM	Electro discharge machining
HRC	Rockwell hardness
ISO	International organization for standardization
LN_2	Liquid nitrogen
MQL	Minimum quantity lubrication
OHNS	Oil hardened non shrinkage steel
PCBN	Polycrystalline cubic boron nitride
PD	Polycrystalline diamond
SEM	Scanning electron microscopy
TiC	Titanium carbide
TiN	Titanium nitride
WC	Tungsten carbide
XRD	X-ray diffraction

Greek Letter Symbols

γ	Rake angle

Roman Letter Symbols

a_p	Depth of cut, mm
f	Feed, mm/rev

Ra	Average surface roughness, μm
r_c	Insert nose radius, mm
Rt	Maximum height of the profile, μm
Rz	Average maximum height of the profile, μm
VB_B	Flank Wear
V_c	Cutting speed, m/min

LIST OF TABLES

Table 1.1 Comparison of different cooling/lubrication techniques [79] 30

Table 1.2 Comparison of carbon dioxide and liquid nitrogen [83] 32

Table 1.3 Tool life results (AISI 4150 steel at 52 HRC) 40

Table 2.1 The chemical composition of AISI 52100 steel and the effects of its alloying elements on the steel [18], [108]–[110] 51

Table 2.2 Some physical and mechanical properties of hardened AISI 52100 [18], [109] 51

Table 2.3 Cutting parameters 53

Table 2.4 The dimensions and some properties of CBN inserts 55

Table 2.5 Technical specifications of the dynamometer and the amplifier 62

Table 2.6 X-ray diffraction parameters 64

LIST OF FIGURES

Figure 1.1 Hard machining operation (Hard turning) 6

Figure 1.2 Comparison of grinding and hard machining processes [8] 7

Figure 1.3 Conventional production line of bearings [23] 8

Figure 1.4 Hard turning assisted manufacturing [23] 9

Figure 1.5 Estimated temperature fields in a hard machining process [30] 10

Figure 1.6 Flank wear of high CBN (H1) and low CBN content tools during the hard turning of AISI 52100 steel [39] 11

Figure 1.7 Elements of tool signature [40] 12

Figure 1.8 Effect of side cutting edge angle on the cutting force distribution [42] .. 13

Figure 1.9 Single point tools with (a) positive and (b) negative rake angle [3] 13

Figure 1.10 Cutting edge preparations [43] 14

Figure 1.11 Inserts with (a) wiper and (b) conventional geometries [46] 15

Figure 1.12 Schematic representation of worn cutting tool (a) [3] and SEM images of tool wear forms (b) [37]; crater wear (1), flank wear (2), BUE (3), notching (4), nose wear (5), and thermal cracks (6) 16

Figure 1.13 Characterization of wear patterns on rake (A) and flank (B) faces of single point cutting tool according to ISO 3685 [14]. 18

Figure 1.14 Typical wear types (A) and SEM image of a worn CBN insert in hard turning. 19

Figure 1.15 Surface Roughness [57] 20

Figure 1.16 Mean value (Ra) of the roughness profile [62] 22

Figure 1.17 Cutting temperatures generated during (a) high-speed machining of hardened steels, and (b) conventional machining of unhardened steels [64] 23

Figure 1.18 White and dark layers in AISI 52100 steel after hard machining [27] .. 24

Figure 1.19 The influence of cutting speed and workpiece hardness on the white layer formation [11] 25

Figure 1.20 Axial and hoop residual planes (Edited from Figure 1 of the reference [72]) 26

Figure 1.21 Effect of phase transformations on the residual stresses during the hard machining at cutting speeds of a) 75 m/min and b) 250 m/min [34] 28

Figure 1.22 Different cooling/lubrication techniques in turning processes [76] 29

Figure 1.23 Classification of cutting fluids (Edited from the Fig. 1 of the reference [77]) 29

Figure 1.24 MQL application [80] 31

Figure 1.25 Cryogenic cooling application using an external nozzle [86]..... 32

Figure 1.26 A) hybrid strategy with cryogen application on the rake face and MQL application on the flank face, B) hybrid strategy with cryogen application on the flank face and MQL application on the rake face (Edited from Fig. 2 of the reference [92]) 33

Figure 1.27 Application methods; (A) precooling, (B) from the rake and (C) from the flank [93]..... 34

Figure 1.28 Effect of cutting speeds of 200 and 800 m/min on the chip and workpiece temperatures [95] 35

Figure 1.29 Effect of cutting conditions on the cutting temperatures in turning of AISI 1040 steel [97]..... 36

Figure 1.30 Variation of cutting temperature with cutting speed and cooling direction under dry and cryogenic conditions [98] 37

Figure 1.31 Flank wear values at different cutting speeds under dry and MQL conditions [101] 38

Figure 1.32 Flank wear pictures under dry, MQL and cryogenic conditions at 120 m/min [16]..... 39

Figure 1.33 Performance of wiper inserts in terms of the average surface roughness [105]..... 41

Figure 1.34 Comparison of surface roughness in dry and cryogenic hard turning of AISI 52100 steel [1]..... 42

Figure 1.35 Comparison of surface roughness values under conventional cutting fluid and cryogenic conditions [107]..... 43

Figure 1.36 Effect of cryogenic cooling on the white layer thicknesses [1]..... 45

Figure 1.37 White layer thickness values under wet and cryogenic conditions [107] 45

Figure 1.38 Influence of the cutting speed on the circumferential and tangential residual stresses [36] 46

Figure 1.39 (a) Axial and (b) hoop residual stresses under dry and cryogenic conditions [1] 47

Figure 1.40 Effects of dry, MQL, cryo and cryoMQL conditions on the flank wear [93]..... 48

Figure 1.41 Effects of dry, MQL, cryo and cryoMQL conditions on the surface roughness [93]..... 48

Figure 2.1 Schematic illustration of performance criteria and their measurement methods 50

Figure 2.2 Detailed dimensions of the workpiece materials prepared for (a) surface integrity and (b) tool wear..... 52

Figure 2.3 The tailstock and its dimensions used in the tests 52

Figure 2.4 Experimental set-up 53

Figure 2.5 Cutting fluid application through the tool holder; (a) conventional cutting fluid and (b) MQL oil 54

Figure 2.6 Dimensions of PCLNR 2525M12 jet tool holder 54

Figure 2.7 Cutting conditions 55

Figure 2.8 Conventional cutting fluid application from (a) tool holder and (b) during the machining operation 56

Figure 2.9 MQL system 57

Figure 2.10 Spraying of the mixture of the pressurized air and oil droplets from tool holder nozzles 57

Figure 2.11 Application of cryogenic cooling with (a) an external nozzle of (b) LN_2 and (c) CO_2 58

Figure 2.12 A schematic representation of hybrid conditions; (a) front and (b) side views 59

Figure 2.13 Hybrid conditions; (a) CO_2 and (b) LN_2. 59

Figure 2.14 Measurament of flank wear formation 60

Figure 2.15 Measurement of crater wear area by using AutoCAD software 60

Figure 2.16 SEM measurements by using (a) JEOL–JSM–6060 LV SEM device and the wear formations; (b) crater wear, (c) flank wear 61

Figure 2.17 Cutting force measurements 61

Figure 2.18 Taylor Hobson Talysurf PGI 1230 profilometer 63

Figure 2.19 White and dark layer observations under the Nikon ECLIPSE MA100 optical microscope 64

Figure 2.20 Seifert XRD 3003 PTS 65

Figure 3.1 Effect of (a) high and (b) small cutting depth values on the cutting forces 67

Figure 3.2 The variations of cutting forces depending on the time for a conventional insert under dry conditions 67

Figure 3.3 The variations of cutting forces depending on the time for a wiper insert under dry conditions 68

Figure 3.4 Cutting force values for conventional and wiper inserts under dry conditions 68

Figure 3.5 Surface roughness values measured under different cooling/lubrication conditions; (a) Ra and (b) Rz 70

Figure 3.6 Surface textures generated by using (a) conventional and (b) wiper cutting tool. 71

Figure 3.7 Comparison of external cryogenic cooling conditions to hybrid conditions in terms of (a) Ra and (b) Rz values 74

Figure 3.8 The effects of cutting edge geometry 75

Figure 3.9 (a-c) Hoop and (b-d) axial residual stress values for conventional and wiper inserts. 76

Figure 3.10 (a) Hoop and (b) axial residual stress values for conventional inserts .. 77

Figure 3.11 Microscopic examinations of specimens under dry conditions: (a) optical microscope and (b) SEM..... 79

Figure 3.12 (a) Hoop and (b) axial residual stress values for conventional inserts .. 80

Figure 3.13 Comparison of external cryogenic cooling to hybrid method in terms of residual stresses for (a-b) conventional and (c-d) wiper cutting tools 82

Figure 3.14 SEM images of the worn conventional and wiper inserts under dry, wet, MQL and hybrid conditions. 83

Figure 3.15 Flank wear values and SEM images of wiper and conventional CBN inserts under different cooling/lubrication conditions 84

Figure 3.16 Cooling characteristics of a) MQL+ CO_2 and b) MQL+ LN_2 hybrid conditions. 87

Figure 3.17 EDS analysis of the machined surface..... 87

Figure 3.18 Crater wear values and SEM images of wiper and conventional CBN inserts under different cooling/lubrication conditions 88

Figure 3.19 Tool wear types under dry and CO_2 conditions..... 90

Figure 3.20 (a) Flank wear and (b) crater wear values under dry and CO_2 conditions 91

CHAPTER 1

INTRODUCTION

Throughout history, manufacturing has been an essential issue. Different materials and processing techniques were developed in order to produce various parts and/or tools from a wide range of engineering materials [1]. Today, many conventional manufacturing methods such as forging, welding, machining and casting are still in use in manufacturing sector commonly and they sustain to be popular research topics in both industrial and academic areas. Machining is a material removal process in which excessive material called chip from a workpiece material is cut by means of a sharp cutting tool [2,3]. As the subtitles of machining processes, turning and grinding are commonly used in many manufacturing sectors such as defense, food, energy, chemistry, and automotive. Turning is a form of machining processes used to create rotational parts by removing excessive material. In this process, workpiece is rotated around its central axis and cutting tool is linearly fed horizontally and vertically [4]. On the other hand, grinding is a finish machining operation which uses the wheels containing abrasive particles and binder material in order to obtain finish workpieces with good surface finish and dimensional accuracy [3,5]. Each abrasive particle bonded on the wheel surface cuts a small chip from the workpiece. These two different machining operations have different physical and technological aspects. When compared to grinding, higher material removal rates, more production flexibility, capability of performing multiple machining operations and easier clamping of workpiece are some of the well-known advantages of turning.

Nowadays, low cost and high quality products are desired in order to meet industrial demands and customer satisfaction [6–9]. Thus, new and promising machining methods are increasingly gaining more importance with the developing technologies. Hard machining is one of these methods and it provides some significant benefits over the abrasive processes [7,10]. It is well-known that a grinding operation is generally applied to the finishing cuts of difficult-to-cut materials such as hardened steels. On

the other hand, hard machining is an important machining process with above-mentioned advantages of turning in case of finishing cuts. It can be defined as a machining operation of a workpiece (mostly hardened steels) which has hardness values in the range of 45-70 HRC using ceramic or CBN cutting tools. It plays an increasingly important role by replacing time-consuming and expensive grinding process [6]. Good surface finish and dimensional accuracy can be obtained with the hard machining processes in shorter processing periods. It is commonly used in many leading industries such as automotive, bearing, die and mold, etc. In particular, the hard turning which is a subclass of hard machining, is quite suitable for the bearing production in which conventional turning and grinding processes are widely employed. As it is well-known, the bearings are produced with three steps. Firstly, a rough turning operation is conducted on bearing steel bars. Then, the turned parts are hardened using a heat treatment cycle and finally, a grinding operation is performed to obtain good surface quality and dimensional accuracy [8]. At that point, this conventional technological chain can be shortened significantly and an increase in productivity and a reduction in machining costs can be achieved with hard turning operations replacing of grinding operation.

During the conventional machining of bearings, AISI 52100 (100Cr6) steel is generally in unhardened state for easier machining. This steel can be hardened up to 64 HRC and also it has good wear resistance and corrosion resistance due to high Cr and C content. Thus, it is highly recommended for the bearings as a workpiece material. During the hard turning of AISI 52100 bearing steel, various complications might occur in terms of mainly surface integrity and tool wear because of the higher cutting temperatures generated at the cutting zone. Due to its excellent wear resistance and high hardness, cutting temperature can exceed 900 °C [11] and subsequent rapid cooling can lead to phase transformations in the surface and subsurface newly generated after turning. Thus, several problems might develop in terms of the surface integrity such as white and dark layer formations, undesired residual stresses and surface roughness. White layer is a few micron thick martensite formation which is more brittle and harder than the bulk material [12]. And this formation is followed by

overtempered dark layer which is softer than both white layer and bulk material due to slower cooling rate. Since these two layers have different hardness values and microstructures, differences at the residual stresses can arise significantly. These differences at the distribution and magnitude of residual stresses directly influence the fatigue life of the material [7] due to premature crack formations. Because of that, residual stress is one of the most important subjects in terms of surface integrity and service life of the machined product, especially for the bearings which operated under cyclic loads. Another subject of the surface integrity is the surface roughness and it is critically important for the bearing elements which have constant contact and rubbing with counterparts. Considering desired surface quality requirement, cutting tool geometry is one of the most influential parameters on the surface roughness. At this point, wiper cutting tools which have additional cutting edges, attract attention. With the use of the wiper inserts, surface roughness can be significantly improved or feed values can be increased without any increase in the surface roughness. On the other hand, the tool life is another performance criterion [8,13] which represents the performance of machining [14]. Tool life is determined by observing and measuring wear formations on the cutting tool such as flank and crater wears according to ISO 3685 [15]. In addition, excessive thermal cracks and fracture failure show that the tool life is ended. These formations are mainly triggered by chemical (diffusion and adhesion) and mechanical (abrasion) interactions. In order to prolong tool life, frictions and temperatures at the cutting zone which accelerates wear formations should be reduced.

When the encountered problems in terms of the tool life and surface integrity are considered, it can be seen that the main factor is the cutting temperature generated due to plastic deformation of workpiece material and frictions at tool-chip and tool-workpiece [16]. To minimize higher cutting temperatures at the cutting zone, some coolants and/or lubricants can be used in hard machining. In this way, it is avoided from harmful effects of excessive cutting temperatures leading to shorter tool life and undesirable surface integrity. Thus, effective lubrication and/or cooling conditions must be provided in order to reduce friction and heat [17]. The basic and the most

preferred method is conventional cutting fluid application for the machining processes in which higher heat and friction are the problems. At this method, a water based oil emulsion is applied to the cutting zone at high flow rates. Even though conventional cutting fluid shows better performance than dry machining, it provides limited cooling and lubrication effects under especially hard machining conditions. Thus, it can be said that it is not an efficient method for the hard turning processes at which cutting temperatures are extremely high. Also the water based oil solution has some harmful effects on environment and the human health [18]. Therefore, some sustainable machining techniques such as MQL (Minimum Quantity Lubrication) and cryogenic cooling are increasingly gaining more importance in hard turning processes [17] to increase productivity and to provide a green machining environment. An MQL system is developed as an alternative to conventional cutting fluids. At this method, oil droplets along with pressurized air are sprayed through nozzle(s) to the cutting zone. These droplets can lower heat at the cutting zone by providing adequate lubrication at tool-chip and tool-workpiece interfaces and consequently reducing frictions. Besides, they evaporate without leaving any residue on the workpiece and the cutting tool in a short while. On the other hand, cryogenic cooling presents efficient cooling media in machining of difficult-to-cut materials such as titanium alloys, super alloys and hardened steels in which excessive heat are generated during the cutting. Therefore, it become popular research topic in especially machining of difficult-to-cut materials recently. It improves machining performance by means of various cryogens such as LN_2 (Liquid nitrogen) [13] and CO_2 (Carbon dioxide) [19]. Although cryogenic cooling presents an efficient cooling media, lubrication characteristics of the cryogens are very limited. Therefore, nowadays, hybrid machining which combines the cryogenic cooling and MQL (Cryo-MQL) become a new research topic. This technique gives an opportunity to set up different cooling/lubricating methods (direct or indirect cooling and lubrication) during the machining. By choosing the appropriate method, hybrid machining can exhibit better results in comparison to other techniques in terms of surface integrity and tool life.

With the light of above information, it is seen that a hard turning process which presents ideal surface integrity and tool life is a need in order to remove time-consuming and expensive grinding operations in especially bearing production. To meet this need, some conventional and innovative cooling and/or lubrication methods have been tried in this study. These are dry, conventional cutting fluid (wet), MQL, cryogenic cooling (LN_2 and CO_2), and hybrid cooling (MQL+LN_2 and MQL+CO_2). Thus, the effects of conventional and sustainable cooling conditions were investigated and compared to each other. On the other hand, it is well-known that conventional and wiper inserts have different effects on the surface integrity and tool life. Therefore, the performances of two different cutting inserts (conventional and wiper inserts) were extensively investigated in terms of tool wear and surface integrity (surface roughness, white and dark layer formations, residual stresses) under conventional and new cooling and/or lubrication conditions. By this way, in hard turning of AISI 52100 bearing steel, the effects of different tool geometry and cutting conditions on tool wear and surface integrity are determined.

The rest of this chapter presents general information about AISI 52100 bearing steel, hard turning, surface integrity, tool wear and sustainable machining. In addition, a review of some related works is given in this section. The rest of the thesis is organized as follows:

- Chapter two presents experimental setup and procedure of the study. The materials, instruments and experimental and assessment procedures used in this thesis study are also described.
- Chapter three discusses the test results for each cutting condition.
- Chapter four presents concluding remarks of the study and some recommendations for future works.

1.1 Hard Machining

To increase productivity and to provide sustainability in machining, shorter machining time and higher flexibility are key factors. Conventionally, hardened steels are

machined using abrasive processes such as a grinding operation. However, the recent improvements in cutting tool materials allow the hardened steels to cut using machining processes other than abrasive processes. Because of that, non-conventional machining methods such as hard machining become more popular [20,21] in machining of complex components increasingly [22]. Hard machining is a method developed for the machining of hardened steels with hardness more than 45 HRC [5]. The red color chip formation during the hard turning due to high cutting temperature is given in the Figure 1.1.

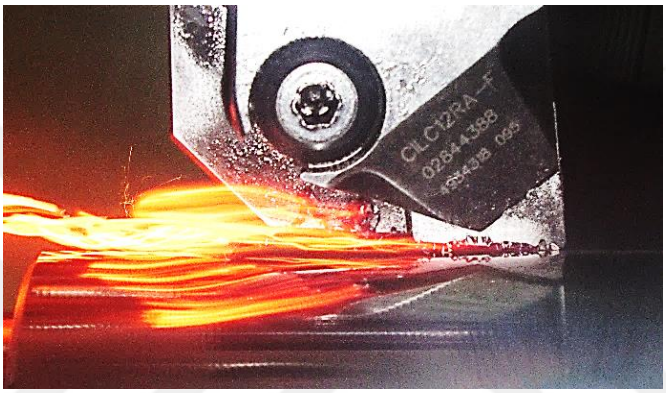

Figure 1.1 Hard machining operation (Hard turning)

This cheap and time-efficient method basically substitutes to the expensive and time-consuming grinding operations [5,19,21,23] . In order to substitute to the grinding processes, hard machining should provide sufficient surface integrity and long tool life. Even though grinding offers slightly better surface integrity, hard machining is an important machining strategy due to its notable properties such as higher material removal rate, process flexibility and sustainable machining capabilities. At this content, comparison of these techniques can be clearly seen in the Figure 1.2.

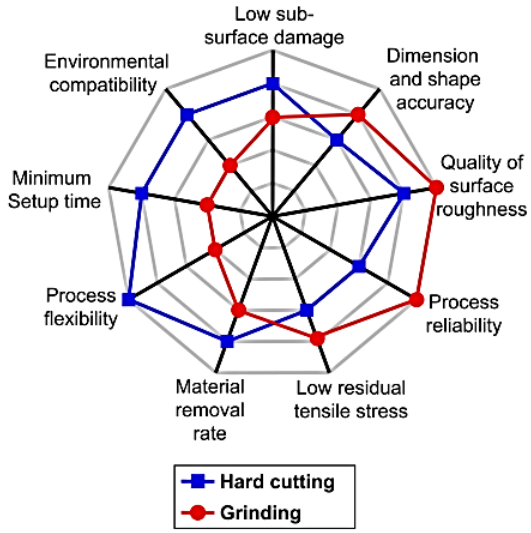

Figure 1.2 Comparison of grinding and hard machining processes [8]

Hard machining is mainly divided into two processes; hard milling and hard turning. While the hard milling is generally used in the mold industry, hard turning is commonly employed in order to produce several parts such as shafts, gears and bearings in automotive industry. Due to cyclic loads and harsh working conditions, the parts employed in these sectors are requested to be wear- and fatigue-resistant. Because of these requirements, they have high hardness and good surface integrity. As it is well known, during the manufacturing of bearings there are several steps. In the first step, workpiece bars in unhardened state is machined by a rough turning process. Then it is heat treated (quenching) in order to increase its hardness. After this hardening process it is ground for better surface integrity and tolerances as shown in Figure 1.3.

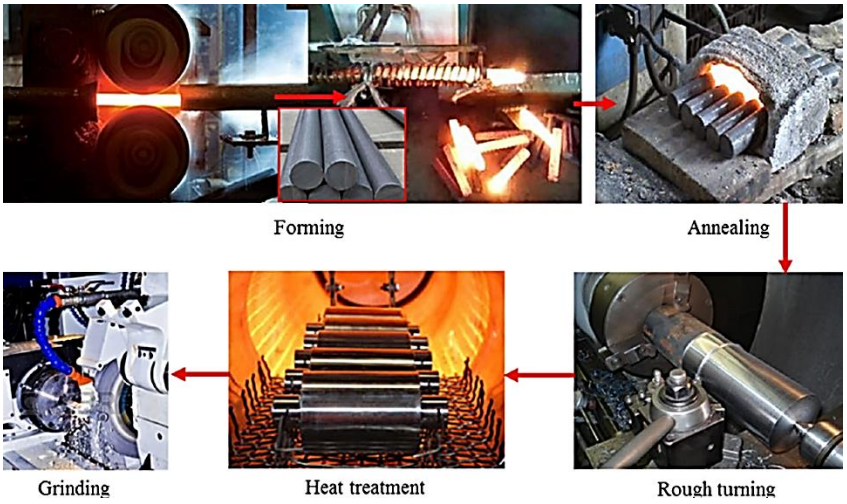

Figure 1.3 Conventional production line of bearings [24]

On the other hand, hard turning is a good alternative to grinding thus it promises a great potential for bearing production. Hard turning offers several advantages on grinding and they can be listed as:

- Similar surface roughness values can be achieved by using hard turning instead of grinding [21,25]
- More complex shapes can be machined easily contrary to grinding operations [26,27]
- Higher cutting speeds can be achieved using hard turning technique [5]. Thus material removal rate can be increased while the machining time can be decreased up to 60% [19,28]
- Hard turning produces recyclable long chips, on the other hand, grinding produces metal dust which is hard to collect, dispose or recycle.

Thus, a possible manufacturing method of bearings by using hard turning operations is illustrated as shown in Figure 1.4.

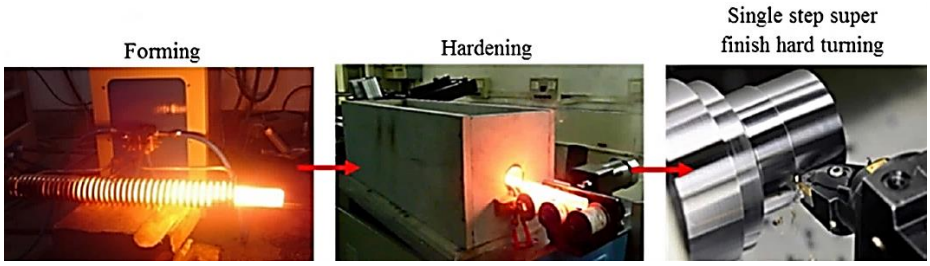

Figure 1.4 Hard turning assisted manufacturing [24]

Besides these substantial advantages, hard turning has an important drawback originated from the aggressive cutting conditions. At this process, high hardness of the workpiece leads to extreme cutting temperatures [2]. Because of that, rapid tool wear, high residual stresses and undesired phase transformations in the microstructure are commonly observed during the hard turning processes and these formations negatively affects the machining costs (rapid tool wear) and product quality (surface integrity). In order to increase the applicability of the hard turning process, mentioned disadvantages must be minimized by using appropriate cooling conditions and high performance cutting tools.

As a branch of hard to cut materials, hardened steels which are commonly used in the tool, die and gear industry are frequently studied in industrial and applications [27], [29]. Manufacturing of roller bearing is one of the most common applications of hardened steels in addition to the gear, die and tool industry [22]. Roller bearings consist of three main parts (balls, inner and outer races) and these parts are connected to each other under various loads and vibrations. Therefore, bearings must be produced by using certain type of materials which have high fatigue life and wear resistance in order to cope with unstable and difficult working conditions. AISI 52100 (100Cr6) tool steel is widely used in engineering applications [20] and especially for the manufacturing of bearings because of its superior properties. Because of its wide usage at the bearing industry, this steel is referred as bearing steel at the literature [30]. Bearing steels in unhardened state are subjected to turning operations due to its geometric features (in generally cylindrical and conical forms). Therefore, hard turning has a vital importance for bearing steels.

1.1.1 Cutting Tool Materials and Geometries

With the developments on the machining processes such as hard machining and high speed machining, higher productivity can be provided. Thus, cutting temperature have increased and it reached to excessive levels in the machining of hardened steels [30]. This heat generation mainly affects the workpiece and the cutting tool. Even though the large amount of this heat is absorbed and dissipated by chips, cutting zone is still subjected to excessive temperatures as shown in Figure 1.5.

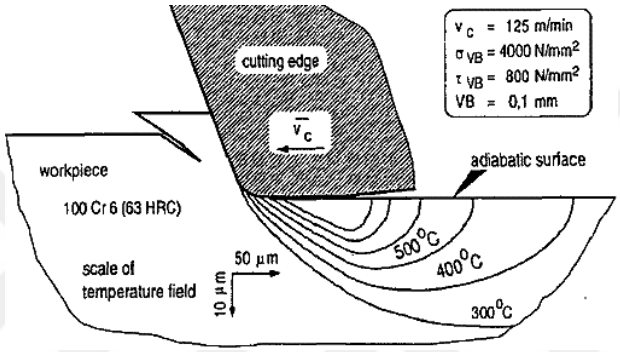

Figure 1.5 Estimated temperature fields in a hard machining process [31]

In investigations conducted on cutting tools, two main topics that is directly related to difficult cutting conditions mentioned above are studied. The first one is cutting tool material that influences the performance of the cutting tool. WC (tungsten carbide), PCD (polycrystalline diamond), ceramics, cermets and CBN (cubic boron nitride) are common cutting tool materials at the industry. WC cutting tools are one of the most preferred cutting tool material groups for the conventional machining operations but they are not suitable for the hard turning due to their low hot hardness and wear resistance. PCD is known as the hardest material found in nature [32] but it is not appropriate for the machining of ferrous metals because of its high chemical affinity with steels. Ceramic inserts, although not as hard as PCD, have high hardness even so. Additionally, they have higher thermal resistance and longer tool life than WC tools [33] but they are very prone to fracture in case of the tensional and bending stresses. When the harsh cutting conditions of hard turning are considered, cutting performance of the ceramics which are cheap alternative to CBN are not sufficient at especially

higher speeds. On the other hand, CBN cutting tools are preferred during the turning of hardened steels due to its higher hot hardness, chemical stability [34] and corrosion resistance. Also CBN is the second hardest cutting tool material after the diamond and it does not react with iron or nickel [1,27,28,30,35–37]. CBN inserts contain different amounts of CBN particles with various grain sizes. The properties of the CBN cutting tool material can be varied by altering the crystal size, content and the type of binder to make various grades, namely:

- The straight PCBN grade consisting of a high percentage of CBN (about 90wt.%) and a metal second phase (Al).
- High content composite CBN (CBN about or less than 80wt.%) and a metal/ceramic second phase.
- Low content composite CBN (CBN less than 70 wt.%) and ceramic (TiN or TiC) second phase [38]

Instead of producing inserts from only CBN particles, CBN particles are generally bound using metal or ceramic binders due to some limitations during the sintering process [39]. With the uniform configuration of the CBN particles, machining performance changes in accordance with particle size and density. As it can be seen from the Figure 1.6, high CBN content cutting tools exhibit worse performance during the hard turning operation in terms of flank wear formations.

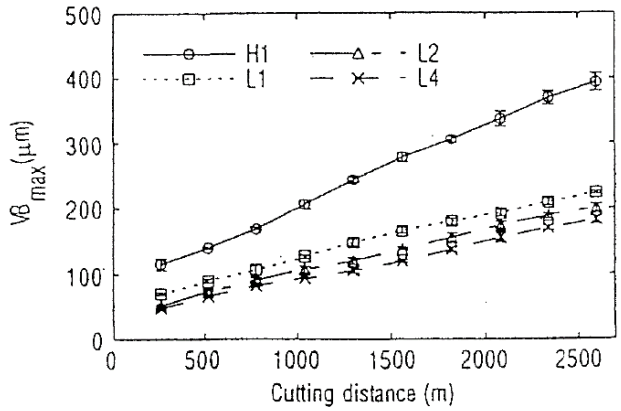

Figure 1.6 Flank wear of high CBN (H1) and low CBN (L1, L2, L4) content tools during the hard turning of AISI 52100 steel [40]

Since CBN cutting tools have hard and brittle structures, these inserts are prone to fracture under harsh cutting conditions at which cutting forces are very high. They are also are relatively expensive with resp"ect to ceramic tools [2]. Thus, industrial usage of CBN tools is very limited. However, in case of manufacturing of strategic parts with higher dimensional accuracy and being economical alternative to grinding, the use of the CBN tools may be very reasonable.

In addition to the cutting tool material, cutting tool geometry is another important issue which directly influences the cutting performance. The geometry of single point cutting tool widely used in turning operations is represented with seven parameters (tool signature) as shown in Figure 1.7.

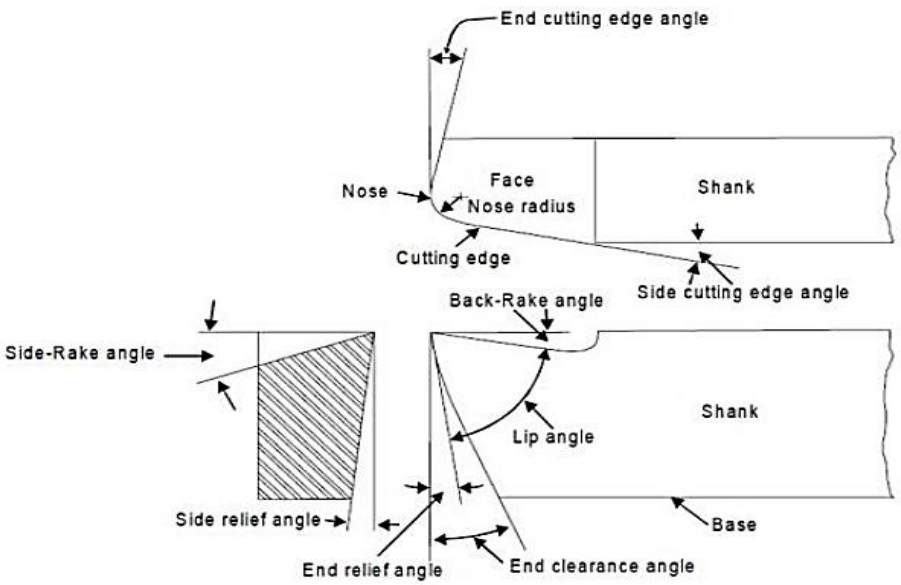

Figure 1.7 Elements of tool signature [41]

Nose radius is one of the basic parameters of cutting tool geometry which connects the side and end cutting edges. Any change in the size of nose radius directly affects the tool wear and surface roughness. With an increase in nose radius, surface roughness values decrease due to higher tool-workpiece contact length. On the other hand, an enlargement in the contact length significantly increases the stresses and frictions in the cutting zone [42]. In addition to the nose radius, side cutting edge angle (lead angle)

is another factor on the stress formation of inserts. Increasing lead angle also increases tool-workpiece contact length and decreases chip thickness. As a result, the cutting force is diffracted on a longer cutting edge and longer tool life is obtained due to smaller force components as shown in Figure 1.8.

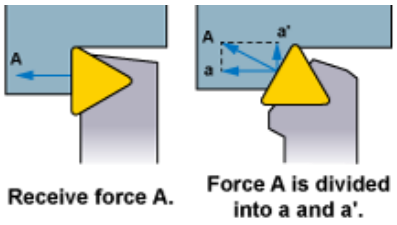

Figure 1.8 Effect of side cutting edge angle on the cutting force distribution [43]

As a third parameter, end cutting edge angle takes place between the end cutting edge and a line perpendicular to the shank. This angle minimizes frictions by providing a clearance between minor cutting edge of the tool and the workpiece. Back rake angle is an angle between the rake face of the tool and a plane parallel to its base. This angle highly affects the cutting forces and chip flow. Additionally, side rake angle represents the angle between the rake face and the shank of the tool. It performs similar functions with the back rake angle. In general, side and back rake angles have two configurations; positive and negative angles as shown in Figure 1.9.

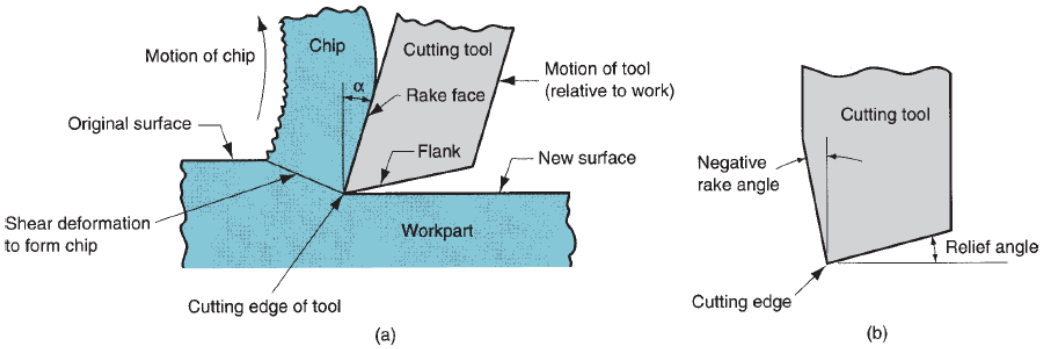

Figure 1.9 Single point tools with (a) positive and (b) negative rake angle [3]

As seen in the Figure 1.9a, positive rake angle (α) creates sharp cutting edge. Thus, it reduces cutting forces and surface roughness. However, it also decreases the cutting

edge strength. Therefore, it is not preferred in machining of hard-to-cut materials. On the other hand, negative rake angle presents higher tool life and it provides an opportunity to roughing cuts and machining of hard-to-cut materials such as hardened steels. For these cutting tools, ceramics that have high compressive strength are preferred as an insert material due to presence of compressive stresses. Other two parameters are side and end relief angles. These angles allow cutting without rubbing against the workpiece and the values of these angles are selected by considering workpiece material. As an example, end relief angle varies from 0° to 15° (usually 8°) and side relief angle is preferred in the range of 6° - 10° for the machining of steels. In addition to these seven parameters, shape of the cutting tool is determined by the cutting edge preparations such as chamfering or honing as shown in Figure 1.10.

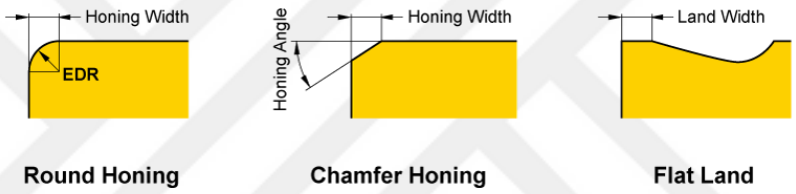

Figure 1.10 Cutting edge preparations [44]

These preparations on the cutting edge significantly improves the machining performance [45] by reducing fractures and micro-chippings on especially the super-hard cutting tools such as CBN, diamond and ceramics. In addition to the improvements on the cutting tool strength, chamfered or honed cutting inserts are prone to produce less compressive residual stresses than large edge honed inserts during the hard turning processes [46]. These cutting edge preparations are implemented for the same objectives but they have different characteristics in terms of surface roughness. At this content, chamfered cutting edges produce better surface roughness than the honed cutting edges [1]. In order to obtain optimum machining performance honing width is preferred as half of the feed [44].

In addition to the cutting edge preparations and cutting edge geometries, there are specially designed wiper inserts which have an auxiliary nose radius behind the primary cutting edge as shown in Figure 1.11.

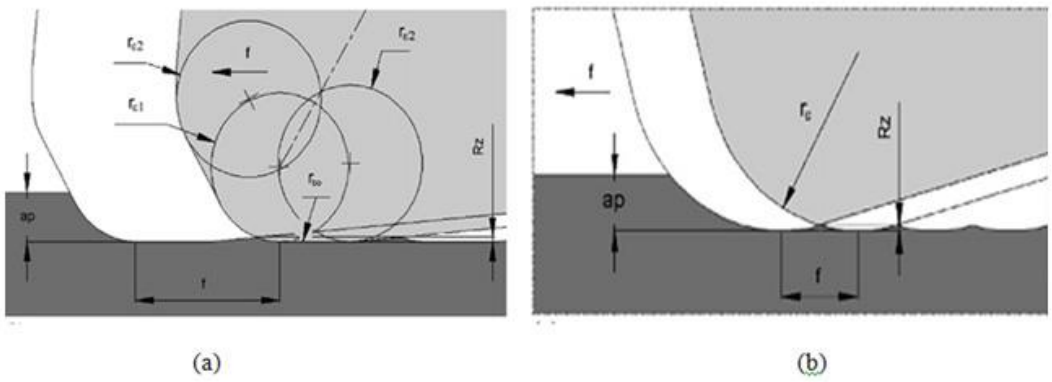

Figure 1.11 Inserts with (a) wiper and (b) conventional geometries [47]

Thanks to this secondary cutting edge, tool-workpiece contact length increases independently from the nose radius. Thus, these inserts produce better surface roughness than conventional inserts during the hard turning operations.

1.2 Tool Wear

During the machining operations, cutting tools are subjected to high localized stresses, temperatures, sliding of the chips through the rake face, and sliding of the tool along newly machined surface. These situations lead to tool wear, which is one of the major assessment criteria for all machining operations. They adversely affect tool life and the machined part quality, and therefore, the economics of machining operation [14]. The wear rate of a tool depends on cutting tool and workpiece material, tool geometry, cutting parameters, cooling/lubrication environment, and the characteristics of the machine tool [48]. The tool wear takes place in accordance with the employed cutting conditions during a machining operation [49] and its types is generally classified as flank wear, crater wear, nose wear, chipping, notching, plastic deformation, and gross fracture. The principal wear types and their locations are given in Figure 1.12.

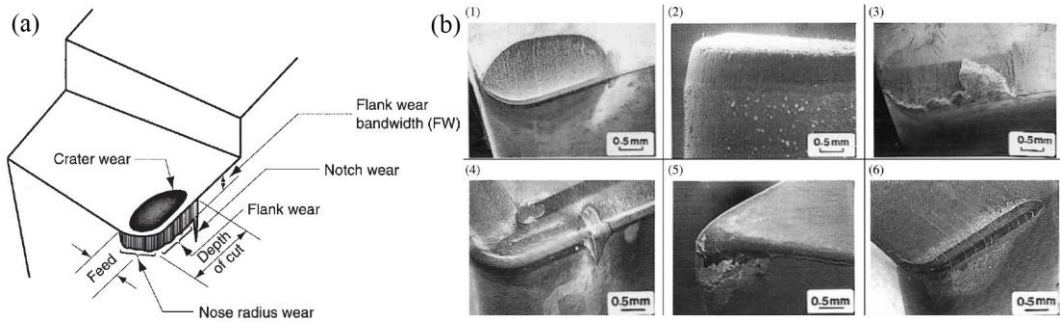

Figure 1.12 Schematic representation of worn cutting tool (a) [3] and SEM images of tool wear forms (b) [38]; crater wear (1), flank wear (2), BUE (3), notching (4), nose wear (5), and thermal cracks (6)

In order to understand the advantages and limitations of a selected cutting condition, it is important to analyze the resulted tool wear and its mechanisms. Flank wear (Figure 1.12 b2) takes place on flank face of the cutting tool. It occurs owing to rubbing motion between tool and the machined surface. Therefore, abrasive wear mechanism is the main reason for formation of flank wear [30]. In addition, high cutting temperatures also adversely affect flank wear formation [16] due to poor mechanical properties of a tool material at high temperatures. On the other hand, crater wear occurs on the rake face of the cutting tool (Figure 1.12 b1). The high temperature at the tool-chip interface and the chemical affinity between cutting tool and workpiece material are the most significant factors which are responsible for crater wear. The principal wear mechanism leading to crater wear is diffusion. It generally occurs with the movement of carbon atoms from high carbon content tool material to low carbon content work material and diffusion rate increases with increasing cutting temperature. Therefore, to reduce crater wear, proper cutting conditions should be selected and/or protective coating materials for the cutting tool [50,51] should be employed. Excessive formation of crater wear weakens the cutting edge and this can cause to deformation or catastrophic failure of cutting tool. Built-up edge (BUE), shown in Figure 1.12 b3, occurs when the work material welds to the tool cutting edge especially during machining of soft low-carbon steels, ductile stainless steels, and nonferrous materials (such as aluminum, titanium, cobalt, and nickel alloys) at low cutting speed and feed values. It causes a change in effective depth of cut and thus unstable cutting. Therefore,

it leads to severe attritious wear and tool chipping. Notch wear (Figure 1.12 b4) takes place when workpiece surface is harder and/or more abrasive than the inner material. This can occur due to several reasons such as work hardening (caused by cold drawing or previous machining operation) or sand particles in the workpiece surface from casting [3]. As a result of the harder external surface, wear is accelerated at this location. Notch wear can lead to tool fracture especially in machining of workpiece materials such as austenitic stainless steels, titanium alloys and nickel-based superalloys with their high work hardening tendency. In order to minimize this tool wear type, tools with chamfered and rounded cutting edge geometries should be preferred and small depths of cut should be avoided [38]. Nose wear (Figure 1.12 b5) is rounding of a sharp tool tip owing to insufficient abrasive wear resistance of the tool material at high mechanical loads and temperatures during a machining operation. It leads to deterioration of surface integrity [48]. In interrupted cutting operations, such as milling, cyclic heating and cooling occurs and develops thermal cracks (Figure 1.12 b5), perpendicular to cutting edge of the tool. After a machining time, lateral cracks may occur and together with thermal cracks, they lead to fracture of the tool. In addition to wear formation, cutting tools can undergo chipping, as a consequence, small pieces from the cutting edge break away. In general, it occurs in brittle cutting tool materials such as ceramic and diamond tools. Chipping also may take place in a region of the tool where small defects such as cracks are already existing. Unlike gradual process in wear formation, it is a sudden loss of the tool material and shape. Therefore, it has a major detrimental effect on surface integrity. Mechanical shocks and thermal fatigue are of the two main causes of the chipping.

Considering the tool life in machining, there are three possible modes in failure of the tool: fracture failure, temperature failure, and gradual wear. Fracture and temperature failures are occurred due to excessive cutting forces and cutting temperatures, respectively. Therefore, these failure modes are regarded as reasons for premature failure of the tool. On the other hand, gradual wear is a preferred wear mode due to its economic advantage of longer tool use. This wear mode occurs at two principle locations on a tool; rake face and flank face. As explained above, the main types of

tool wear are flank wear and crater wear (Figure 1.12). Dimensional characteristics of these wear types (crater, flank, nose and notch wears) can be directly measured for HSS, carbide, and ceramic tools according to ISO 3685 “Tool-life testing with single-point turning tools” standard, as shown in Figure 1.13. As indicated in Figure 1.13 A, crater wear is represented in terms of depth (KT) and width (KF-KB). Its value can be determined by the measurement of crater depth, or 2D [52] or 3D [53] measurement of wear area. On the other hand, flank wear measurement (Figure 1.13 B) can be performed on the active major cutting edge length (b). It is divided into three zones as zone C (includes the rounded part of the cutting edge at the corner (r_ε)), zone B, and zone N. In general, the wear land forms uniform and it is defined as VB_B in the central zone (zone B). On the other hand, in case of variations that may occur in wear land, maximum wear land (VB_{Bmax}) can be observed. According to ISO 3685, the allowable wear amount for effective tool life is defined depending on several criteria for HSS and carbide tools. Accordingly, VB_B=0.3 mm or VB_{Bmax}=0.6 mm are the allowable wear banwidth limits for both materials. In addition, crater wear criterion is also determined for sintered carbide tools as $KT=0.06+0.3f$, where f is the feed rate.

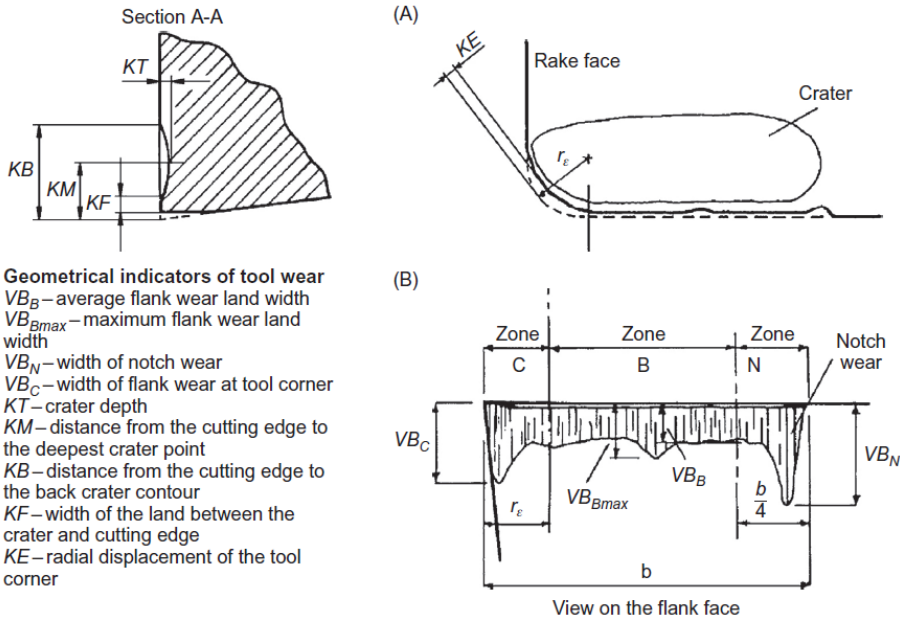

Figure 1.13 Characterization of wear patterns on rake (A) and flank (B) faces of single point cutting tool according to ISO 3685 [15].

Considering CBN turning of hardened steels, the abrasion, adhesion and diffusion are regarded as the primarily CBN tool wear mechanisms also with combination of several tool wear mechanisms [54]. The wear patterns CBN cutting tools can be crater wear, flank wear, nose wear, cracks, and microchipping according to regarded cutting condition. In order to determine tool life criteria in hard turning, it is recommended to use both crater wear depth and/or area and flank wear bandwidth measurements. Figure 1.14 indicates a typical worn CBN insert with crater and flank wears (Figure 1.14 B) and wear types in CBN hard turning (Figure 1.14 A).

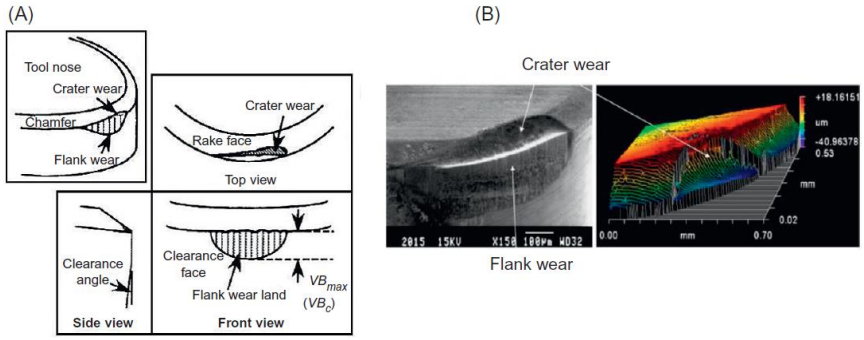

Figure 1.14 (A) Typical wear types [55] and (B) SEM image of a worn CBN insert in hard turning [54]

1.3 Surface Integrity

An important indicator for the machining performance is the surface integrity and it describes the final condition of machined surface based on several parameters. Surface integrity is frequently studied because it directly affects the quality and working performance of the final product [35,56]. The factors that constitutes surface integrity in hard machining can be listed as surface roughness, phase transformations (white-dark layer formation) and residual stresses. These properties of the product are generally influenced from two main factors; thermal (due to cutting temperatures) [57] and mechanical factors (due to plastic deformations). Even though these mechanically and thermally induced formations can reach to excessive levels during especially hard machining operations, they can be generally minimized with the selection of proper cutting fluids and usage of high performance cutting tools [2].

1.3.1 Surface Roughness

Surface roughness is one of the most important components of the surface integrity [58] and it shows the quality of the surface finish in a defined area. During the machining processes, positive or negative deviations occur in the direction of a normal vector relative to the nominal surface and these deviations are referred as the surface roughness as shown in Figure 1.15.

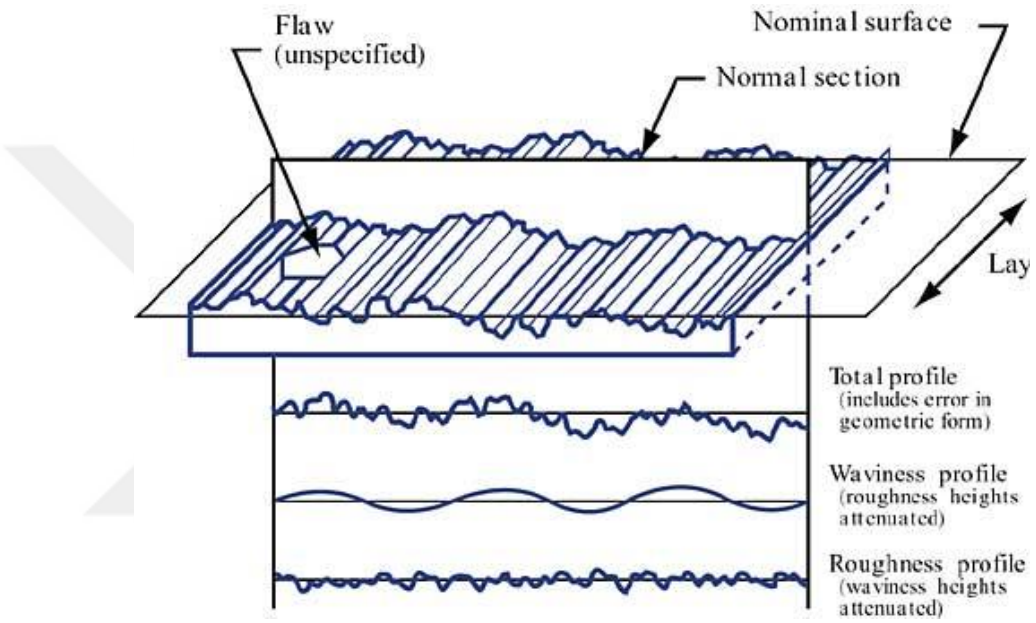

Figure 1.15 Surface Roughness [59]

In this context, high surface roughness values are undesired for machine elements such as bearings that usually operated at high rotational speeds. Under these working conditions, rough surfaces are subjected to rapid wear and plastic deformation due to their high friction coefficients.

Surface roughness is influenced by the cutting parameters, tool geometry, tool wear, cutting forces and vibrations. In order to perform a comprehensive evaluation of surface quality, surface roughness and its driving factors should be carefully analyzed. As the cutting parameters, feed [60] and cutting speed mainly influence the surface roughness. By decreasing feed and increasing cutting speed smoother surfaces can be

obtained. In the turning operations where the lower feeds are used, contact point of the insert moves slower and it deforms the surface more steadily. This situation reduces surface roughness by increasing the number of peaks and converging these deviations on the workpiece axis direction. Even though low feeds produce low surface roughness values, they are avoided due to longer machining periods. Because of that, increasing cutting speed is considered as an alternative solution under machining conditions where the machining time is limited. In this context, increasing cutting speed also presents similar effect but the influence of the feed is higher than the cutting speed in the turning operations.

In addition to the cutting parameters, [11] tool geometry is another important factor of the machining performance [57,61] and surface roughness values [22]. For example, cutting tools with larger nose radius produces better surface roughness values by increasing the sweeping area for each peak. Thanks to increased sweeping area with larger radii of curvature, height of peaks is limited and the deviations reduce. Thus, cutting tools with larger nose radius can be preferred for their ability of improving surface roughness without changing feed or cutting speed. Another alternative to cutting inserts with larger nose radius is wiper cutting inserts. In contrast to conventional inserts, wiper inserts have multiple radii that consist of large main radius and commonly two additional smaller radii as shown in Figure 1.11.

Thanks to their additional radii, wiper inserts are capable of generating better surface finish when compared to conventional inserts and it can give comparable surface roughness values with grinding operations. By using these wiper cutting tools, surface roughness values obtained at low feeds or cutting speeds become possible at higher feeds [22] or cutting speeds [62]. Thus, these tools which provide significant improvements on the surface roughness and machining time are becoming widespread increasingly.

In order to determine the surface roughness, the defined area is generally examined by using several linear measurements. These measurements are evaluated from three different types of surface roughness values; Ra (average roughness), Rt (maximum

height of the profile) and Rz (average maximum height of the profile). Rt represents the vertical distance between the highest and lowest points that takes place on the sampling length. Thus, Rt shows the maximum height difference on the measured length. On the other hand, Rz is calculated as the average of five maximum heights measured from sampling length. As a third measurement, Ra defines the arithmetic average of the profile heights along the measured length according to ISO 4287 and its equation is given on the Figure 1.16.

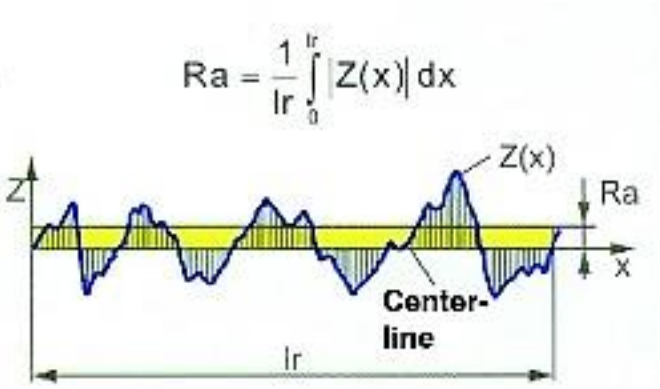

Figure 1.16 Mean value (Ra) of the roughness profile [63]

During the turning and grinding operations, Ra values are generally obtained in the range of 6.3-0.4 μm and 1.6-0.1 μm respectively. Because of their low roughness values, high precision parts are ground after conventional turning and heat treatment operations. In the hard turning operations which are going to replace to grinding operations, Ra values below the 0.4 μm are considered sufficient in the literature [1].

Tool wear and cutting temperatures are also other important factors affecting the surface roughness. Rapid tool wear and excessive cutting temperatures are effective on the surface texture by affecting machining performance. High temperatures in the cutting zone cause ductile cutting by decreasing the hardness of workpiece. In this case, worn cutting tools perform unstable cutting. Rapid tool wear and excessive cutting temperatures that increase surface roughness values can be commonly observed during especially hard turning operations.

1.3.2 Subsurface phase transformations

1.3.2.1 White and dark layer

During the machining processes, thermo-mechanical energy dissipated into work-tool surfaces, leads to the subsurface alterations (such as residual stresses and subsurface phase transformations) [64]. While the mechanical form of the dissipated energy leads to a grain refinement on the machined surface and subsurface of the workpiece, thermal energy imitates a heat treatment process. It is possible to observe this effect of the cutting temperature during high-speed machining of difficult-to-cut materials such as superalloys and hardened steels rather than conventional machining processes (Figure 1.17).

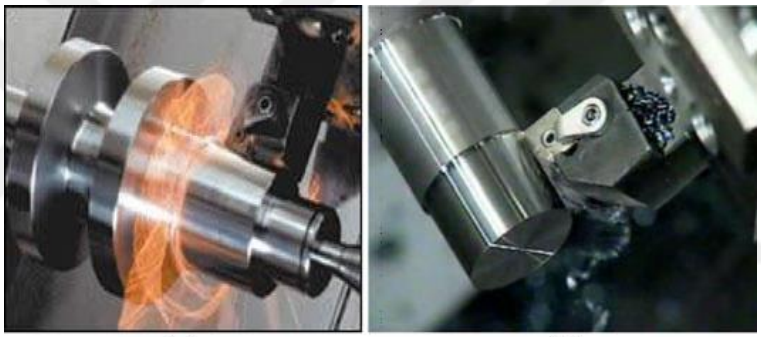

Figure 1.17 Cutting temperatures generated during (a) high-speed machining of hardened steels, and (b) conventional machining of unhardened steels [65]

During the machining operations, rising of the temperature above the austenite transformation temperature (≈800°C for the AISI 52100 steel [66]) and the following rapid cooling [21] creates a martensitic structure at the surface [38]. This martensitic microstructure generally contains low austenite around 10-33% [67] and it is called “white layer” because it is observed in white color under an optical microscope after polishing and etching [28,50,68]. In addition to these white layer formations, an overtempered dark layer is also formed due to slower temperature changes. These two different layers which have different microstructure and hardness because of subjecting to different temperature levels and cooling rates are shown in Figure 1.18

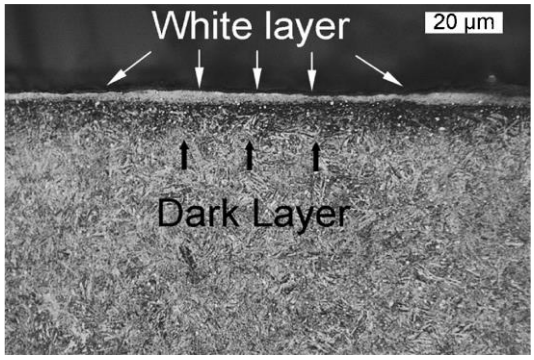

Figure 1.18 White and dark layers in AISI 52100 steel after hard machining [28]

As a result of these subsurface properties, different residual stresses occur on the white and dark layers [35]. It is well-known that the fatigue life of the material significantly decreases with an increase at the thickness of white layer which creates residual stresses. Then, at a certain period, white layer can partially delaminate and cause to a failure under high contact pressure [5]. The effect of these residual stresses are discussed at the Section 1.3.2.2.

It is believed that the white and dark layers is primarily generated by a thermal effect during machining of hardened steels. Thermally induced formations such as white and dark layers in hardened steels depend on temperature level generated in cutting zone and the cooling rate [26,41]. During the machining process, surface of the workpiece is subjected to the maximum cutting temperature due to direct contact and rubbing of cutting tool. Then it cools faster than subsurface because of the exposure to the coolant or air. Because of these rapid changes in the temperature, martensitic white layer takes place near surface as a thin layer. The cutting temperature is mainly affected by two parameters; cutting speed and workpiece hardness. Thus, white layer formation is indirectly related to cutting speed and workpiece hardness as shown in Figure 1.19.

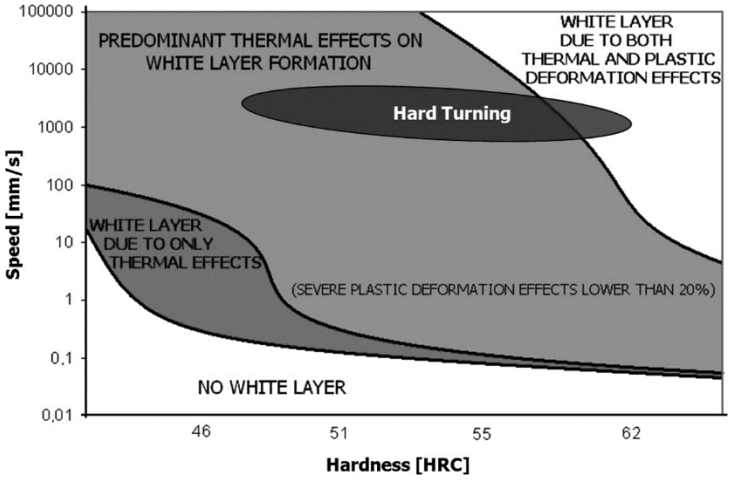

Figure 1.19 The influence of cutting speed and workpiece hardness on the white layer formation [12]

On the other hand, dark layer forms between the white layer and the bulk material. Due to moderate heating distributed on the subsurface and followed cooling, dark layer thickness is relatively higher than the white layer. This layer is softer than both white layer and the base material [69] due to overtempering caused by limited heat transfer.

During the hard turning operations, this phenomenon is significantly observed due to excessive cutting temperatures caused by higher cutting speed and workpiece hardness. In order to obtain allowable white and dark layer formations, decreasing of the cutting temperature during the machining of hardened steels is not an efficient and cost-effective solution. Therefore, proper cooling and/or lubrication methods are currently utilized to lower both cutting temperatures [50] and tool wear [70] in metal cutting industry.

1.3.2.2 Residual Stresses

As a third subclass of the surface integrity, residual stresses are defined as the stresses resident inside a component or structure after all applied forces and thermal shocks have been removed. Residual stresses are classified as beneficial or undesired according to its type (tensile or compressive) and distribution (uniform or disordered). Even though the compressive residual stresses are beneficial for the fatigue life of a

machinery part [37], non-uniform stresses and distributions in different phases lead to premature crack initiation and decrease fatigue life significantly [71].

In order to determine the overall performance of the workpiece material, residual stresses are measured using XRD (X-Ray Diffraction) technique and evaluated in detail. This method basically measures the angle of irradiated crystalline particles where the maximum diffracted intensity takes place [72]. Since the turning is a machining technique that performs cutting operations on two directions (axial and circumferential), two measurement directions are considered adequate in order to evaluate residual stress formations in turning operations. Because of that, the machined parts are examined on either axial or hoop (circumferential) measurement planes in terms of residual stresses after the turning operations as shown in Figure 1.20.

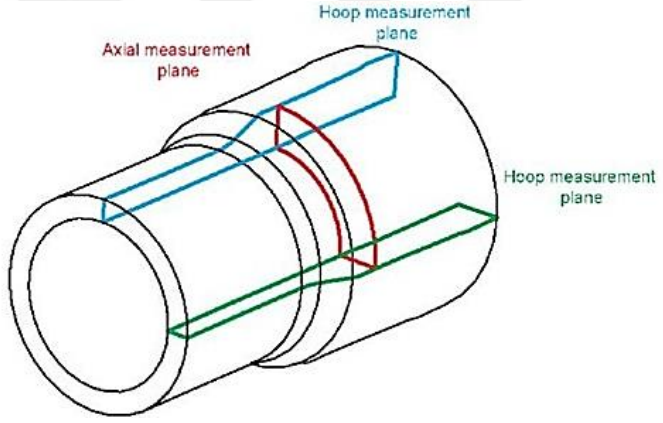

Figure 1.20 Axial and hoop residual planes (Edited from Figure 1 of the reference [73])

Main reasons for the residual stresses are high temperature gradients, plastic deformations and chemical reactions. The residual stresses might be also produced by a combination of temperature changes and plastic deformation which can be observed during the machining processes [38].

As known, residual stresses can be derived from the disconformity between different phase structures in a workpiece material. Therefore, any influence that generates a variation in the phase structure of workpiece material generates residual stresses. In this context, there are two factors which affect residual stresses during the machining

operations. These are mechanical (plastic deformation) and thermal effects (phase transformations) which become dominant at low and high cutting speeds respectively [26,74,75]. The combination of these two mechanisms can be commonly observed as thermal/plastic deformation. In this model, the generated heat leads volumetric expansion of the surface layer then it is relieved by plastic deformation. After the cutting process, cooling of the surface layer causes to residual stresses.

As mentioned above, these mechanisms are dependent on two main factors in the turning operations; cutting speed and workpiece hardness. As a result, the combined effect of these parameters determine the overall residual stresses remaining within the machined work part material. Even though the workpiece hardness is considered as a secondary factor on conventional machining processes, cutting speed is the dominant factor for the residual stress formations. With the increase of cutting speed, residual stresses increase due to severe plastic deformation on the surface and high cutting temperatures distributed towards the bulk material. After the removal of heat source (material removal process), different cooling rates produce various phase structures and residual stresses. Due to phase transformation from austenite to martensite, different residual stress values occur from the bulk material to the surface. In addition, the location of the maximum stresses is also determined by the cutting speed and they are shifted towards the rotation axis of the workpiece at higher cutting speeds as a result of exposure to higher cutting temperatures.

In this context, white layer formations generated by the effect of cutting temperature are directly related to the residual stresses. In case of white layer formation in an orthogonal machining process, tensile residual stresses occur where the white layer thickness is relatively low. As the thickness of the white layer increases, residual stresses become more compressive near surface and the maximum stresses are observed around the white-dark layer transition zone [35] due to phase differences. The effect of cutting speed and the white layer on the residual stresses are shown in Figure 1.21.

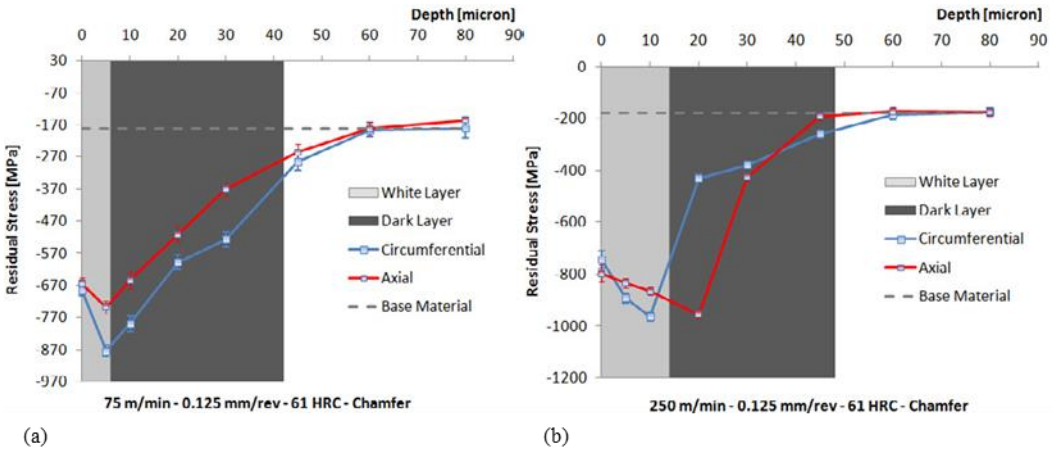

Figure 1.21 Effect of phase transformations on the residual stresses during the hard machining at cutting speeds of a) 75 m/min and b) 250 m/min [35]

During the hard turning operations, workpiece hardness is considered as a second parameter that significantly effects the residual stresses on these two measurement directions. In this context, an increase in the workpiece hardness produces more compressive stresses in both axial and hoop directions due to higher cutting temperatures caused by higher cutting force requirements.

1.4 Sustainable machining

As explained above in detail, tool wear and surface integrity are two important criteria for the evaluation of machining performance. In this subject, the cutting conditions are commonly studied by the researchers in order to improve surface integrity and tool wear. During the cutting process, elevated temperatures and frictions negatively affecting tool wear and surface integrity are the basic issues. In machining of some engineering materials, these cutting temperatures and frictions can be minimized using several coolants and/or lubricants in order to lower the machining costs and to enhance the product quality [76] as shown in Figure 1.22.

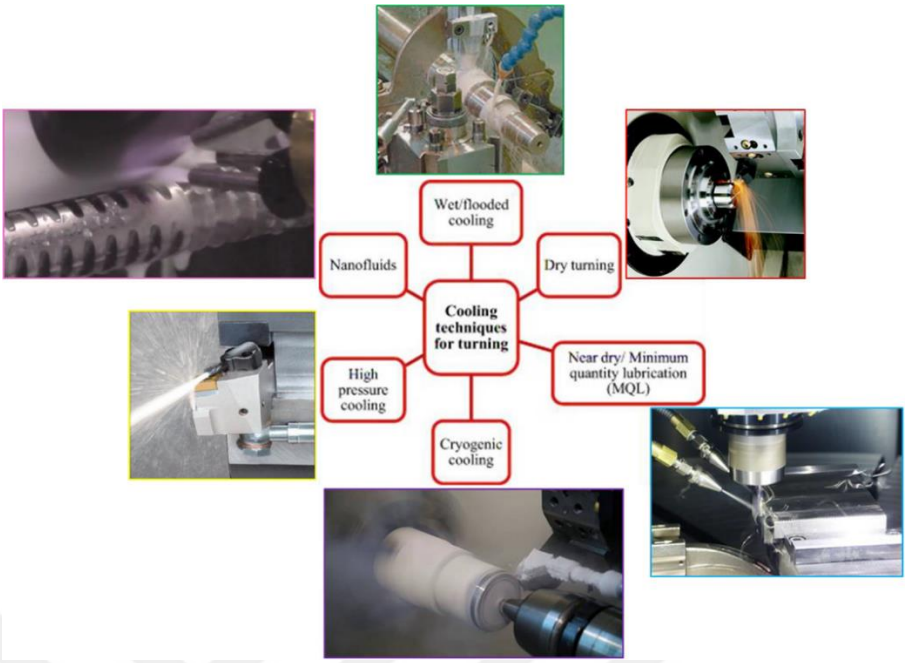

Figure 1.22 Different cooling/lubrication techniques in turning processes [77]

During conventional cutting processes of easy-to-cut materials, the cutting temperatures commonly reduced using conventional cutting fluids [57] which is a simple, cheap and convenient technique. These cutting fluids are applied from the tool holder (internal application) or an external nozzle to the cutting zone at low pressures such as 5-10 Psi [78] and they have various forms as shown in Figure 1.23.

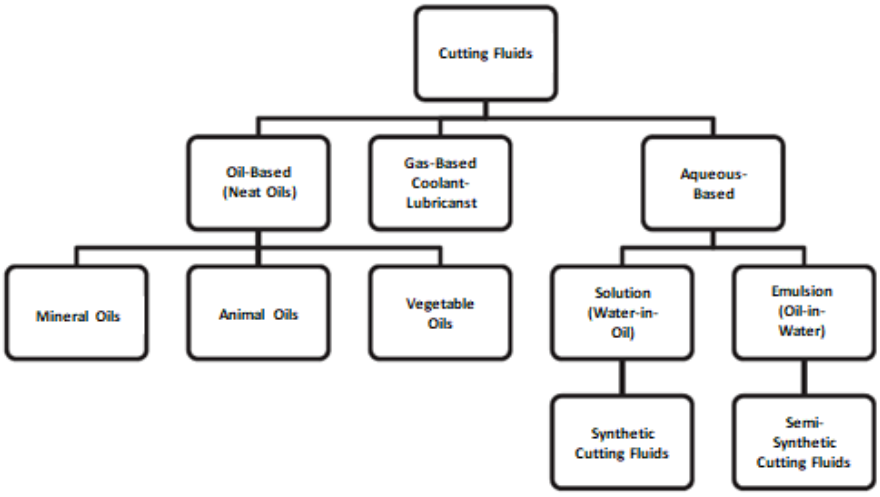

Figure 1.23 Classification of cutting fluids (Edited from the Fig. 1 of the reference [78])

Due to the fact that the cooling and lubrication properties of conventional cutting fluids are limited, they are not sufficient for the hard machining processes in which excessive temperatures are generated [76]. Additionally, conventional cutting fluids have harmful effects to environment (contamination) and human health (dermatological problems) [79].

Because of these drawbacks of the usage of conventional cutting fluids, eco-friendly and efficient cooling/lubrication techniques such as MQL, cryogenic cooling and hybrid cooling (CryoMQL) are recently one of the popular research topics among researchers [78,79]. In the research works in the literature, these cooling/lubrication techniques are compared to each other according to various parameters as shown in Table 1.1.

Table 1.1 Comparison of different cooling/lubrication techniques [80]

	Effects of the cooling and lubricating strategy	Conventional cutting fluid (Emulsion/Oil)	Dry (Compressed Air)	MQL (Oil)	Cryogenic (LN2)	Hybrid (LN2 + MQL)
Primary	Cooling	Good	Poor	Marginal	Excellent	Excellent
	Lubrication	Excellent	Poor	Excellent	Marginal	Excellent
	Chip Removal	Good	Good	Marginal	Good	Good
Secondary	Machine Cooling	Good	Poor	Poor	Marginal	Marginal
	Workpiece Cooling	Good	Poor	Poor	Good	Good
	Dust Particle Control	Good	Poor	Marginal	Marginal	Good
	Product Quality	Good	Poor	Marginal	Excellent	Excellent
	Sustainability Concerns	Water pollution, microbial infestation and high cost	Poor surface integrity due to thermal damage	Harmful oil vapor	Initial cost	Initial cost, oil vapor

1.4.1 MQL (Minimum Quantity Lubrication) system

In the MQL systems, only necessary amount of lubricant (high quality oil) with air is sprayed using nozzle(s) onto cutting zone at a certain pressure as shown in Figure 1.24. In a MQL system, an air reservoir and compressor provide constant pressure air (≈5-6 Bar) and the oil kept in the container is pumped and mixed with the pressurized air. Finally, the pressurized air-oil mixture is sprayed to the cutting zone by means of the nozzles. The pressurized air-oil mixture applied using these nozzles and the MQL system coats the tool-chip and tool-workpiece interfaces in form of a thin film with 0.1-50 μm droplets to minimize heat generation via friction reduction.

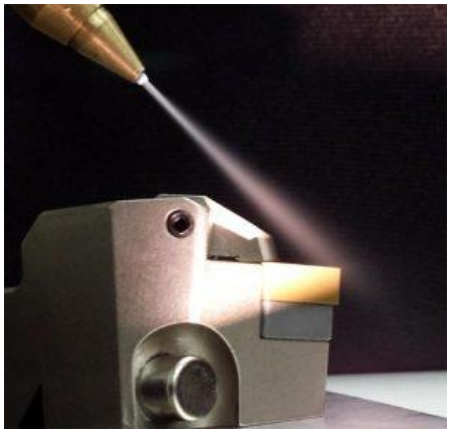

Figure 1.24 MQL application [81]

With a high quality MQL lubricant, frictions at the tool-chip and tool-workpiece interfaces and thus, heat generation is significantly reduced. As a result, it can reduce tool wear significantly [82,83]. In addition, the MQL systems provide some environmental benefits. Many MQL lubricants are mainly composed of vegetable oils and they are completely safe for human health as well as being renewable, eco-friendly material. Thus, it is not only more effective but also eco-friendly.

In hard turning operations, MQL systems are capable of reducing friction based tool wear where the negative rake angle and/or wiper inserts are used. On the other hand, due to their limited cooling capacity, they can remain insufficient in reducing of extreme temperatures such as 900-1000 °C which can be generated during the hard turning processes. Therefore, more innovative solutions for efficient cooling and lubrication are currently needed.

1.4.2 Cryogenic Cooling

Cryogenic cooling is an innovative and sustainable method utilized cryogens under the harsh cutting conditions such as machining of hardened steels. Liquid nitrogen (LN_2) [78] and carbon dioxide (CO_2) are the most common cryogens used in machining operations. These two cryogens have different cooling/lubrication properties as shown in the Table 1.2.

Table 1.2 Comparison of carbon dioxide and liquid nitrogen [84]

	Advantages	Disadvantages
Liquid nitrogen (LN_2)	- Higher cooling capacity (-196 °C) - No exhaust systems are needed inside machine-tools - Lubricant properties	- A bit more expensive than CO_2 - Storage at low temperature involves leakages by cooling - Higher expansion rate (≈700 times)
Liquid carbon dioxide (CO_2)	- Pressurized bottles (60 bar) at 20-25 without loss by cooling - A bit cheaper than LN_2 - Dissolves oil in supercritical state	- Lower cooling capacity (-78 °C) - Harmful in high concentrations - If output pressure is not controlled, dry ice can be formed

These cryogens are commonly applied to the cutting zone using external nozzles (Figure 1.25) or cutting tools (or tool holder) with internal cooling/lubrication channels. On the other hand, the cryogens are supplied from cryogenic tanks in different shapes and sizes in accordance with experimental setups [85,86].

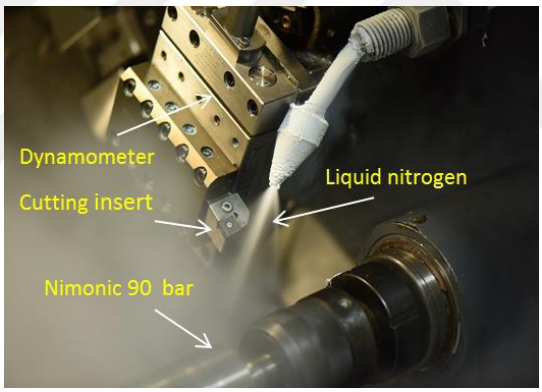

Figure 1.25 Cryogenic cooling application using an external nozzle [87]

With the use of LN_2 and CO_2, excessive cutting temperatures can be decreased significantly [88] because of the lower boiling temperatures of liquid nitrogen (-196 °C) and carbon dioxide (-78.5 °C) during the machining of hardened steels. Due to lower cutting temperatures, the effects of tool wear mechanisms on the cutting tool are restricted. Thus, sharpness of the cutting edge can be maintained [89] and productivity can be increased up to 23% [30]. Cryogenic cooling can provide excellent cooling, for example, a decrease in the cutting temperature more than 30% [90,91]. However, this method has a limited lubrication effect. Even though this method is not capable of

providing a sufficient decrease in friction, it is one of the most effective method in reducing of temperature due to high heat transfer. As a result, cryogenic cooling is an important and effective cooling method especially in providing of low the tool wear [92] and better surface integrity during the hard turning operations.

1.4.3 Hybrid Cooling

Hybrid cooling or the CryoMQL system is basically the combination of cryogenic cooling and MQL techniques. It is developed in order to provide both excellent cooling and adequate lubrication. In this method, lubricant might be applied externally while the cryogen sprayed from the tool holder (internal cooling) or an external nozzle (Figure 1.26), or it can be sprayed from a custom-designed nozzle for the cryogenic coolant [93].

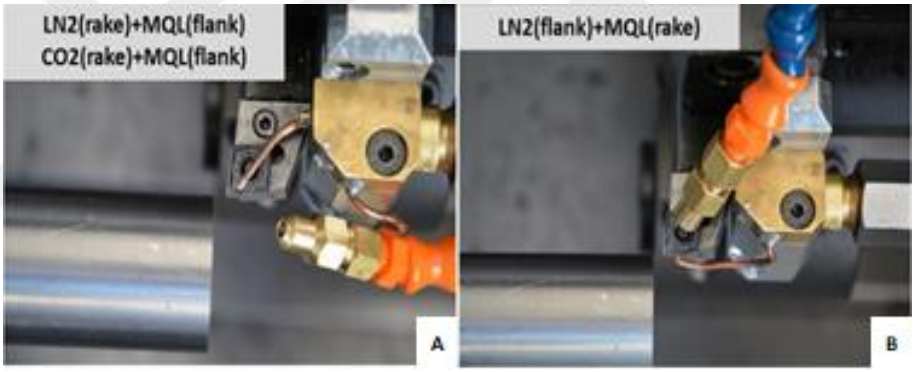

Figure 1.26 A) hybrid strategy with cryogen application on the rake face and MQL application on the flank face, B) hybrid strategy with cryogen application on the flank face and MQL application on the rake face (Edited from Fig. 2 of the reference [94])

Even though the hybrid method come to the fore because of its significant benefits, this method has an important drawback regarding its method of application. When the hybrid cooling is applied using the techniques mentioned above, both lubricant and the cutting tool experience extreme cooling. Therefore, oil mist can freeze before reaching the cutting zone and it can lose lubrication effect during the application. Furthermore, when the cutting tool exposes direct and extreme cooling, it become more brittle as it is mentioned earlier. In order to prevent these two undesired situations, a third

application method can be used during the hybrid cooling/lubrication technique. In this method, oil is sprayed from tool holder onto the cutting zone directly and the cryogens are also supplied from an external nozzle which is placed in front of the tool holder with an adequate clearance. In this way, workpiece is subjected to precooling and thus, extreme cooling and embrittlement of the cutting tool is prevented as shown in Figure 1.27.

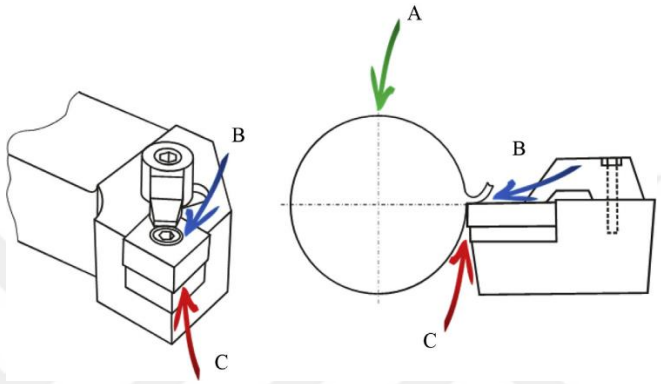

Figure 1.27 Application methods; (A) precooling, (B) from the rake and (C) from the flank [95]

1.5 Literature Review

Recently, turning of hardened steels is an important research topic due to its high potential of application in the industrial area. Because of industrial importance of hard turning operations, there are many research works conducted by academicians and industrial researchers in the literature to overcome their constraints such as higher cutting temperatures and shorter tool life. Elevated temperatures are considered as the primary reason for worse surface integrity and rapid tool wear in hard turning operations. Thus, measurements of cutting temperatures are frequently performed during turning process of the hardened steels and several cooling/lubrication strategies are studied in order to decrease excessive temperatures for better surface integrity and longer tool life. During the machining of hardened steels, temperatures in the cutting zone might exceed 900 °C [28,96]. Aramcharoen et al. [97] observed that the chip temperature reached to 800 °C as a result of higher cutting speed (800 m/min) during the machining of hardened AISI H13 tool steel (57 HRC), as shown in Figure 1.28.

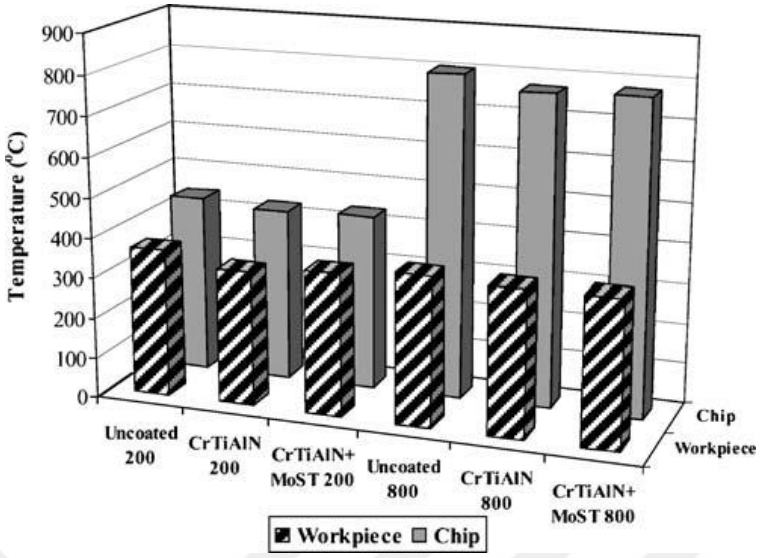

Figure 1.28 Effect of cutting speeds of 200 and 800 m/min on the chip and workpiece temperatures [97]

Nowadays, in order to reduce the cutting temperatures in hard turning operations, several cooling/lubrication techniques including conventional cutting fluid (oil and water emulsion), MQL and cryogenic cooling are employed in the literature. Conventional cutting fluid is the most common cooling/lubrication technique to lower cutting temperatures in machining of a wide range of engineering materials. Even though the conventional cutting fluids can be currently applied at low to medium cutting speeds, it remains inadequate to minimize higher cutting temperatures generated during the machining of hard-to-cut materials such as titanium alloys, super alloys and hardened steels. Therefore, alternative cooling/lubrication techniques to conventional cutting fluid are still investigated to provide better surface integrity and longer tool life in machining of hard-to-cut materials in academic and industrial fields. In this regard, Jerold et al. [98] conducted several experiments regarding cryogenic cooling and they observed that LN_2 showed better performance than conventional cutting fluid and it reduced cutting temperature by approximately 22% in the machining of AISI 1045 steel. On the other hand, CO_2 is another cryogen used at several studies in order to provide moderate cooling. Kaynak et al. [96] carried out an experimental study that reveals the cooling capacities of CO_2 and LN_2 during the

turning of AISI 4140 steel (42 HRC). Experimental results showed that cutting temperatures elevated up to 900 °C under dry conditions and decreased down to 300 °C and 400 °C using LN_2 and CO_2 respectively. In another turning study of AISI 1040 carbon steel using multilayer coated carbide inserts, the cooling capacities of conventional cutting fluid, CO_2 and LN_2 at two cutting speed and four feed values are shown in Figure 1.29.

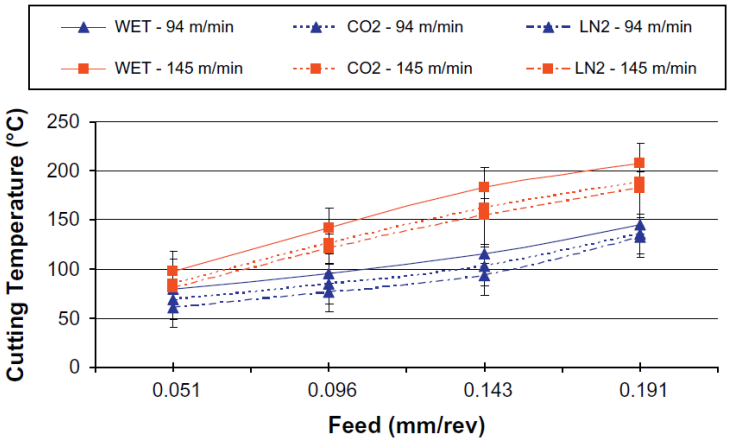

Figure 1.29 Effect of cutting conditions on the cutting temperatures in turning of AISI 1040 steel [99]

As can be seen from Figure 1.29, CO_2 and LN_2 decrease the cutting temperatures in the range of 6–21% and 9–34% respectively when compared to conventional cutting fluid. Besides, LN_2 performed better than CO_2 by about 3–17% in reducing of temperatures due to its lower application temperature.

As well as the cooling/lubrication strategy, its application method to the cutting zone is also very important. In order to study the effect of cooling direction, Hong et al. [100] performed several turning tests on Ti6Al4V alloy under dry and cryogenic conditions. During the tests, they measured cutting temperatures using some thermocouples embedded into the cutting tool. The results showed that the type of application significantly influences the cutting temperatures as shown in Figure 1.30.

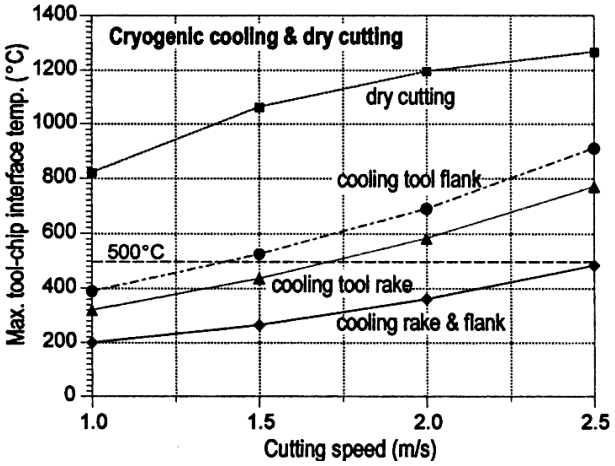

Figure 1.30 Variation of cutting temperature with cutting speed and cooling direction under dry and cryogenic conditions [100]

As shown in Figure 1.30, cutting temperatures generated as a result of cooling of the rake face are less by around 100-150 °C in comparison to those of the cooling of flank face. Besides, it is observed from the figure that simultaneous cooling of rake and flank faces becomes the best cooling strategy and lowers cutting temperatures by around 75% when compared to dry machining.

It is well-known that the cutting temperature is one of the main factors affecting the tool life and surface integrity. In this context, tool life and the tool wear are frequently studied on many engineering materials including hardened steels [27,101]. Liu et al. [34] performed a research on turning of hardened AISI 52100 steel (64 HRC) using CBN cutting inserts. They investigated flank wear and cutting temperature at different cutting speeds. The test results showed that cutting temperature triggered by increasing cutting speed accelerates the tool wear significantly. In another study on the hard turning of AISI 52100 bearing steel (64 HRC), Attanasio et al. [50] found that crater wear strongly depends on feed and cutting speed. On the other hand, it is another finding of the study that cutting speed is effective on flank wear. It is well-known that the cutting speed is directly related to the cutting temperatures. That is, an increase in cutting speed drastically increases the temperatures in the cutting zone. This case also leads to rapid tool wear and shorter tool life. Various cooling/lubrication strategies are

employed to improve tool life at higher speeds in the literature. For instance, MQL method can enhance tool life up to 90% when compared to dry conditions in machining of AISI 420 martensitic stainless steel (47-48 HRC) [102]. As a supportive research, Das et al. also found that the MQL conditions suppress the tool wear and prolongs tool life as shown in Figure 1.31.

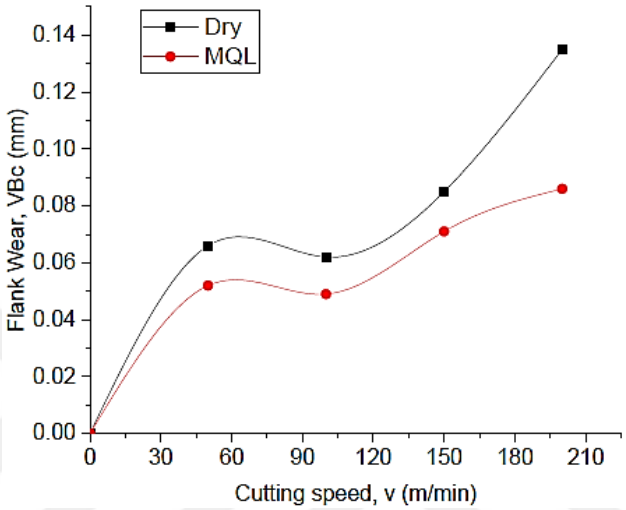

Figure 1.31 Flank wear values at different cutting speeds under dry and MQL conditions [103]

In addition to the MQL systems, cryogenic cooling is another method studied in the literature. In this context, Kaynak [17] conducted some turning tests on Inconel 718 using uncoated carbide inserts under dry, MQL and cryogenic cutting conditions. It is found that applications of MQL and cryogenic cooling (LN_2) decreased flank wear by 64% and 77% respectively in comparison to dry machining after machining time of 30 seconds. Additionally, it was observed that the cryogenic cooling performed by 36% better than MQL in terms of flank wear as shown in Figure 1.32 due to reduced cutting forces during the machining with LN_2.

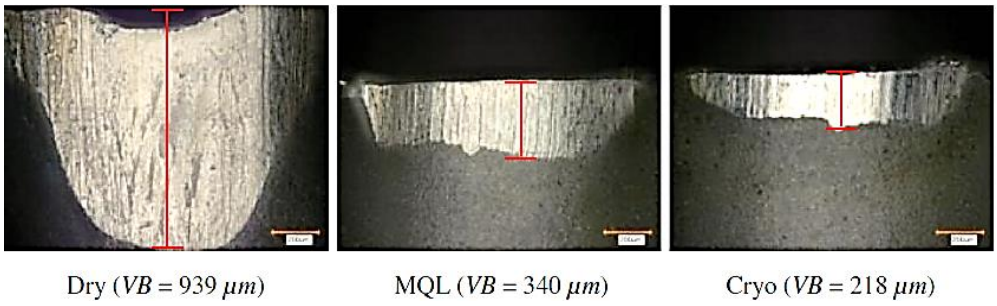

Figure 1.32 Flank wear pictures under dry, MQL and cryogenic conditions at 120 m/min [17]

Bicek et al. [30] conducted several tests on the hardened AISI 52100 steel (64 HRC) under dry and cryogenic conditions in order to determine the tool wear. At the end of the tests, it was observed that the cryogenic cooling provided 15% more tool life than the dry turning. In addition, another finding of the study is that cryogenic conditions provided less tool wear than dry MQL and conventional cutting fluid conditions. Paul et al. [57] compared cutting performance of uncoated carbide inserts under dry, conventional cutting fluid and cryogenic conditions in terms of tool life. After machining time of 30 min of AISI 1060 steel, it was determined that cryogenic cooling provided by 53% and 57% less tool wear in comparison to dry and conventional cutting fluid conditions respectively. Dhar et al. [2] also performed a number of turning tests under same conditions and they obtained the lowest tool wear in the turning of AISI 4037 steel under LN_2 conditions. In this study, authors stated that the conventional cutting fluid did not exhibit as effective performance as LN_2 but it showed better results than dry turning. Similarly, Magadum et al. [104] performed some turning tests on hardened EN24 steel (45 HRC) at three cutting speeds under conventional cutting fluid and LN_2 conditions. Experimental results showed that the cryogenic cooling improved tool life up to 38.6% when compared to conventional cutting fluid due to lower cutting temperatures, higher bulk hardness of cutting tool and better integrity of the cutting edge. In addition, it is one of other findings of the study that cryogenic machining is more effective at especially higher cutting speeds. Navas et al. [105] performed an comparison regarding tool life under dry, conventional cutting fluid and LN_2 conditions in which the flank wear is the tool life criterion (VB_B = 0.3 mm). They

observed that the cryogenic cooling performs better than other cutting conditions as shown in Table 1.3.

Table 1.3 Tool life results (AISI 4150 steel at 52 HRC)

Cooling method	Total machined length (mm)	Total machining time (min)	Total removed volume (mm^3)
Dry	408	4.75	156809
Emulsion	457	8.35	275818
LN_2	904	9.25	306022

In addition to LN_2, CO_2 also is another cryogen commonly used as an effective coolant in machining tests in the literature. CO_2 is applied to the cutting zone at temperature of around -78 °C, thus it has lower cooling capacity than LN_2 (-196 °C). Therefore, LN_2 is able to increase tool life more than four times [106]. Kaynak et al. [96] observed that the LN_2 is more effective in minimization of flank wear in comparison to CO_2. Even though CO_2 has secondary importance according to the LN_2 according in terms of cooling capacity, it also reduces tool wear significantly. In this context, two research works become prominent that resulted better machining performance with CO_2. In the first study, Pereira et al. [62] conducted turning experiments on AISI 304L stainless steel (209 HBN) using both cryogens. As a result, cooling with CO_2 and LN_2 improved tool life 35% and 17% respectively. Sartori et al. [94] also reported that with the use of CO_2, less tool wear takes place in the turning of Ti6Al4V alloy with respect to LN_2. At the end of the study, flank wear (75 μm) under dry conditions reduced to 55 μm and 65 μm by using CO_2 and LN_2 respectively. In addition to these studies, Pereira et al. [19] performed hard turning tests on AISI M3CL2 cold work steel (66 HRC) using CO_2 as a cryogen and they reported that the cryogenic cooling improved tool life by about 20% when compared to dry machining. On the other hand, surface integrity is another issue directly influenced from the cutting conditions in machining. In this context, surface roughness is one of the most important parameters which is a subtitle of surface integrity and shows product quality. It is well-known that cutting conditions (feed and cutting speed) and tool geometry significantly affects the roughness values of the machined surfaces. In the literature, cutting tool geometry (for instance, conventional or wiper insert geometry) is commonly studied in order to improve surface roughness values. Guddat et al. [107] performed a study on the cutting

performance of PCBN with conventional and wiper insert geometries in terms of surface roughness in turning of hardened AISI 52100 steel (60 HRC). At the end of their experiments, the authors revealed that the wiper inserts reduced the surface roughness by more than 80% as shown in Figure 1.33.

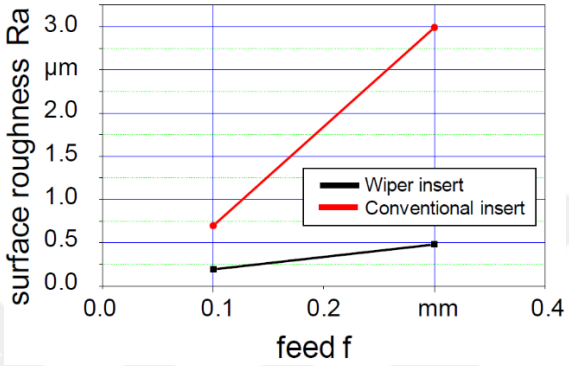

Figure 1.33 Performance of wiper inserts in terms of the average surface roughness [107]

In another study, D'Addona et al. [22] conducted an experimental study on the 55 OHNS tool steel (AISI 0-1) with hardness of 55 HRC using conventional cutting tools and they measured the surface roughness value of 0.652 µm. Then they repeated same experiments with wiper inserts and achieved surface roughness value of 0.197 µm which can be obtained from the grinding operations. Additionally, Gaitonde et al. [108] carried out a number of hard turning experiments on AISI D2 (60 HRC) cold work steel using conventional and wiper inserts. Experimental results showed that surface roughness improved by 50% owing to the use of wiper inserts. On the other hand, as well as tool geometry, cooling/lubrication media is another influential factor on the surface roughness frequently studied in the literature. Elmunafi et al. [102] studied on surface roughness in hard turning of AISI 420 SS (47-48 HRC) under dry and MQL conditions. They observed that surface roughness values reduce by about 22% under MQL conditions. In addition to the MQL, cryogenic cooling is another method studied by researchers for obtaining better surface roughness values. Paul et al. [57] reported that the cryogenic cooling provides better surface integrity. At the

cutting tests of AISI 1060 steel, it was found that cryogenic cooling with LN_2 resulted in better surface roughness values up to 40% than dry machining thanks to effective cooling, preserving of tool hardness and cutting zone interactions. Umbrello et al. conducted a number of tests on hard turning of AISI 52100 steel under dry and cryogenic (LN_2) conditions. They observed that the surface roughness reduced by around 50% under cryogenic conditions as shown in Figure 1.34. In addition, they reported that the surface quality of grinding process was achieved using LN_2 during the experiments.

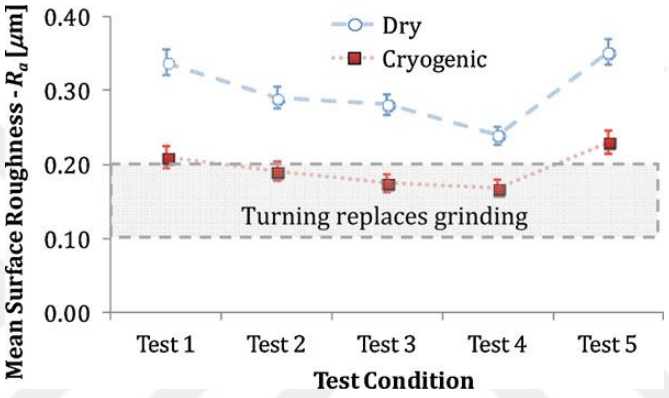

Figure 1.34 Comparison of surface roughness in dry and cryogenic hard turning of AISI 52100 steel [1]

Conventional cutting fluid is the most common cooling/lubrication strategy in the industrial area. It is easy-to-use and cheap and it does not need any extra equipment to mount to machine tools. This method also is capable of providing adequate lubrication as well as cooling. However, it is not sufficient for the hard turning operations. Thus, conventional cutting fluids cannot improve the surface quality as much as cryogenic cooling due to their limited cooling capacity. When compared to the conventional cutting fluid conditions, cryogenic cooling performs better up to 35% in terms of surface roughness as shown in Figure 1.35.

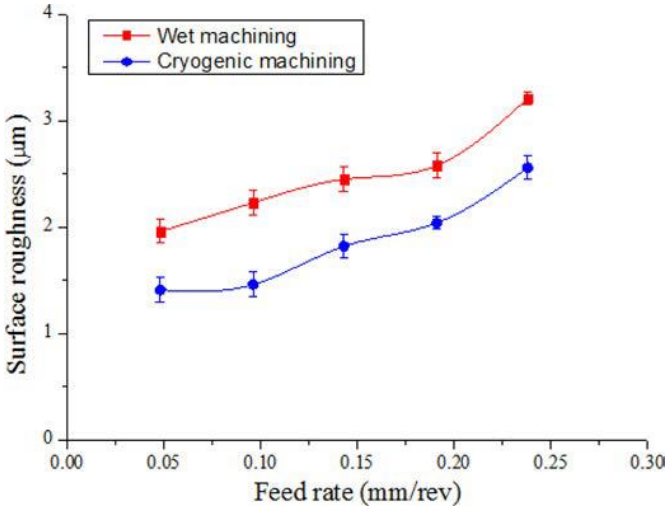

Figure 1.35 Comparison of surface roughness values under conventional cutting fluid and cryogenic conditions [109]

In the literature, some information exists about which surface roughness values reduce with the use of CO_2 as a cryogen. Pereira et al. [19] reported that the use of CO_2 improved surface roughness by around 25-30% during the hard turning of ASP23 steel (66 HRC). Authors attributed the improvements on the surface roughness to the more stable cutting conditions of cryogenic cooling with CO_2. In another study, it was revealed that the CO_2 application exhibits better performance in terms of surface roughness in comparison to dry, conventional cutting fluid and LN_2 conditions. After the tests, it was found that CO_2 application produced better surface finish by around 3–24% and 2–14% in comparison to conventional cutting fluid and LN_2 conditions respectively. These results were related to the limited tool wear that caused by increased tool hardness and decreased friction on the cutting zone during the cryogenic turning operations [99].

As another subclass of the surface integrity, subsurface phase transformations are also frequently studied by the researchers in order to improve product quality. Subsurface phase transformations take place with the effects of thermo-mechanical factors during cutting and their thicknesses might increase up to 10 μm [67]. The thermally induced phase transformations (white and dark layers) are dominant in hard turning due to excessive cutting temperatures and rapid and moderate cooling conditions. With

increasing cutting temperatures in the hard turning operations, while the white layer thickness increases, dark layer thickness decreases due to white layer thickness and position of the penetration depth [35]. Ramesh et al. carried out a study on the hard turning of AISI 52100 steel (62 HRC) and they observed that the white layer thickness and grain size increase with the increasing cutting speed from 91.4 m/min to 274.3 m/min [26]. In another study, Hosseini et al. conducted a number of experiments on hard turning of AISI 52100 steel in order to determine the effect of tool wear on the white and dark layer formations. They reported that flank wear has a significant impact on the white layer formation as well as the cutting speed. In addition, it was observed that white and dark layer thickness can increase up to 3±1 μm and 10±2 μm respectively due to dominant effect of flank wear that leads to thermomechanical alterations [69].

Since white and dark layers take place by excessive cutting temperatures generated during the hard turning process, cryogenic cooling can be a solution in order to minimize or to eliminate these layers. Therefore, several studies were conducted on cryogenic turning of hardened steels in the literature. Umbrello et al. [36] conducted a study on hard turning of AISI 52100 steel (56.5 HRC) in order to reveal the relationship between the cryogenic cooling and subsurface phase transformations. At the end of experimental study, the authors reported that white layer thickness values range between 3.2-6.57 μm under the dry conditions and these values lower below the 1 μm with the use of LN_2. In another study on hard turning of AISI 52100 steel (54-61 HRC), Umbrello et al. [1] examined the effect of cryogenic cooling (LN_2) on the white layer formation and they observed that a significant decrease in white layer ticknesses was achieved using cryogenic cooling as shown in Figure 1.36.

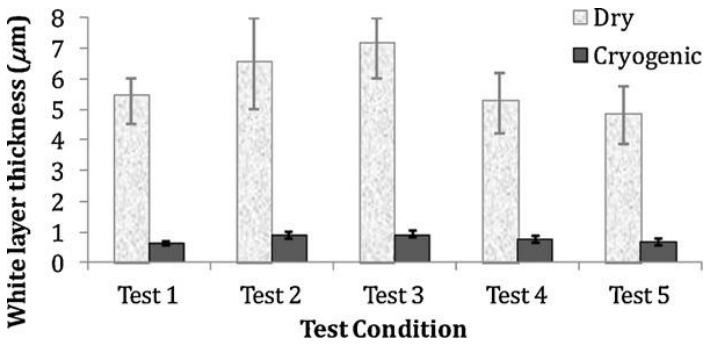

Figure 1.36 Effect of cryogenic cooling on the white layer thicknesses [1]

Authors reported that the higher white layer thicknesses under dry conditions can be attributed to the higher cutting temperatures and localized thermal softening of the workpiece material. As shown in Figure 1.36, white layer thicknesses lower down to below 1 μm after the cryogenic machining while they reach up to 5-8 μm under the dry conditions. Cryogenic cooling also produces better subsurface than conventional cutting fluid conditions as well as dry conditions due to their insufficient cooling conditions. In this context, Sivaiah et al. [109] conducted several turning experiments on 17-4 PH stainless steel under wet and cryogenic (LN_2) conditions. At the end of the tests it was found that cryogenic cooling performs better significantly in terms of white layer thickness in comparison to conventional cutting fluid conditions as shown in Figure 1.37.

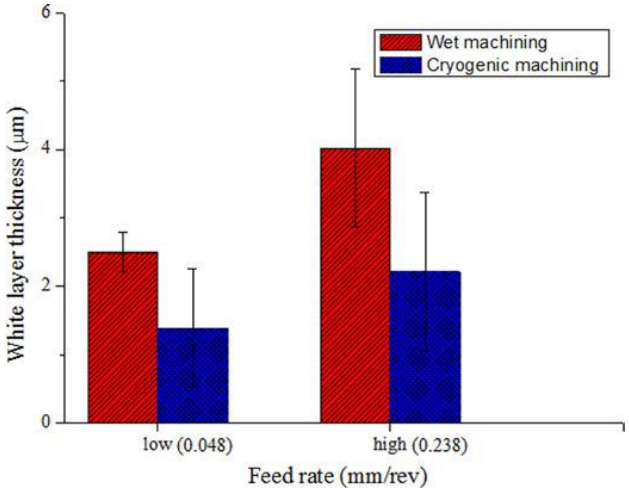

Figure 1.37 White layer thickness values under wet and cryogenic conditions [109]

The residual stresses (tensile stresses) play an important role in premature fatigue crack initiation negatively affecting service life of any machine element and they considerably increase with increasing cutting temperatures [68]. On the other hand, compressive residual stresses in surface and subsurface of the workpiece material are requested for longer fatigue life of the machinery elements. Unlike grinding, hard machining produces compressive residual stresses which serve longer fatigue life. Umbrello et al. [35] reported that both axial and circumferential (hoop) compressive residual stresses increase with increasing cutting temperatures. They also stated that the highest residual stresses develop at the transition region between the white and dark layer. In another study, Revel et al. [37] observed that the cutting speed (and the cutting temperature) have a great influence on the residual stress formation and distribution in hard turning of the AISI 52100 bearing steel (61 HRC). In addition, they reported that in case of increasing cutting speed, residual stresses turn into higher compressive stresses as shown in Figure 1.38.

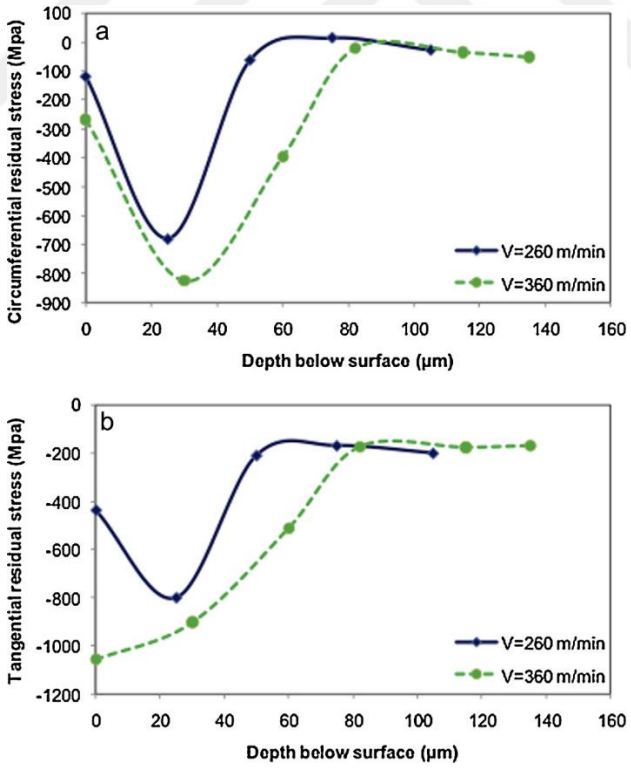

Figure 1.38 Influence of the cutting speed on the circumferential and tangential residual stresses [37]

In order to investigate the effects of cryogenic cooling on residual stresses, Umbrello et al. [1] conducted some hard turning tests on AISI 52100 steel (61 HRC) and they found that the use of LN_2 reduces residual stresses by around 20% as shown in Figure 1.39. Authors have concluded the lower residual stress values of the cryogenic machining to the effective cooling and lower white layer formations.

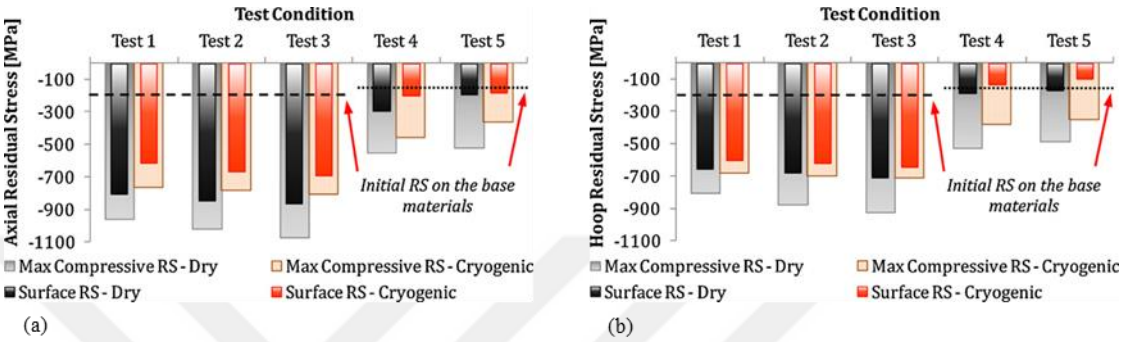

Figure 1.39 (a) Axial and (b) hoop residual stresses under dry and cryogenic conditions [1]

In the light of the literature review, it is possible to say that low cutting performance and product quality can be observed due to excessive cutting temperatures in hard machining processes. On the other hand, it is clearly stated that the appropriate cooling/lubrication strategy significantly improves the product quality and tool life. In addition to the cooling/lubrication methods mentioned above, an additional technique which provides an efficient cooling and lubrication is increasingly gaining more importance in the literature due to its beneficial properties. Hybrid cooling/lubrication or CryoMQL is a new and effective method which combines the cryogenic cooling and MQL technique. Due to simultaneous efficient usage of lubrication and cooling effects of MQL and cryogens, this method becomes more common recently in the literature. Although there are some research works on hybrid machining of Ti6Al4V alloy [94], AISI 304 steel [62] and Inconel 718 [93,95] in the literature but it is not possible to observe any study on hard machining.

Within this scope, Pusavec et al. [95] conducted a comprehensive research that compares cooling/lubrication methods according to tool wear and surface roughness. In this study, authors performed several turning experiments on Inconel 718 as a

workpiece material and they observed that the hybrid cooling performs better than other cooling/lubrication techniques in terms of tool wear and surface roughness values due to the combined effect of effective cooling and lubrication of hybrid cooling as shown in Figure 1.40 and Figure 1.41 respectively.

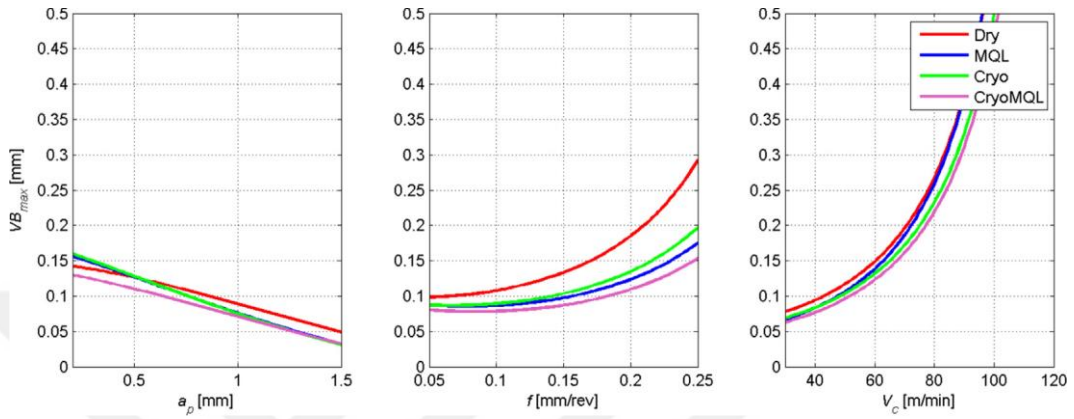

Figure 1.40 Effects of dry, MQL, cryo and cryoMQL conditions on the flank wear [95]

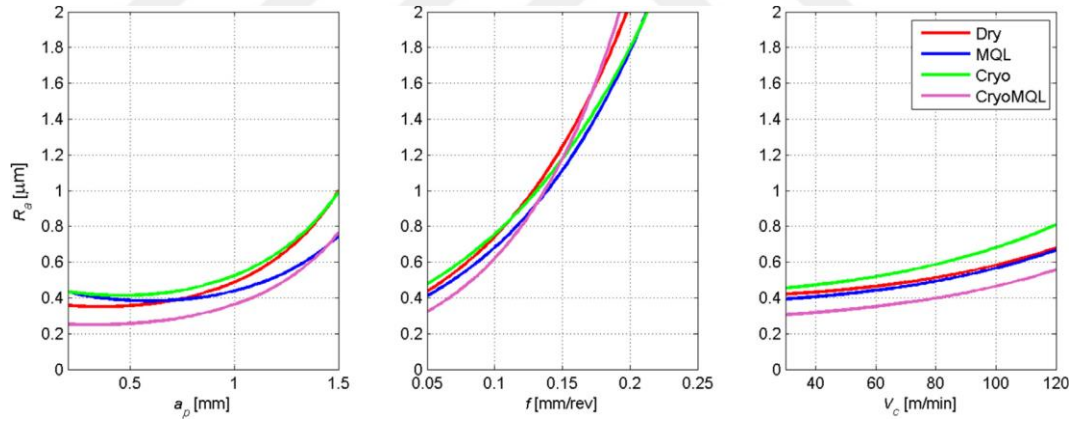

Figure 1.41 Effects of dry, MQL, cryo and cryoMQL conditions on the surface roughness [95]

1.6 Aim of this Study

The aim of this study is to investigate the effect of different cutting conditions in the hard turning of AISI 52100 bearing steel on tool wear and surface integrity. In this context, five cooling/lubrication strategies were studied; dry, wet, MQL, MQL+CO_2 and MQL+LN_2. Under these conditions, coolants and/or lubricants were applied

through the tool holder and cryogens were sprayed from an external nozzle as a precooling method. In addition to the cutting conditions, two different insert geometries were selected as conventional and wiper insert geometries that directly influences surface quality. As a result, combined effect of cutting tool geometry and cutting conditions were observed in terms of not only tool wear but also surface integrity. Novel aspects of this study can be listed as follows;

- Pre-cooling based hybrid conditions (MQL+CO_2, MQL+LN_2) are applied for the first time in the literature to a hard turning process of AISI 52100 bearing steel in which both conventional and wiper inserts are employed.
- Performance of both conventional and wiper CBN inserts under different cooling/lubrication conditions in terms of tool wear and surface integrity (surface roughness, residual stress, white/dark layer formations) is discussed in detail.
- Low (CO_2, -78 °C) and very low temperature cryogens (LN_2, -196 °C) are employed in the hybrid conditions to determine the effects of pre-cooling level on performance criteria.

CHAPTER 2

EXPERIMENTAL SETUP AND PROCEDURE

In this chapter, experimental set-up employed for the tests under different cutting conditions (dry, wet, MQL, cryogenic and hybrid), and measurement and evaluation methods used for the performance criteria such as tool wear, cutting forces, surface roughness, residual stresses, and subsurface phase transformations (white and dark layers) are discussed in detail. Schematic illustration of performance criteria and their measurement methods is shown in Figure 2.1.

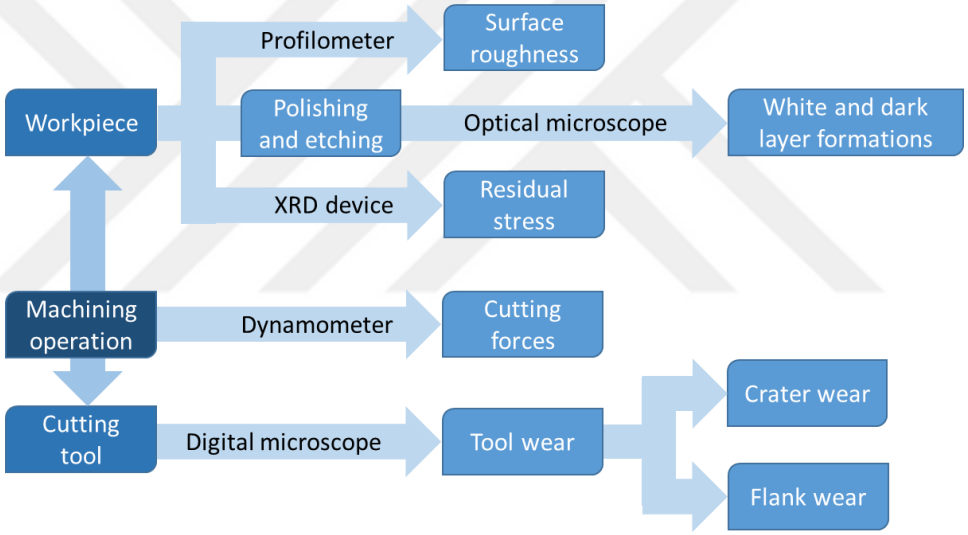

Figure 2.1 Schematic illustration of performance criteria and their measurement methods

2.1 Workpiece Material

AISI 52100 bearing steel (100Cr6) was selected as workpiece material due to its common usage in the industrial area. AISI 52100 steel is a very suitable material for production of bearings owing to its balanced chemical composition, and good physical and mechanical properties. Besides, this steel can be hardened up to 64 HRC using a proper heat treatment procedure. As a result, AISI 52100 steel is mostly preferred in bearing industry due to its higher hardenability, corrosion resistance and wear

resistance. The chemical composition and some physical and mechanical properties of AISI 52100 steel are given in Table 2.1 and Table 2.2 respectively. In addition, the effects of its alloying elements on the steel are also represented in Table 2.1

Table 2.1 The chemical composition of AISI 52100 steel and the effects of its alloying elements on the steel [20,110–112]

Alloying element	Allowed percentage	Effect
Carbon (C)	0.98 - 1.1	Principal hardening element
Manganese (Mn)	0.25 - 0.45	Strong hardening element, deoxidizer
Phosphorus (P)	< 0.025	Increases tensile strength, generally considered as impurity
Sulphur (S)	< 0.025	Improves machinability
Silicon (Si)	0.15 - 0.3	Deoxidizer
Chromium (Cr)	1.3 - 1.6	Increases hardenability, abrasion resistance, heat resistance and corrosion resistance
Nickel (Ni)	0.3	Improves toughness, hardenability and corrosion resistance
Copper (Cu)	0.3	Provides corrosion resistance. Occasionally, used for hardening

Table 2.2 Some physical and mechanical properties of hardened AISI 52100 [20,111]

Hardness	Young modulus	Density	Melting point	Thermal conductivity	Specific heat
60 - 67 HRC	190-210 GPa	7.81 g/cm^3	1424 °C	46.6 W/mK	458 J/KgK

In the study, two different type workpieces with diameters of 40 mm were prepared by taking into consideration the tool wear and surface integrity measurements. A group of the short ones with length of 75 mm were machined in accordance with maximum capacity of the XRD device for residual stress measurements. A number of the long ones with length of 250 mm were also machined to obtain consistent results from the tool wear tests. Besides, axial through holes with diameters of 20 mm were drilled on all specimens in order to obtain a homogeneous hardness value throughout a workpiece material. The workpiece dimensions are shown in detail in Figure 2.2. In addition, for rigid clamping of short and long workpieces between a chuck and tailstock, a large chamfer of 8.66 mm×30° was created on the one edge of the axial hole. For this

purpose, a custom-designed tailstock was manufactured. The detailed dimensions of the tailstock are shown Figure 2.3.

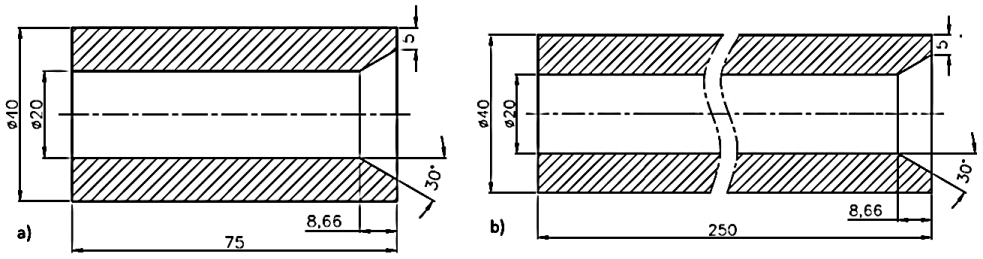

Figure 2.2 Detailed dimensions of the workpiece materials prepared for (a) surface integrity and (b) tool wear

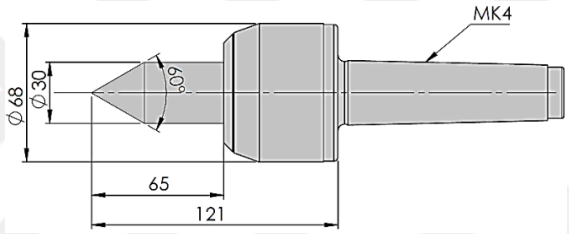

Figure 2.3 The tailstock and its dimensions used in the tests

Even though the AISI 52100 bearing steel has a ductile structure prior to the heat treatment, it can be hardened up to 64 HRC with a proper heat treatment procedure as mentioned above [113]. In this study, the bearing steel specimens were hardened to 62 HRC using the appropriate heat treatment procedure. Firstly, specimens were austenitized at 845 ℃ for 40 minutes. Then, they were quenched within a water/salt bath. As a final process, specimens were tempered at 195 ℃ for 90 minutes in order to reduce internal stresses and martensite brittleness.

2.2 Experimental Setup and Cutting Conditions

The tests were conducted using HAAS ST-20Y CNC lathe which is suitable for hard turning operations due to its highly rigid structure and adequate machining power (15kW). The experimental setup used for the hard turning of AISI 52100 bearing steel is shown in Figure 2.4.

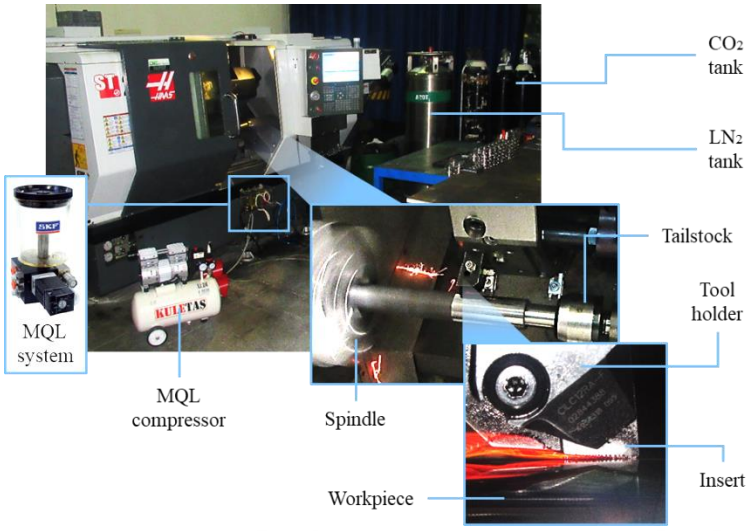

Figure 2.4 Experimental set-up

As mentioned earlier, the effects of tool geometry (conventional and wiper inserts) and cooling and/or lubrication conditions (dry, wet, MQL, cryogenic and hybrid) on tool wear and surface integrity were experimentally investigated in hard turning of AISI 52100 bearing steel in this study. Therefore, cutting speed, feed and depth of cut values were kept constant during all experiments. These values were determined in accordance with literature studies and tool manufacturers' catalogues (Table 2.3).

Table 2.3 Cutting parameters

Cutting speed (Vc)	Feed (f)	Depth of cut (a_p)	Cutting distance	
			250 mm specimen	75 mm specimen
200 m/min	0.1 mm/rev	0.1 mm	5596.119 m	75.021 m

As shown in Table 2.3, cutting distances for the specimens used for tool wear and surface integrity studies are different from one another. It is considered adequate to perform turning operations on the short specimens at a cutting distance of 75.021 m (machining time of 22.5 seconds) for the surface integrity evaluations. This machining distance was considered enough for the mechanical and thermal steady state condition of experiments [36]. On the other hand, in consequence of preliminary tests conducted to obtain the comparable flank wear and crater wear, it is found to be sufficient a cutting distance of 5596.119 m (machining time of 28 minutes) for the tool wear assessments.

2.3 Tool Holder and Cutting Inserts

PCLNR 2525M12 JET tool holder with internal passageways for effective cooling and/or lubrication during the cutting was used. This tool holder have three nozzles with diameter of 1 mm. Two nozzles are directed to the rake face while the other nozzle is oriented to the flank face of the cutting tool. During the tests, conventional cutting fluid and MQL oil were applied to cutting zone by means of the tool holder with internal passageways as shown in Figure 2.5. Additionally, the dimensions of the tool holder are illustrated at the Figure 2.6.

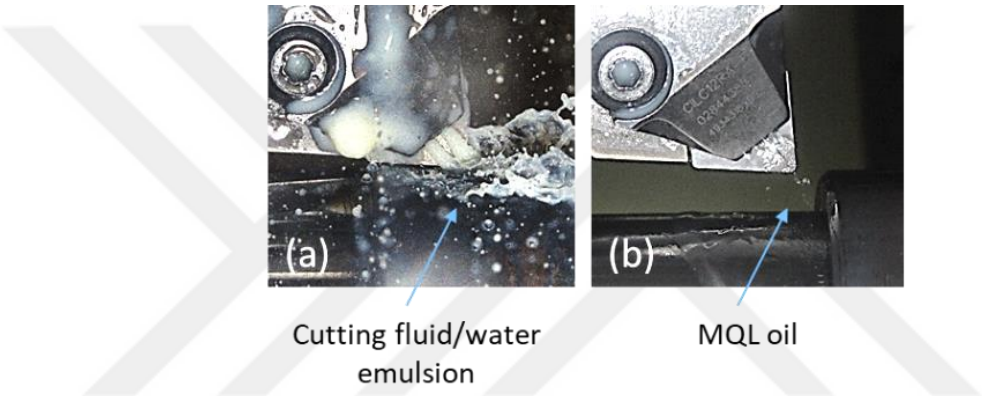

Figure 2.5 Cutting fluid application through the tool holder; (a) conventional cutting fluid and (b) MQL oil

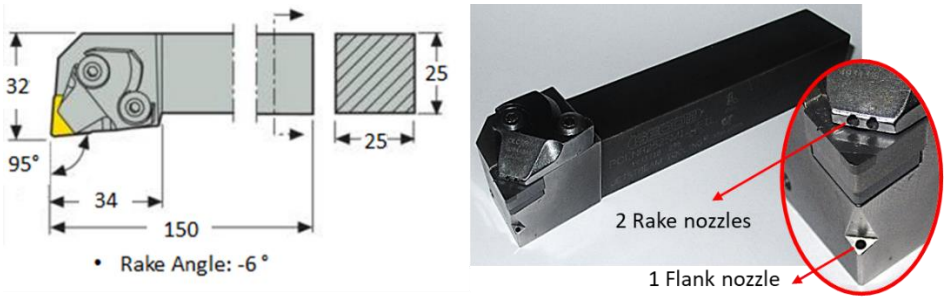

Figure 2.6 Dimensions of PCLNR 2525M12 jet tool holder

During the tests, the PCBN (Polycrystalline Cubic Boron Nitride) cutting tools with two different geometries (conventional and wiper) produced by SECO tools were employed. The CBN inserts (Secomax CBN010) have low CBN content (50% CBN)

with average grain size of 1.5-2 µm in the TiC (Titanium carbide) binder. Low CBN content cutting tools were preferred due to being more suitable for finish operations [65]. The dimensions and some properties of CBN inserts are shown in Table 2.4.

Table 2.4 The dimensions and some properties of CBN inserts

	Wiper insert CNGA 120408S-01020-1WZB	Conventional insert CNGA 120408S-01020-L1-B
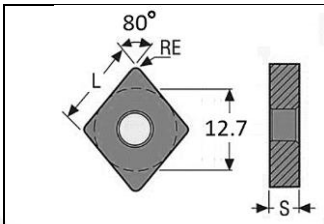	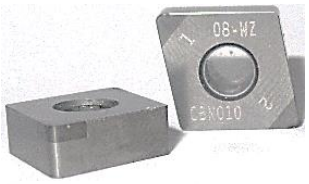	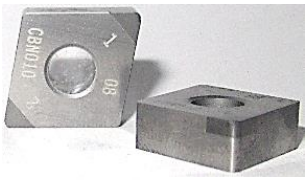
Wiper edge length	0.8 mm	None
Number of cutting edge	2	
Insert included angle	80°	
Theoretical cutting edge length (L)	12.9 mm	
Cutting edge effective length	3.4 mm	3.6 mm
Nose radius (RE)	0.8 mm	
Insert thickness (S)	4.78 mm	
Cutting edge chamfer	0.1 mm x 20°	

2.4 Cooling and/or Lubrication Conditions

The tests were conducted under dry, wet (conventional cutting fluid), MQL, external cryogenic and hybrid (MQL+cryogen) conditions (Figure 2.7) in order to reveal the effects of cooling and/or lubrication conditions on cutting performances of conventional and wiper inserts in hard turning of AISI 52100 bearing steel.

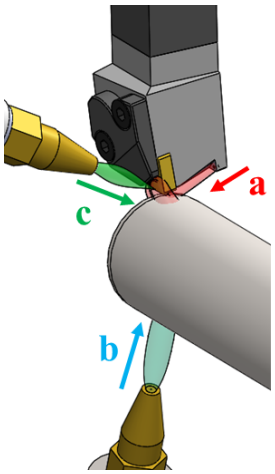

Method	Coolant	Application	
Wet	Semi-synthetic cutting fluid	Internal	a
MQL	Biodegradable oil mist	Internal	a
Cryogenic	LN_2 CO_2	External	c
Hybrid	Biodegradable oil mist	Internal	a
	LN_2 CO_2	External (Precooling)	b

Figure 2.7 Cutting conditions

2.4.1 Conventional Cutting Fluid

The conventional cooling fluid employed during the tests consists of a mixture of water of 95% and semi-synthetic cutting fluid (ISOPAL 6018) of 5%. As shown in Figure 2.8, conventional cutting fluid was applied to both flank and rake faces of the cutting inserts via internal passageways of the tool holder at a pressure of 8 bar in order to provide effective cooling and lubrication.

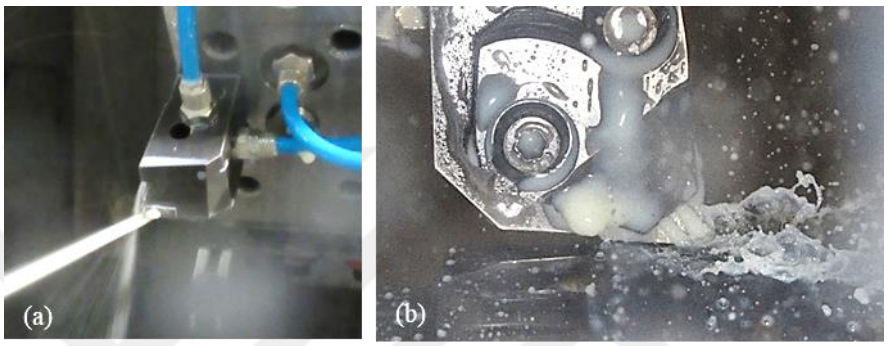

Figure 2.8 Conventional cutting fluid application from (a) tool holder and (b) during the machining operation

2.4.2 Minimum Quantity Lubrication

During the tests, a SKF VectoLub VE1B MQL system with two micro-pumps were used and SKF LubriOil (Fatty Acid Ester based) biodegradable oil as a lubricant were sprayed onto the cutting zone via the passageways of the tool holder at a pressure of 5.5 bar and a flow rate of 0.001 l/min. MQL system and its components employed in this study are shown in Figure 2.9. Spraying of the mixture of the pressurized air and oil droplets from tool holder nozzles onto the cutting zone is illustrated in Figure 2.10.

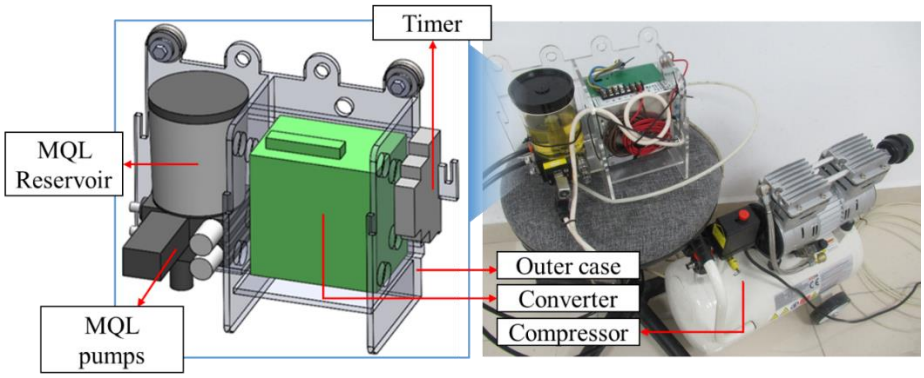

Figure 2.9 MQL system

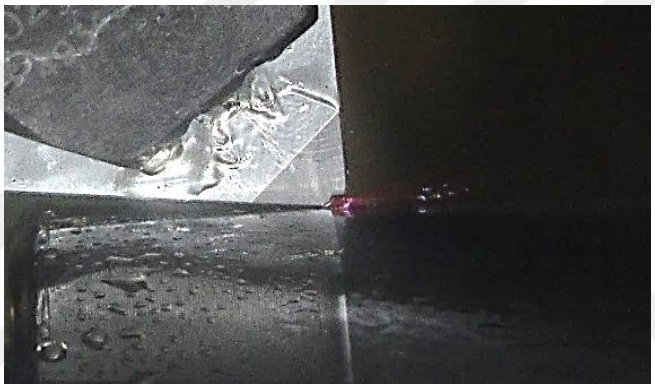

Figure 2.10 Spraying of the mixture of the pressurized air and oil droplets from tool holder nozzles

2.4.3 Cryogenic Cooling

During the tests, cryogenic cooling was performed using two different cryogens; LN_2 (Liquid nitrogen) and CO_2 (Carbon dioxide). Application conditions of these two cryogens are different from each other. While LN_2 was sprayed at -196°C and 15 bar, CO_2 was applied at -78.5°C and 54 bar during the tests.

During the hard turning tests, cryogens were directly delivered onto cutting zone by means of an external nozzle with diameter of 0.5 mm. The nozzle position in external cooling method is shown in Figure 2.11.

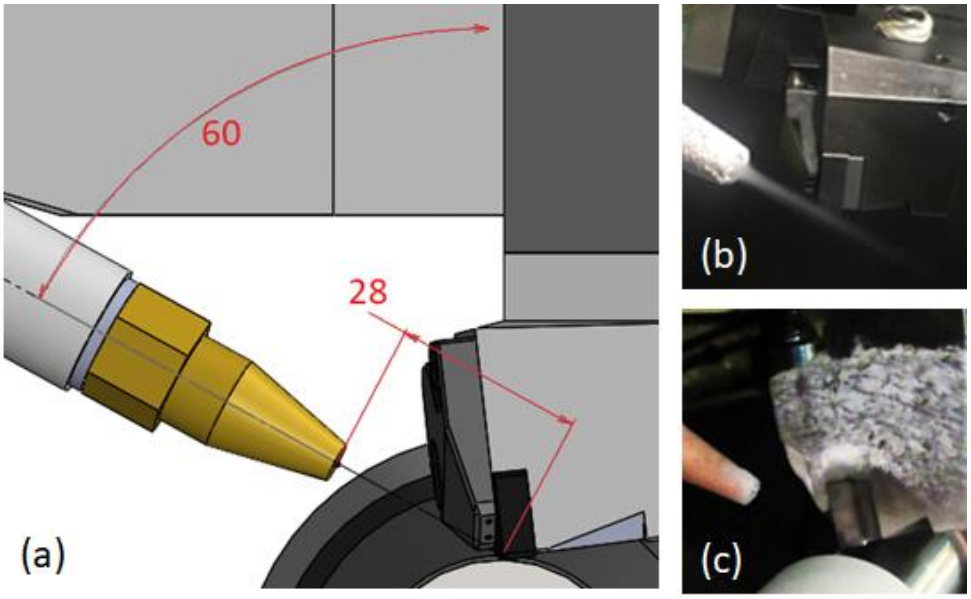

Figure 2.11 Application of cryogenic cooling with (a) an external nozzle of (b) LN_2 and (c) CO_2

After a stable gas flow was provided, the cryogens were applied to the cutting zone during the turning processes.

2.4.4 Hybrid Conditions

The effective cooling and lubrication condition newly employed in this study is hybrid conditions which basically combines the MQL and cryogenic cooling. With the use of this cutting condition, it is aimed to ensure both effective cooling and lubrication. In this method, the mixture of pressurized air and MQL oil were applied onto cutting zone via passageways of the tool holder while cryogens were directed onto workpiece material for precooling purposes by means of an external nozzle. Precooling method was selected in order to prevent an extra embrittlement of CBN inserts due to excessive cooling capacities of the cryogens. As a result, MQL was applied directly to the high friction zones (tool-chip and tool-workpiece interfaces) while cryogens were applied to the opposite side of the cutting zone to minimize extreme temperatures generated during the hard turning as shown in Figure 2.12. In this way, embrittlement and premature failure risks of CBN inserts was minimized. Hybrid conditions with two different cryogens are shown in Figure 2.13

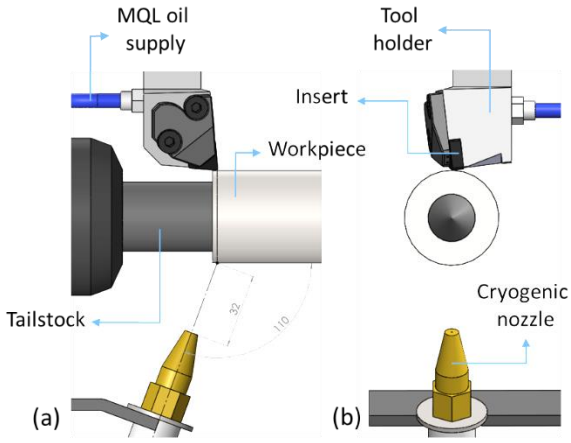

Figure 2.12 A schematic representation of hybrid conditions; (a) front and (b) side views

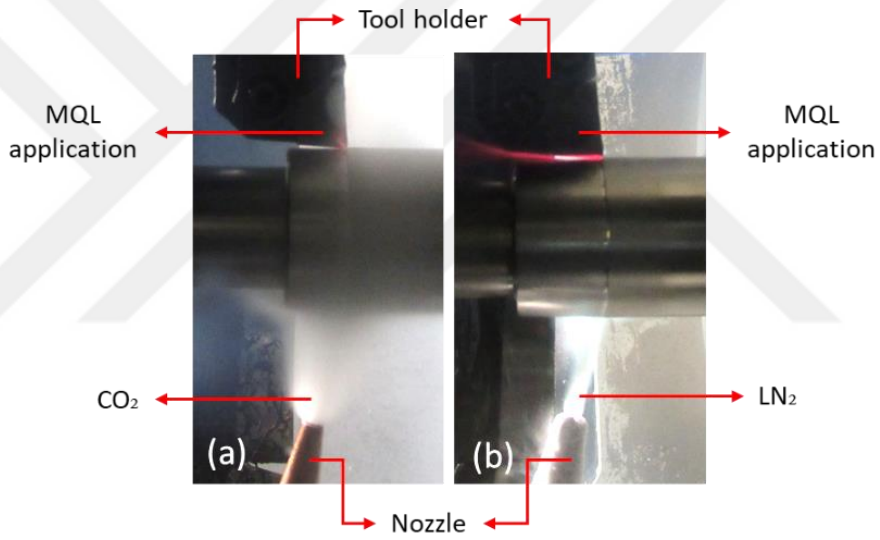

Figure 2.13 Hybrid conditions; (a) CO_2 and (b) LN_2.

2.5 Measurement Techniques

At the end of the tests, several measurements were performed in order to evaluate cutting performance of conventional and wiper inserts in terms of tool wear and surface integrity. These measurements can be examined under two different subjects. One of them is tool wear (flank wear and crater wear) and another one also is the surface integrity including surface roughness, white/dark layer formations and residual stresses.

2.5.1 Tool wear

Tool wear tests were conducted on hardened AISI 52100 bearing steel at a certain cutting distance of 5596.119 m. Flank wear was directly measured by using a Dino-Lite digital microscope with magnification capacity up to 250X . Maximum flank wear (VB_{Bmax}) on the inserts were evaluated as a flank wear due to its non-uniform bandwidth. Non-uniform structure and measurement method of the flank wear are illustrated in Figure 2.14.

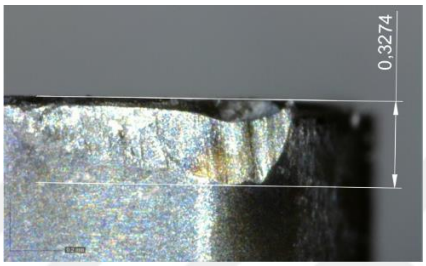

Figure 2.14 Measurament of flank wear formation

As mentioned in earlier sections, crater wear can be characterized by its depth or area. In this study, the magnitude of crater wear was defined by its area because tool-chip contact distances on rake faces of conventional and wiper inserts are different from one another. To determine crater wear area, rake face images of cutting inserts were captured under a Dino-Lite digital microscope and then the captured images were exported into AutoCAD software. Thanks to this CAD software, the crater wear area was precisely measured as shown in Figure 2.15.

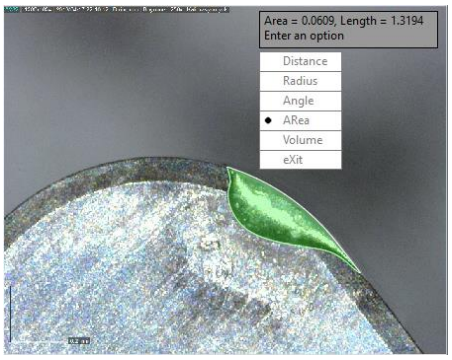

Figure 2.15 Measurement of crater wear area by using AutoCAD software

Additionally, for better understanding of the wear types and mechanisms on cutting inserts, the SEM images were taken using JEOL–JSM–6060 LV SEM device as shown in Figure 2.16.

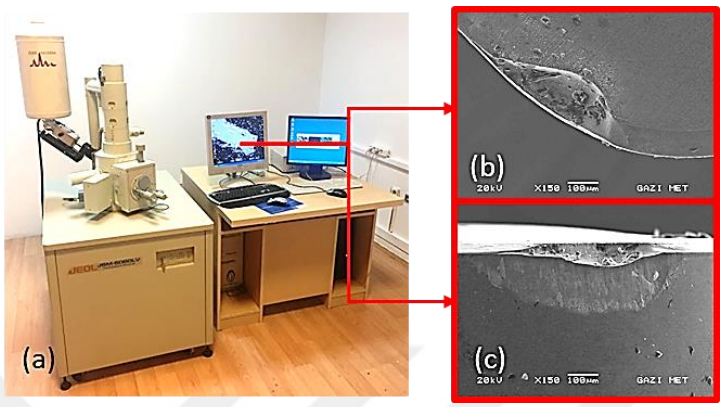

Figure 2.16 SEM measurements by using (a) JEOL–JSM–6060 LV SEM device and the wear formations; (b) crater wear, (c) flank wear

2.5.2 Cutting Forces

In a turning process, cutting force is one of the most important indicators for the machinability of engineering materials. Therefore, three components of cutting forces (tangential force, thrust force and radial force) were measured during the hard turning operations of conventional and wiper cutting tools under only dry conditions. The cutting forces were measured using a Kistler 9257B multi-component dynamometer as shown in Figure 2.17.

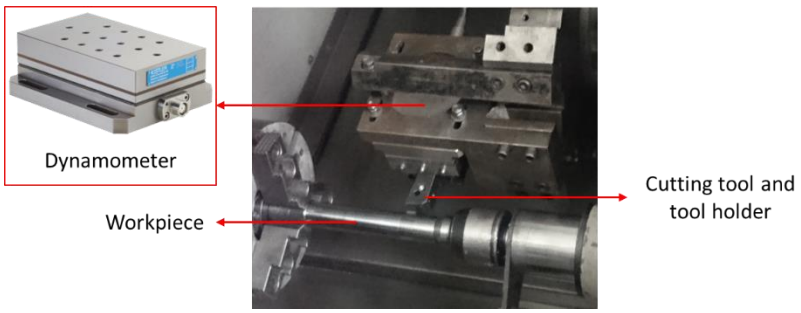

Figure 2.17 Cutting force measurements

The dynamometer was connected to the Kistler Type 5070A multichannel charge amplifier and the measurement results were evaluated using Dynoware software. Technical specifications of the dynamometer and the amplifier are given in the Table 2.5.

Table 2.5 Technical specifications of the dynamometer and the amplifier



Kistler 9257B Multi-Component dynamometer

Range	Fx, Fy, Fz	kN	-5 ... 5
	Fz for Fx and Fy ≤ 0.5 Fz	kN	-5 ... 10
Threshold		N	<0.01
Sensitivity	Fx, Fy	pC/N	≈ -7.5
	Fz	pC/N	≈ -3.7
Natural frequency	Fn (x,y,z)	kHz	≈ 3.5
	Fn(x,y)	kHz	≈ 2.3
	Fn(z)	kHz	≈ 3.5
Weight		kg	7.3
Clamping area		mm	100x170
Connection			Fischer flange 9 pole



Kistler Type 5070A multichannel charge amplifier

Number of channels		8
Connector		Fischer flange 9 pole
Measuring range	pC	200 ... 200000
Frequency range	kHz	≈ 0 ... > 45
Output voltage	V	± 10
Voltage	V AC	100 ... 240
Interface		RS 232C

2.5.3 Surface integrity

In this study, surface integrity was examined in terms of surface roughness, residual stresses and white/dark layer formations. They inherently require different measurement techniques and devices, and specimen preparations. These measurement procedures will be explained in detail in the following sections.

2.5.3.1 Surface Roughness

Surface roughness values of the machined surfaces were measured using a Taylor Hobson Talysurf PGI 1230 profilometer in the Ortadoğu Rulman Sanayi Inc. (Figure 2.18).



Figure 2.18 Taylor Hobson Talysurf PGI 1230 profilometer

As the surface roughness values, Ra (average roughness) and Rz (average maximum height of the profile) values were measured by one scanning along full length (approximately 50 mm) of a machined surface.

2.5.3.2 White and Dark Layer

The specimens must be properly cut, ground, polished and etched before microscopic examinations to clearly observe the white and dark layer formations. In this context, proper small pieces were cut from the machined parts using wire electro discharge machine (Wire EDM) and these pieces were embedded into the bakalite. Then, every piece was ground by means of sandpapers with grit sizes of 320, 400, 600, 800 and 1000. After the grinding with sandpapers, specimens were subjected to a final polishing process by using a suspension containing diamond abrasive particles with a grit size of 3 μm. This process was repeated until the scratches disappeared on the surface. As final process, prior to microscopic examinations, specimens were etched within a solution of 5% nitric acid and 95% alcohol for 6 seconds. After these processes, white and dark layer thicknesses were measured under Nikon ECLIPSE MA100 microscope as shown in Figure 2.19.

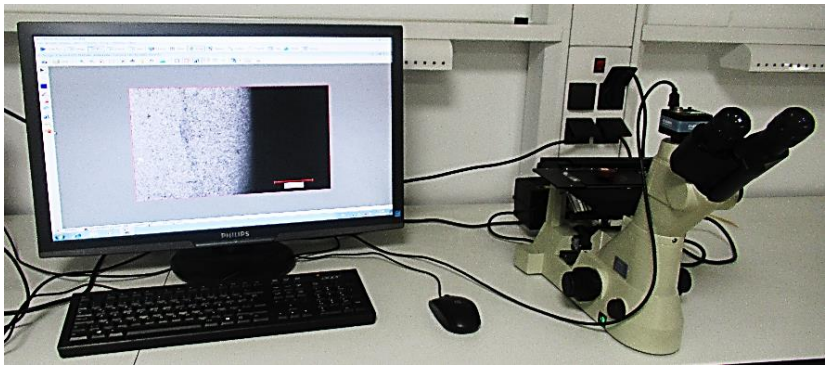

Figure 2.19 White and dark layer observations under the Nikon ECLIPSE MA100 optical microscope

2.5.3.3 Residual Stress Measurements

Residual stresses are the one of the most important subtitles of the surface integrity and strongly related to the cutting conditions and tool geometry. Due to the different cutting forces acting on workpiece material in feed and cutting directions, the residual stresses may change according to directions and magnitudes of forces and may significantly affect the fatigue life of the machinery elements. Therefore, both hoop (in cutting direction) and axial (in feed direction) residual stresses were measured by depending on depth. The residual stress measurements were performed using the parameters in Table 2.6 on a Seifert XRD 3003 PTS XRD device (Figure 2.20) in the Ortadoğu Rulman Sanayi Inc.

Table 2.6 X-Ray diffraction parameters

X-Ray radiation	Cr-K α
Bragg angle (2Θ)	≈ 156°
Lattice plane	{2 1 1}
Number of Ψ angles (±40°)	5
Collimator diameter	1.5 mm
Filter type at the detector	Vanadium
Measurement type	Continuous
Detection methods	Parabolic and C.O.G. (Center of gravity)

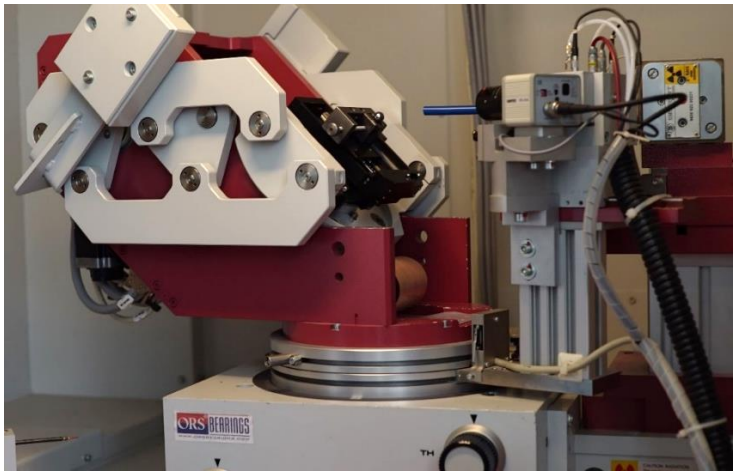

Figure 2.20 Seifert XRD 3003 PTS

CHAPTER 3

RESULTS AND DISCUSSION

In this chapter, the effects of different cooling and/or lubrication strategies on the cutting performances of conventional and wiper CBN inserts in hard turning of AISI 52100 bearing steel are discussed in detail. The performance evaluations are conducted in terms of several parameters such as tool wear, cutting forces, surface roughness, residual stresses and subsurface phase transformations. The test results are evaluated in two sections. The first section presents the tool wear and surface integrity results for conventional and wiper inserts under dry, wet, MQL and hybrid conditions. In the second section, surface integrity results (surface roughness and residual stresses) as the performance criteria for conventional and wiper CBN inserts under external cryogenic cooling and hybrid conditions are presented. The cutting forces for conventional and wiper inserts during the hard turning process under only dry conditions are measured to determine the magnitudes of the three force components and their effects on performance criteria are discussed at beginning of this section.

3.1 Cutting Forces

Cutting forces are one of the indicators that dramatically influence the tool wear and surface integrity. Therefore, feed force (F_f), main cutting force (F_c) and passive force (F_r) were measured using both wiper and conventional cutting inserts to observe the effects of cutting forces on hard turning process under only dry conditions. As shown in Figure 3.2 and Figure 3.3, the highest force component measured for both conventional and wiper inserts is radial force (passive force). It is well-known that main cutting force is the highest force component in conventional turning operations of work materials (especially steels) in an unhardened state in which depth of cut value is larger than a cutting insert nose radius. However, this case is different in a hard turning. In case of being depth of cut value smaller than a cutting insert nose radius as

in many hard turning processes, the passive force is maximal. Both cases are illustrated in Figure 3.1.

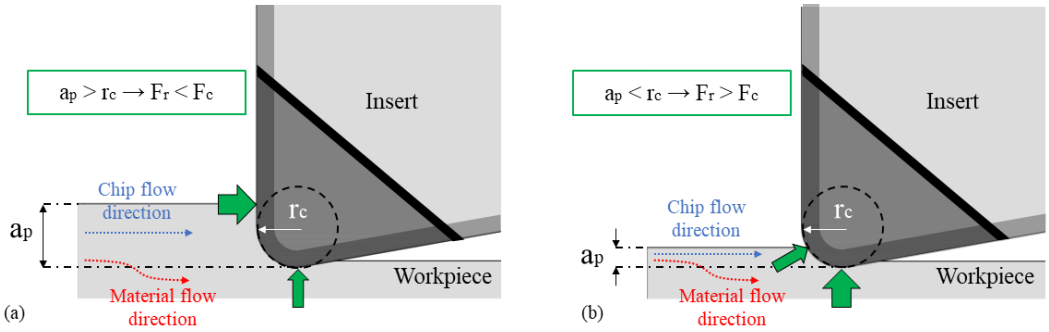

Figure 3.1 Effect of (a) high and (b) small cutting depth values on the cutting forces

Besides, larger negative rake angles (Figure 3.8) is another factor affecting the passive force significantly [38]. It is determined that the magnitudes and trend lines of force components are in a good agreement with the literature studies [5,114].

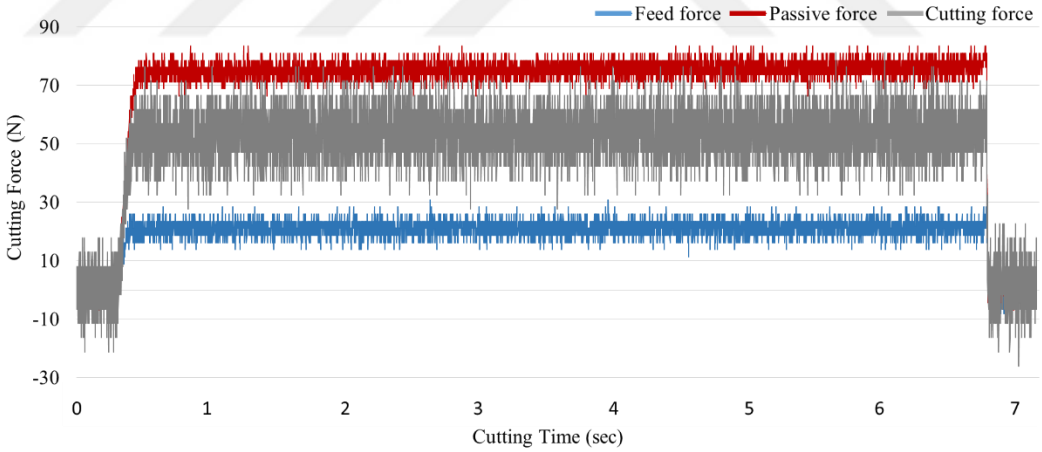

Figure 3.2 The variations of cutting forces depending on the time for a conventional insert under dry conditions

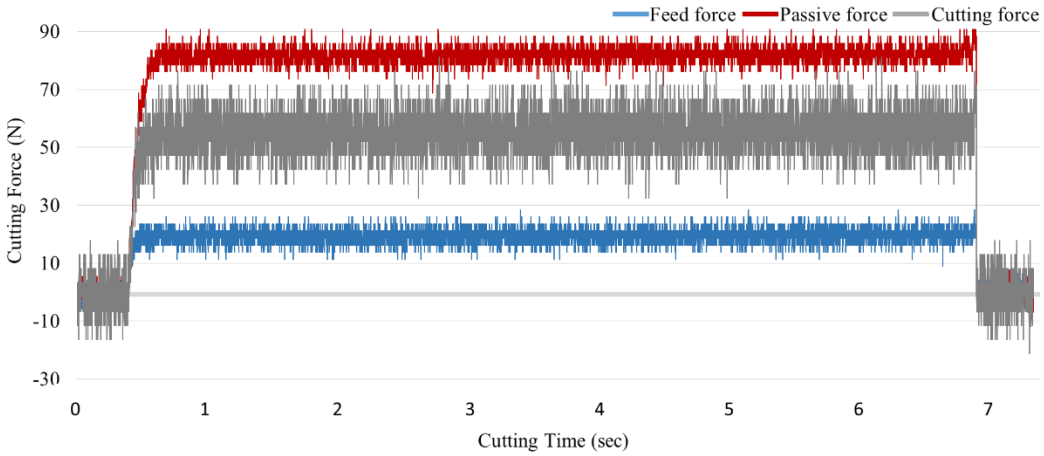

Figure 3.3 The variations of cutting forces depending on the time for a wiper insert under dry conditions

The average values of cutting forces measured during hard turning of AISI 52100 bearing steel are given in Figure 3.4. The first remarkable point in Figure 3.4 is that main cutting and passive force components in the hard turning process are significantly lower than ones in the conventional turning process. This case can be explained with low depth of cut (0.1 mm) and feed (0.1 mm/rev) values in the hard turning process unlike the conventional turning process.

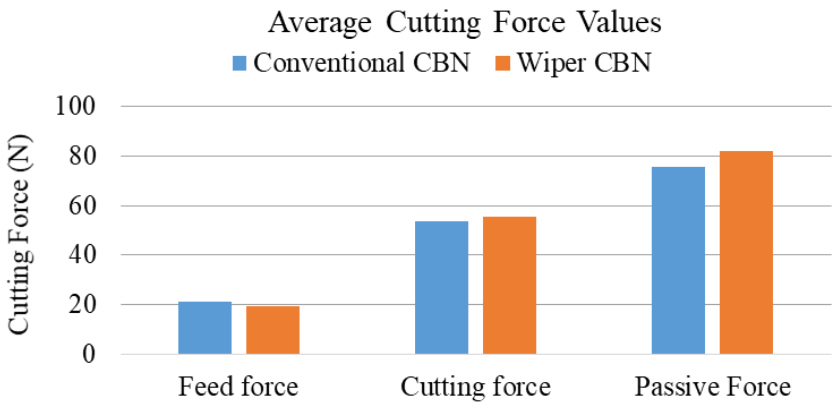

Figure 3.4 Cutting force values for conventional and wiper inserts under dry conditions

Main cutting force and passive force values for the conventional inserts are 53.78 N and 75.51 N respectively while ones for wiper inserts are measured as 55.25 N and 81.8 N. This corresponds to the increases of 2.7% and 8.3% in main cutting and passive forces respectively. Due to the wiper and conventional insert geometries, they are subjected to different friction conditions at the tool-chip and tool-workpiece interfaces. In this context, rectilinear cutting edges of the wiper inserts different from conventional inserts increases rubbing on flank face and rake face [107]. This also leads to the increases in passive and main cutting forces due to the increasing frictions at the tool-chip and tool-workpiece interfaces. In case of the feed force, force values for wiper and conventional inserts were measured as 21.26 N and 19.39 N, respectively. As a result, there is a decrease of 8.8% in feed force generated by wiper inserts in comparison to conventional inserts. It is well-known that tool-workpiece contact distances in axial (feed) direction for both conventional and wiper inserts are equal to one another due to large nose radii (0.8 mm) of cutting inserts and very low depth of cut (0.1 mm) values. The higher frictions on rake face and end flank face of wiper inserts lead to higher temperatures. This also makes the chip formation easy due to thermal softening effect and reduces feed force values.

3.2 Surface Roughness

Surface roughness is one of the most important indicators of part quality significantly affected by the cutting tool geometry and cutting conditions. In this study, both Ra and Rz values were measured in order to perform a comprehensive evaluation on the surface qualities of the workpieces in hard turning of AISI 52100 steel using conventional and wiper inserts under dry, wet, MQL and hybrid conditions. Ra and Rz results for conventional and wiper inserts are shown in Figure 3.5.

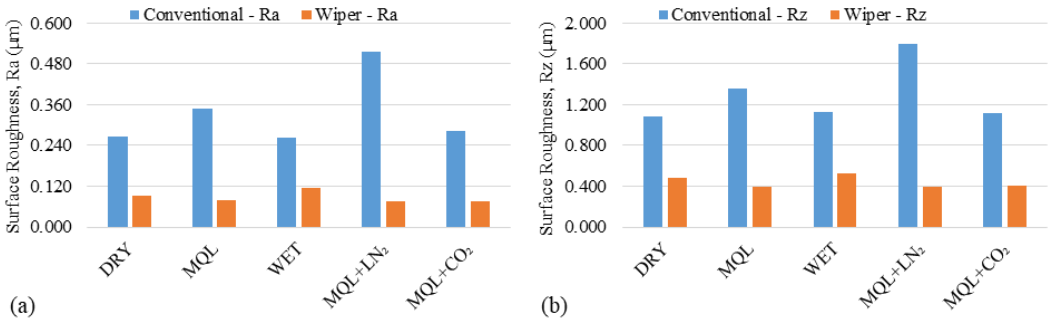

Figure 3.5 Surface roughness values measured under different cooling/lubrication conditions; (a) Ra and (b) Rz

When analyzed Ra and Rz values in Figure 3.5 in terms of tool geometry, the wiper inserts substantially exhibited superior performance to conventional inserts. It is well-known that the wiper inserts provide better surface quality and chip breaking ability at higher feeds in turning operations when compared to conventional inserts. There is only one radius on the nose of a conventional insert. However, the wiper edges are based on several radii formed a large radius or rectilinear cutting edge. In a turning operation with a cutting insert, the surface roughness is determined by feed and nose radius. Therefore, the wiper inserts with large radius or rectilinear cutting edges play an important role in reducing of the roughness values of the machined surfaces in especially hard turning processes in which surface finish has a critical importance. They tend to wipe (the reason for their name) the machined surface and obtain a smoother surface characteristic owing to longer contact length compared to conventional insert geometry [115]. As shown in Figure 3.6, the wiper inserts lead to lower scallop heights (or shallower feed marks) than conventional inserts due to their special geometries.

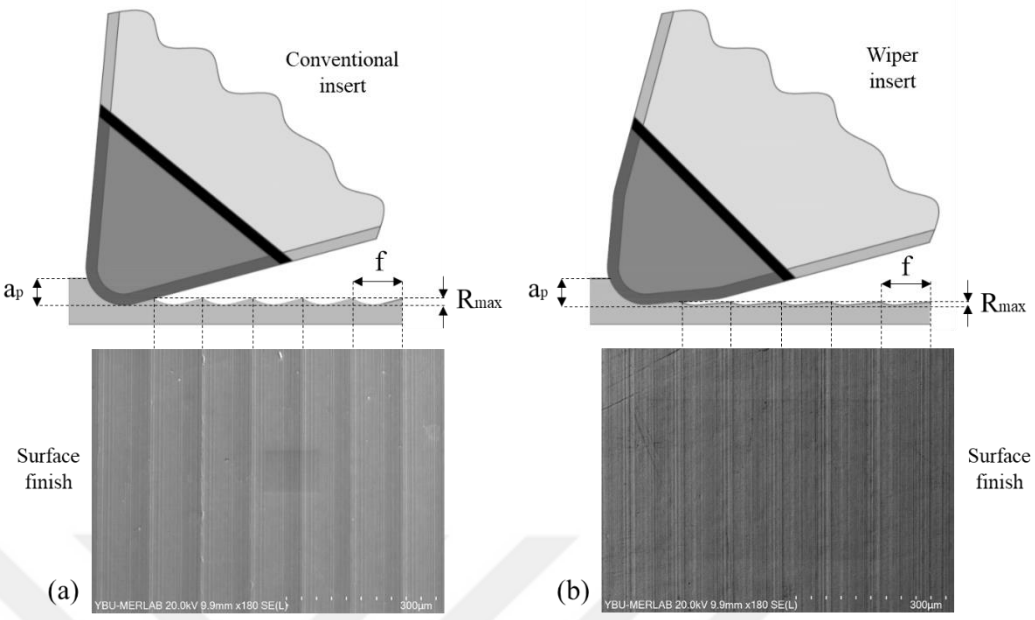

Figure 3.6 Surface textures generated by using (a) conventional and (b) wiper cutting tool.

When considered the surface roughness values under all cooling/lubrication conditions in Figure 3.5, Ra and Rz values reduced by around 73.9% and 65.9% with the use of wiper inserts, respectively. In case of the conventional inserts, similar Ra and Rz values were measured under dry, wet and MQL+CO_2 conditions. These results vary in the range of 0.263 to 0.283 µm for Ra and 1.079 to 1.125 µm for Rz. Besides, the lowest Ra values are measured under dry and wet conditions within the three cutting conditions. A similar trend also is observed for Rz values. This case can be associated with flattening of the minor cutting edge with the effect of the excessive end flank wear. The flattening effect lowers scallop heights between feed marks and thus, the roughness values reduce. The wear results confirm this claim (Figure 3.15). Even though the dry and wet conditions resulted in almost the same Ra values, a slight increase (about 7%) occurred under MQL+CO_2 conditions. This increase can be related to the high cutting forces caused by high level cooling of the workpiece during the MQL+CO_2 application [94,116]. This can also help an increase in vibrations and thus, a more unstable cutting process. It is well-known that the cryogens lead to an excessive embrittlement of workpiece material while the lubricants provide an efficient lubricity at the tool-workpiece interface [105]. Additionally, MQL and

MQL+LN_2 cutting conditions also increased Ra and Rz values. Under MQL conditions, Ra was 0.350 μm whereas the Rz was measured as 1.357 mm. When compared to dry conditions, surface roughness values increased by around 31.7% and 25.7% for Ra and Rz respectively. MQL+LN_2 conditions led to the highest Ra and Rz values. Under MQL+LN_2 conditions, Ra and Rz were measured as 0.516 μm and 1.798 mm respectively that corresponds the increases of 94.2% and 66.6% in comparison to dry conditions. The reason for the increases can be considered as the extreme cooling of the workpiece by means of LN_2 (-196 °C). The high cutting forces produced at extreme low temperatures cause to higher vibrations and the vibrations also tend to deteriorate the surface finish of the machined surface [117].

In case of wiper inserts, the first remarkable point in Figure 3.5 is that surface quality (Ra < 0.2 μm, even Ra < 0.1 μm in the most conditions) in a grinding operation is achieved under all cooling/lubrication conditions. This case shows success of the wiper inserts in ensuring of the surface quality of the machined surfaces. Another prominent point in Figure 3.5 is that the excessive fluctuations in surface roughness values (as in conventional inserts) are not observed due to a more stable cutting process with longer tool-workpiece interface. Similarly, trend lines of Ra and Rz are consistent. However, on the contrary to conventional inserts, dry and wet conditions resulted relatively higher in terms of Ra and Rz values in comparison to MQL and hybrid cutting conditions. Under dry conditions, Ra and Rz values were measured as 0.092 μm and 0.487 μm whereas they became 0.116 μm and 0.529 μm under wet conditions, respectively. Additionally, under MQL, MQL+LN_2 and MQL+CO_2 conditions, Ra and Rz values are almost the same as one another. For these three cutting conditions, Ra values vary between 0.076 and 0.078 μm whereas the Rz values take place between 0.393 and 0.407 μm. As a result, Ra values decreased by around 16.2% and Rz values also reduced in the range of 16.5% to 19.4 % under MQL, MQL+LN_2 and MQL+CO_2 conditions in comparison to dry conditions. These improvements show the importance of efficient lubrication under the MQL and hybrid conditions. However, the precooling of the work material under hybrid conditions did not exhibit a prominent advantage when compared to MQL conditions even though the MQL+CO_2 condition presented

the best results. In this context, precooling application provided a slight improvement on surface quality but the application of MQL emerges as a dominant factor of better surface roughness values obtained from MQL and hybrid cutting conditions when they are compared to the dry machining. As a result, the improvements on the surface roughness of MQL and hybrid conditions are attributed to the easier cutting process provided by effective lubrication.

In addition to hybrid conditions with combination of MQL and cryogenic precooling (LN_2 and CO_2), the efficiency of external cryogenic cooling was also investigated in terms of surface roughness within this thesis study content. Thus, CO_2 and LN_2 as the cryogens were directly applied from an external nozzle to the cutting zone during the hard turning process. In case of conventional inserts, under cryogenic cooling conditions in which LN_2 and CO_2 are employed, the measured Ra and Rz values are slightly lower ones than hybrid conditions. However, the values still are higher than minimal ones under dry and wet conditions. Therefore, it can be said that cryogenic and hybrid conditions are not suitable in ensuring of minimal roughness values. Ra and Rz values under LN_2 conditions were measured as 0.439 μm and 1.667 μm respectively. When compared to MQL+LN_2, the external LN_2 application improved Ra and Rz values by around 14.9% and 7.3%, respectively. In addition to the external LN_2 application, under CO_2 conditions, Ra and Rz values were obtained as 0.277 μm and 1.142 μm, respectively. These values corresponds to a decrease of 2.1% and an increase of 1.8% in Ra and Rz values respectively in comparison to MQL+CO_2 conditions as shown in the Figure 3.7. This case shows that cooling has a priority according to lubrication in the hard turning process in which conventional inserts are employed.

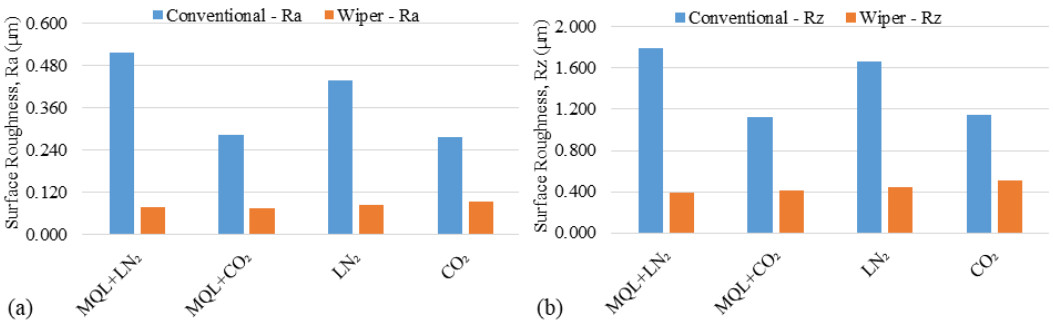

Figure 3.7 Comparison of external cryogenic cooling conditions to hybrid conditions in terms of (a) Ra and (b) Rz values

On the other hand, in case of wiper inserts, surface roughness values increased under external LN_2 and CO_2 cooling conditions in comparison to the hybrid conditions. In this context, Ra and Rz values were measured in the range of 0.086 to 0.094 µm and 0.444 to 0.506 µm respectively under external LN_2 and CO_2 cooling conditions respectively. Under LN_2 conditions, Ra and Rz were increased by around 11.7% and 13% in comparison to MQL+LN_2 conditions as shown in Figure 3.7. Similarly, under CO_2 conditions, Ra and Rz values increased by around 23.7% and 24.3% respectively when compared to MQL+CO_2 condition. These results of the surface roughness values show the importance of lubrication in hard turning process in which the wiper inserts are employed.

3.3 Residual Stresses

In this study, the residual stresses formed during hard turning of AISI 52100 steel by using wiper and conventional cutting tools under different cooling/lubrication conditions were measured by XRD technique. At the end of the hard turning operations, significant compressive residual stress values are observed in both circumferential (hoop) and axial directions due to high workpiece hardness (62 HRC) [118] and high cutting speed (200 m/min) [35]. Additionally, the effect of insert geometry and cutting edge preparation are also some of the important factors that influences the residual stresses as shown in the Figure 3.8.

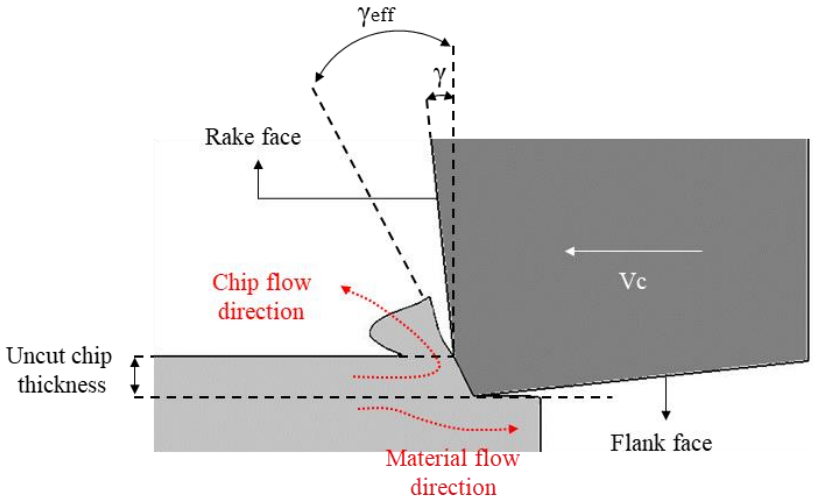

Figure 3.8 The effects of cutting edge geometry

As shown in the Figure 3.8, uncut chip thickness is equal to the width of the chamfer on the cutting edge. Therefore, the effective rake angle is -26° which is the sum of chamfer angle of -20° and rake angle (γ) of -6°. High compressive stresses resulted in both hoop and axial directions are also attributed to larger effective rake angle (γ_{eff} = -26°) [35]. The distribution of elastic stresses beneath the machined surface is significantly affected from the rake angle. Besides, the compressive zone in the subsurface expands prominently when performing machining operations with large negative rake angles [38]. The residual stress values depending on the depth for conventional and wiper inserts under different cooling/lubrication conditions are shown in Figure 3.9.

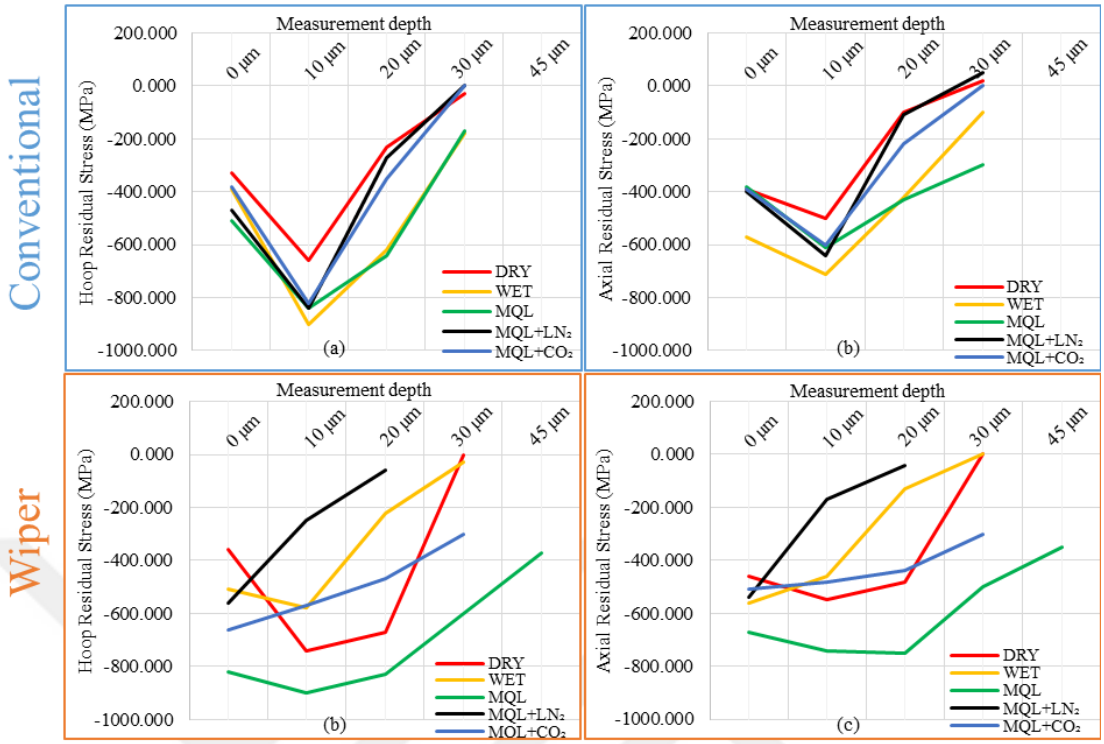

Figure 3.9 (a-c) Hoop and (b-d) axial residual stress values for conventional and wiper inserts.

The first prominent point in Figure 3.9 is that trend lines depending on the depth of residual stresses for the conventional and wiper inserts are different from one another. This case can be related to phase transformation and plastic deformation conditions occurred with the effect of different thermo-mechanical loads. It is well-known that the high temperatures generated during the hard turning can reach up to austenitizing temperatures of the AISI 52100 steel in even for a short while [119]. Therefore, microstructural phase transformations such as white and/or dark layers with different thicknesses can take place on the surface and subsurface of the bearing steel. This case can also lead to different stress distributions in the different phase regions. As mentioned above, plastic deformation also is another factor affecting different stress distributions. Another remarkable point in Figure 3.9 is that compressive residual stresses at the surface of the workpiece material produced by the wiper inserts are higher than ones of the conventional inserts. This can be explained by the fact that the wiper inserts lead to larger BUE formation [120] and tool wear on the minor cutting edge (Figure 3.15) due to their longer tool-workpiece contact distance and thus, cause

to higher frictions and forces (Figure 3.2 and Figure 3.3). In addition, the higher compressive residual stresses can be also linked with slow cooling rate of the machined surface due to longer contact length of wiper inserts [121].

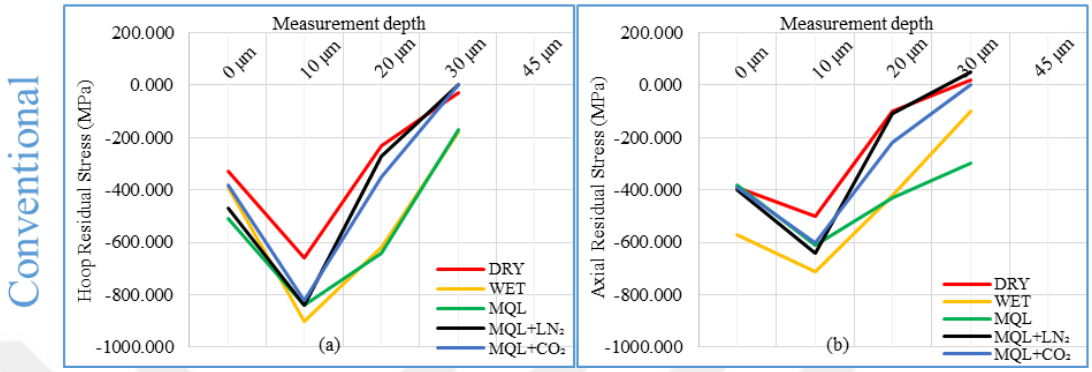

Figure 3.10 (a) Hoop and (b) axial residual stress values for conventional inserts

When considered the conventional inserts in Figure 3.10, it is observed that lower compressive residual stresses are produced at the surface of the workpiece material, the compressive residual stresses reach to maximal at the depth of 10 µm and maximum stresses return towards tensile residual stresses at the depths of 20 µm and 30 µm in both axial and hoop directions under all cooling/lubrication conditions. It is also known as "hook" shaped residual stress profile [122]. As mentioned above, with the effect of effective rake angle (γ_{eff} = -26°) of the CBN inserts, plastic deformation produces the compressive residual stresses at the surface and subsurface of the work material. In addition, the high cutting temperatures and rapid cooling during the hard turning process lead to the local thermal expansion and contraction of the machined surface, which causes to tensile residual stress. This is a reason for being lower compressive stresses at the surface than ones at subsurface of the work material. The phase transformations are another factors affecting the residual stresses. The white layer is formed by combination of the phase transformation and plastic deformation. In addition, the dark layer is a high-temperature tempering structure and dynamic recrystallization is the main formation mechanism of the dark layer [123]. White layer is displayed in white color while dark layer is represented in dark grey color under an optical microscope as mentioned in earlier sections. However, white layer is in the

form of a fine grained dense structure under SEM. As shown in SEM and optical microscope examinations in Figure 3.11, no white and dense layer formations could be observed at the surface of the workpiece material. This also shows that temperatures in the cutting zone did not reach to austenitizing temperatures of the bearing steel. However, as illustrated an optical microscope examination in Figure 3.11a, it is possible to observe a dark layer formation with 15.9 μm thick. This shows that the measurements of the compressive residual stresses at depth of 10 μm in which they are maximal possibly remain within the dark layer region. It is well-known that dark layer is an over-tempered zone at elevated tempering temperatures. Maximal tempering temperatures are generated on the surface of the workpiece material during the hard turning process. Therefore, maximum tensile residual stresses within the dark layer are produced on the surface. However, the tempering temperatures and cooling rate reduce from surface of workpiece material to deeper material regions. This leads to a reduction in local thermal expansion and contraction and thus, in the tensile residual stresses in deeper material regions. The lower tempering temperatures and cooling rates also relieve tensile residual stresses partially (transformation of martensite to tempered martensite). The stress relieving process and plastic deformation ensure higher compressive residual stresses than ones on the surface of workpiece material up to depth of 10 μm. The effects of tempering and plastic deformation is alleviated from surface of workpiece material to further deeper material regions and thus, compressive residual stresses return towards tensile residual stresses as at the depths of 20 μm and 30 μm. Briefly, the tensile residual stress on the machined surface are formed by thermal effects, and the mechanical loads affect deeper material regions.

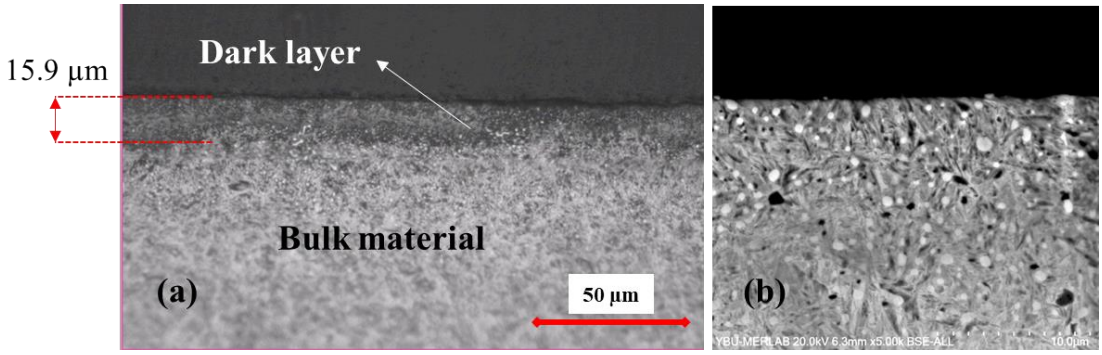

Figure 3.11 Microscopic examinations of specimens under dry conditions: (a) optical microscope and (b) SEM

Additionally, mean value of the maximum stresses in hoop direction is 32.7% more than ones of the residual stresses in the axial direction. This increase in the residual stresses can be directly related to the force components in cutting speed and feed directions. As mentioned earlier, the main cutting force (53.78 N) was significantly higher than the feed force (21.26 N). Thus, high hoop and low axial residual stresses are produced due to different magnitudes of main cutting and feed forces respectively. Dry conditions resulted significantly in minimal axial and hoop compressive residual stresses for the conventional inserts than other cutting conditions due to high cutting temperatures which can produce higher tensile residual stresses within the dark layer. Under the dry conditions, compressive residual stresses at the depth of 10 µm were measured as -660 MPa and -500 MPa for hoop and axial directions, respectively. MQL and hybrid conditions have nearly same trend lines in terms of residual stresses. Higher compressive stresses are achieved under MQL and hybrid conditions in comparison to dry conditions. Under these conditions, hoop and axial residual stresses were measured in the range of -820 to -840 MPa and -600 to -640 MPa respectively that corresponds to the increases of around 26.3% and 23.3% according to dry conditions. This can be explained by the fact that efficient cooling and lubrication reduce the cutting temperatures and thus, make plastic deformation more dominant in producing of compressive residual stresses [95]. Similarly, wet conditions also increased the maximum compressive residual stresses at depth of 10 µm. With conventional cutting fluid application, maximum compressive residual stresses of -900 MPa to -710 MPa

are generated on hoop and axial measurement directions as shown in Figure 3.10. This also corresponds to the increases of 36.4% and 42% in comparison to dry conditions. It is well-known that compressive residual stresses are observed where the plastic deformation is dominant contrary to tensile residual stresses caused by thermal effects [124]. Under wet conditions in which conventional cutting fluid is directly applied to cutting zone, it can be said that thermal effect reduces, and plastic deformation is made more dominant due to its moderate cooling and lubrication effect of the conventional cutting fluid.

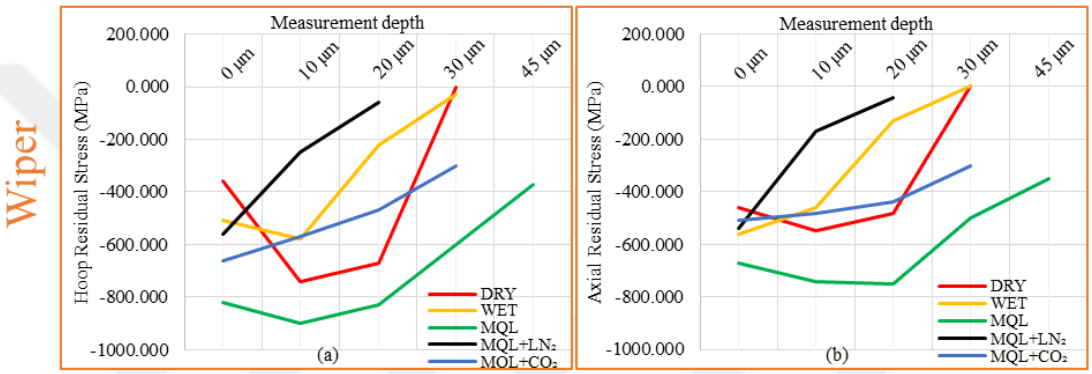

Figure 3.12 (a) Hoop and (b) axial residual stress values for conventional inserts

When considered the wiper inserts in Figure 3.12, the axial residual stresses were also measured lower than hoop residual stresses as in the conventional inserts. Minimal compressive residual stresses on the surface were measured (-360 MPa Hoop and -460 MPa axial) under dry conditions. This case is related to higher cutting temperatures generated at the work surface under dry conditions. However, the subsurface compressive stresses at depths of 10 µm and 20 µm are higher than ones under two hybrid and wet conditions. This case can be associated with higher subsurface plastic deformation in case of higher forces and temperatures during the dry hard turning process. Another interesting case in Figure 3.12 which is different from Figure 3.10 is that trend lines of two hybrid conditions are continuous upward. This case shows that the cryogenic cooling is more effective on the hard turning process under hybrid conditions in which the wiper inserts are employed due to larger tool-workpiece interface. It is thought that the efficient cooling and lubrication lead to the formation

of thinner dark layer than 10 μm. The wear results are good evidences because wiper inserts exhibited superior performance to conventional inserts in terms of flank wear under hybrid conditions (Figure 3.15). A similar trend can be observed under wet conditions in which moderate cooling and lubrication are dominant. Even though the hoop residual stresses under MQL+CO_2 condition are higher due to upper intermediate cooling and efficient lubrication, surface residual stresses are in the range of -510 to -660 MPa and -510 to -560 MPa in hoop and axial directions respectively under hybrid and wet conditions. Minimal compressive stresses are achieved under MQL+LN_2 conditions. This case can be explained by the fact that LN_2 enhances resistance of work material to plastic deformation. The highest compressive stresses were measured under MQL conditions. As a result of MQL application, -900 MPa hoop and -740 MPa axial residual stresses were observed at 10 μm below the surface. This also corresponds to the increases of 21.6% and 34.5% in comparison to dry conditions. This case shows the importance of effective lubrication for better plastic deformation with wiper inserts in the hard turning processes in which frictions are more dominant.

In addition to the dry, wet, MQL and hybrid conditions, external cryogenic cooling methods (with an external nozzle) were also examined in terms of residual stresses to compare to some of previous methods (hybrid conditions). The results are shown in Figure 3.13.

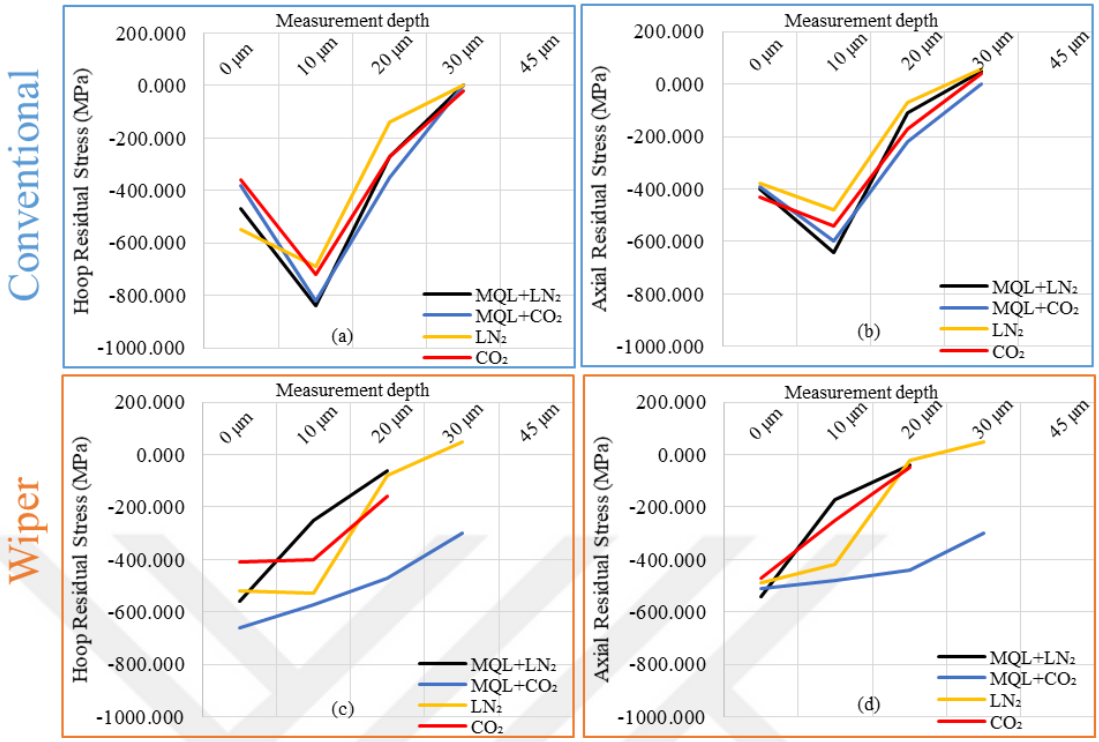

Figure 3.13 Comparison of external cryogenic cooling to hybrid method in terms of residual stresses for (a-b) conventional and (c-d) wiper cutting tools

In case of conventional inserts, maximum residual stress values are observed similar in the hoop direction (-690 MPa for LN_2 and -720 MPa for CO_2) and axial direction (-480 MPa for LN_2 and -540 MPa for CO_2) for external cryogenic cooling. Besides, the compressive residual stresses produced under external cryogenic cooling conditions are lower than ones under hybrid cryogenic conditions although their trend lines are similar to ones under other all conditions. Similarly, external cryogenic cooling generally resulted the lowest compressive stresses for the wiper inserts among all cooling/lubrication conditions. In this context, LN_2 produced -530 MPa hoop and -490 MPa axial residual stresses, while CO_2 generated -410 MPa hoop and -470 MPa axial residual stresses at the surface. As a result, when considered the external cryogenic application (LN_2 and CO_2) for both conventional and wiper cutting tools, the mean values of maximum axial and hoop compressive residual stresses decreased by around 13.5% and 18.4% respectively in comparison to hybrid cutting conditions. This can be associated with higher level cooling and lower level lubrication effects of cryogens in

the cutting zone under external cryogenic cooling conditions in comparison to hybrid conditions.

3.4 Tool Wear

In hard turning of AISI 52100 bearing steel, two dominant wear formations are observed. These are flank wear and crater wear. Figure 3.14 shows the SEM images of the worn conventional and wiper CBN inserts under dry, wet, MQL and hybrid conditions.

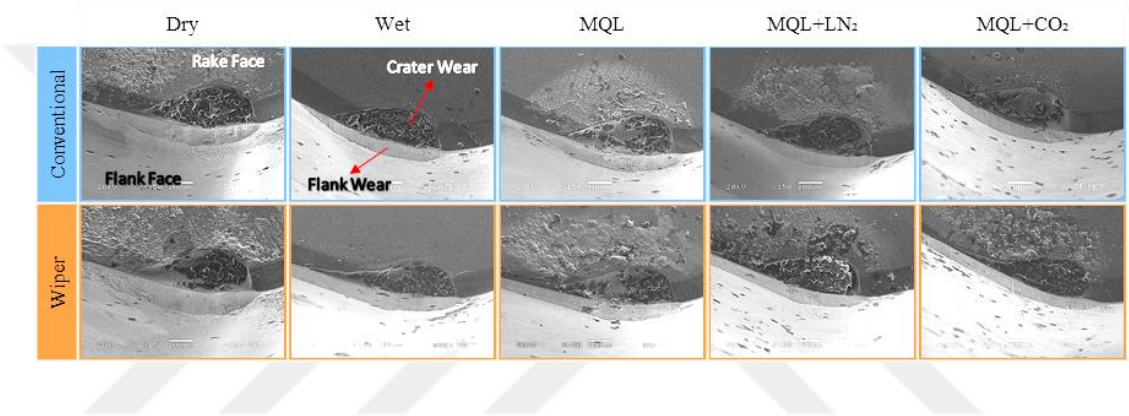

Figure 3.14 SEM images of the worn conventional and wiper inserts under dry, wet, MQL and hybrid conditions.

As illustrated in Figure 3.14, significant crater wear and flank wear formed on the rake face and flank face of cutting inserts in consequence of abrasion and diffusion wear mechanisms. The first remarkable point in the Figure 3.15 is that the lengths of flank wear on the wiper inserts are longer than ones on the conventional inserts. This case is associated with longer tool-workpiece contact distance of the wiper inserts due to their special geometries [125]. Another prominent point in the Figure 3.15 also is that larger flank wear formations were observed on end flank face rather than side flank face. This can be explained with longer tool-workpiece contact distance on minor cutting edge than tool-workpiece contact distance on major cutting edge. Since the depth of cut value (0.1 mm) is lower than the tool tip radius (0.8 mm) the wear processes also takes place at the minor cutting edge [126]. In addition, in this study, the employed CBN insert has a uniform edge preparation all around the corner radius. The uniform edge

micro-geometry through the corner radius of the insert leads to very low edge radius to uncut chip thickness at the minor cutting edge. This leads to higher ploughing than shearing at minor cutting edge [127]. Therefore, it can be said that ploughing action leads to higher contact distance between workpiece and minor cutting edge.

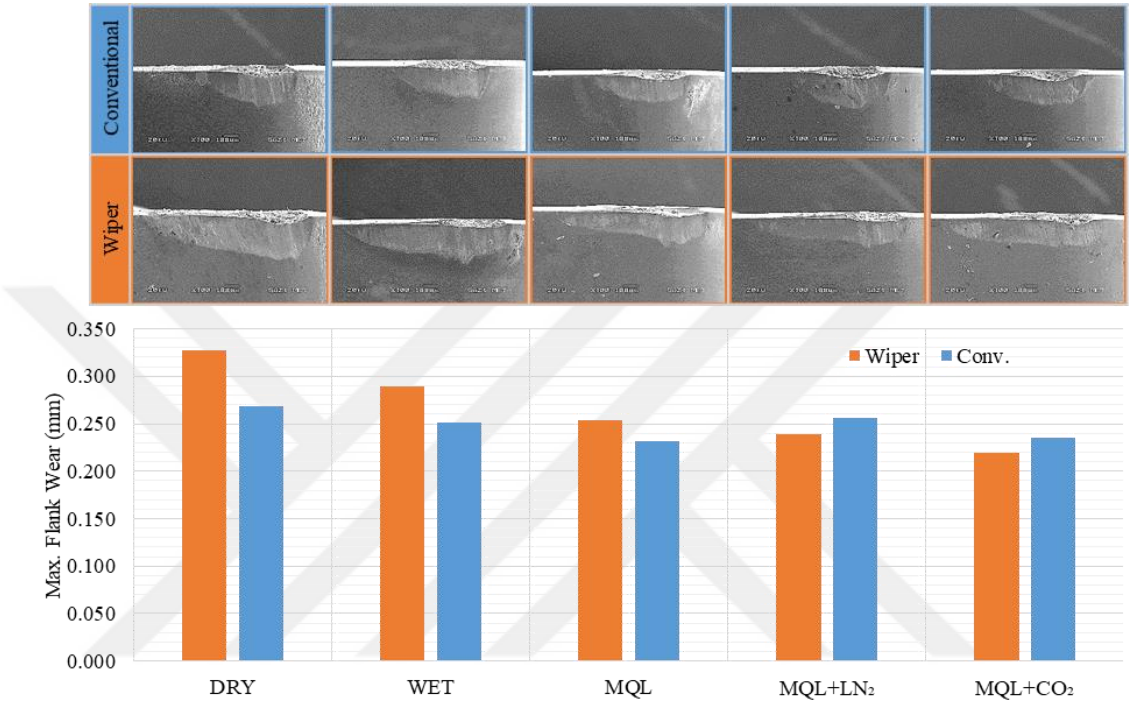

Figure 3.15 Flank wear values and SEM images of wiper and conventional CBN inserts under different cooling/lubrication conditions

As shown in Figure 3.15, the largest bandwidth values of flank wear (VB_{Bmax}) are observed under dry conditions due to absence of cooling and/or lubrication agents during the cutting. Under dry conditions, maximum flank wear values were obtained as 0.327 mm and 0.268 mm for wiper and conventional cutting tools respectively. These results show that maximum flank wear of the wiper insert was measured 22.2% higher than that of the conventional insert tool due to longer tool-workpiece contact distance, and frictions and elevated temperatures generated in the tool-workpiece interface. Under wet conditions, flank wear values were observed as 0.290 mm and 0.251 mm for wiper and conventional cutting tools respectively. When compared to dry conditions, it can be seen that the flank wear value was decreased slightly due to

moderate cooling and lubrication properties of the conventional cutting fluid. As a result of frictions and temperatures reduced with the use of conventional cutting fluid, maximum flank wear values decreased by around 12% and 6.4% in comparison to those under dry conditions, respectively. The remarkable point in the results under wet conditions, the difference between flank wear values for conventional (0.251 mm) and wiper (0.290 mm) inserts is large as in the results under dry conditions. This case shows that semi-synthetic cutting oil addition (5%) into water (95%) and penetration of conventional cutting fluid into tool-workpiece interface remain insufficient. Thus, the frictions at the tool-workpiece interfaces of wiper inserts could not be minimized due to low oil percentage in conventional cutting fluid and insufficient penetration of coolant and lubricant agents along their longer tool-workpiece contact distances. The flank wear values on the wiper inserts, therefore, were higher. The conventional cutting fluid was more successful on the conventional inserts owing to their shorter tool-workpiece contact lengths. Under these conditions, lubricant penetration is easier and frictions are minimal. For this reason, the flank wear bandwidth is less than that on wiper inserts. MQL also provided a significant improvement in flank wear when compared to dry and wet conditions. When the fine oil mist was applied from the cutting tool holder under MQL condition, maximum flank wear values were measured as 0.253 mm and 0.232 mm for wiper and conventional cutting tools respectively. Good penetration into tool-workpiece interface and lubrication effect of oil droplets within the pressurized air lead to a reduction in friction and thus, abrasive effect decreased at the tool-workpiece interface. As a result, maximum flank wear values under MQL conditions decreased by 22.6% and 13.5% in comparison to ones on wiper and conventional inserts under dry conditions, respectively.

Hybrid conditions (MQL+LN_2 and MQL+CO_2) exhibited different performance from other cooling/lubrication conditions in terms of wear performance of the wiper and conventional inserts. Under hybrid conditions, the wiper inserts showed better performance than conventional inserts in terms of flank wear. This case shows that efficient cooling and lubrication conditions (hybrid) are more effective on cutting conditions in which frictions and temperatures are more dominant. Another important

and interesting point is that minimum flank wear value of 0.219 mm is obtained by the use of wiper inserts under MQL+CO_2 conditions. MQL+CO_2 provided a combined effect in terms of efficient cooling and lubrication at tool-chip and tool-workpiece interfaces. Under hybrid conditions, the expected performance on conventional inserts could not be reached in terms of flank wear. The minimum flank wear value for conventional inserts was achieved under MQL conditions due to their good lubrication properties. However, flank wear value (0.236 mm) measured under MQL+CO_2 conditions is very close to flank value (0.232 mm) measured under MQL conditions. In addition, it is possible to say from Figure 3.15 that MQL+CO_2 condition exhibited a superior performance to MQL+LN_2 condition. This case can be explained with higher pressure application of CO_2 (54 bars) than that of LN_2 (15 bars). In this case, it is thought that higher pressure CO_2 showed a cooling effect on cutting zone as well as making precooling onto the work material. It is expected that lower pressure LN_2 performed a more localized precooling on the work material as shown in Figure 3.16. It is known that when CO_2 sprayed from the delivery nozzle and enters the atmospheric pressure, a major pressure droplet occurs and leads to expansion and cooling down (as low as -78.5 °C) owing to phase transformation (sublimation) and Joule-Thomson effect [80,128]. As a result, the liquid CO_2 transforms in 40% CO_2-snow and 60% cold CO_2-gas and flows through the nozzle with a dispersed stream characteristic (Figure 3.16a). On the other hand, it is possible to perform a coherent stream of LN_2 during cryogenic cooling (Figure 3.16b) since it converts from solid into the liquid phase at -210 °C and starts boiling at -196 °C and ambient pressure [80]. Therefore, totally different cooling characteristics are observed for these two cryogenic cooling applications. It can be said that due to mentioned penetration properties, hybrid conditions with CO_2 provides better heat removal from the cutting zone (Figure 3.16).

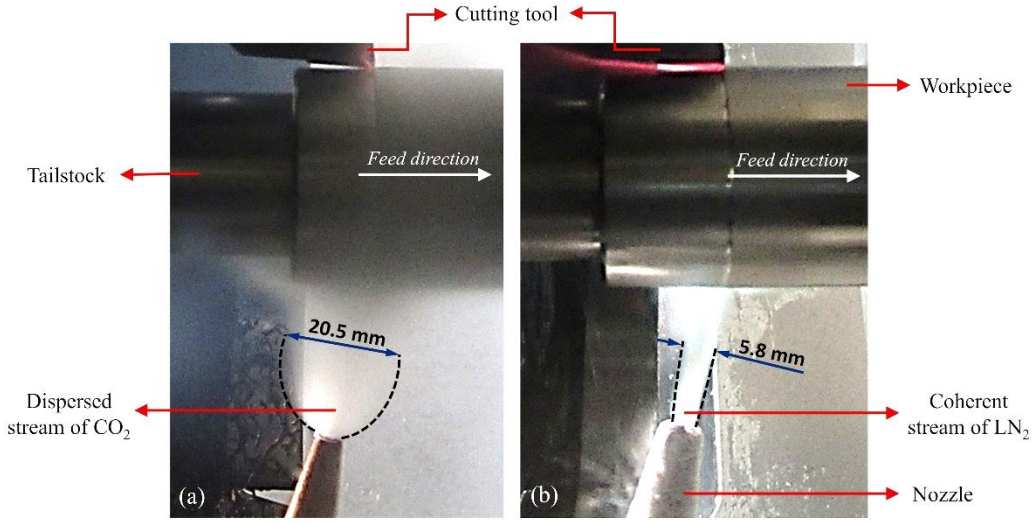

Figure 3.16 Cooling characteristics of a) MQL+ CO_2 and b) MQL+ LN_2 hybrid conditions.

In formation of flank wear, abrasion and diffusion wear mechanisms have an important impact. An EDS analysis on the work material in Figure 3.17 is good evidence for the diffusion. Under normal conditions, AISI 52100 bearing steel contains 1% wt of carbon. However, in consequence of the EDS analysis, carbon content on the turned surface of the bearing steel increases up to 6.2 % wt. This case verifies a carbon diffusion from tool material to work material.

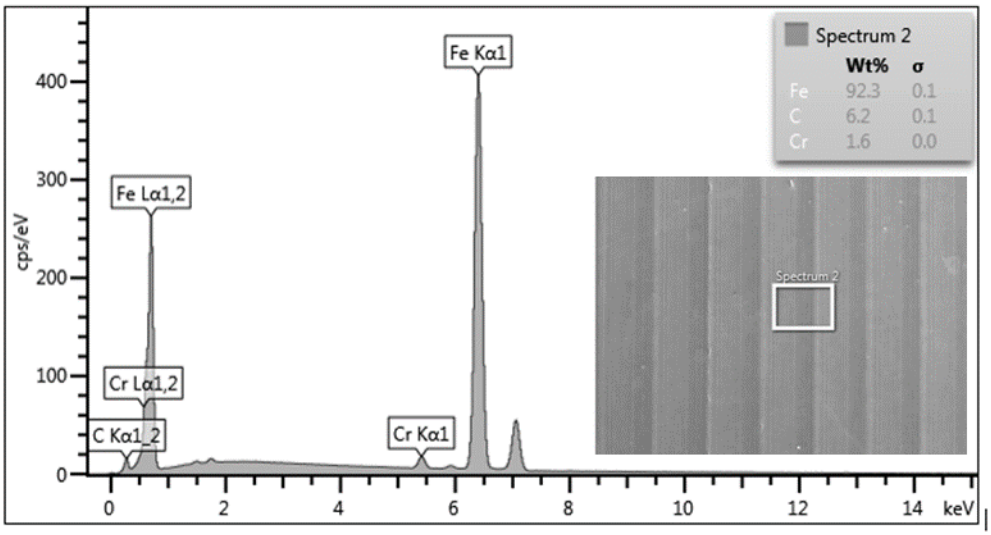

Figure 3.17 EDS analysis of the machined surface

In addition to the flank wear, significant amount of crater wear formed on both wiper and conventional inserts after the hard turning process under different cooling/lubrication conditions as shown in Figure 3.18.

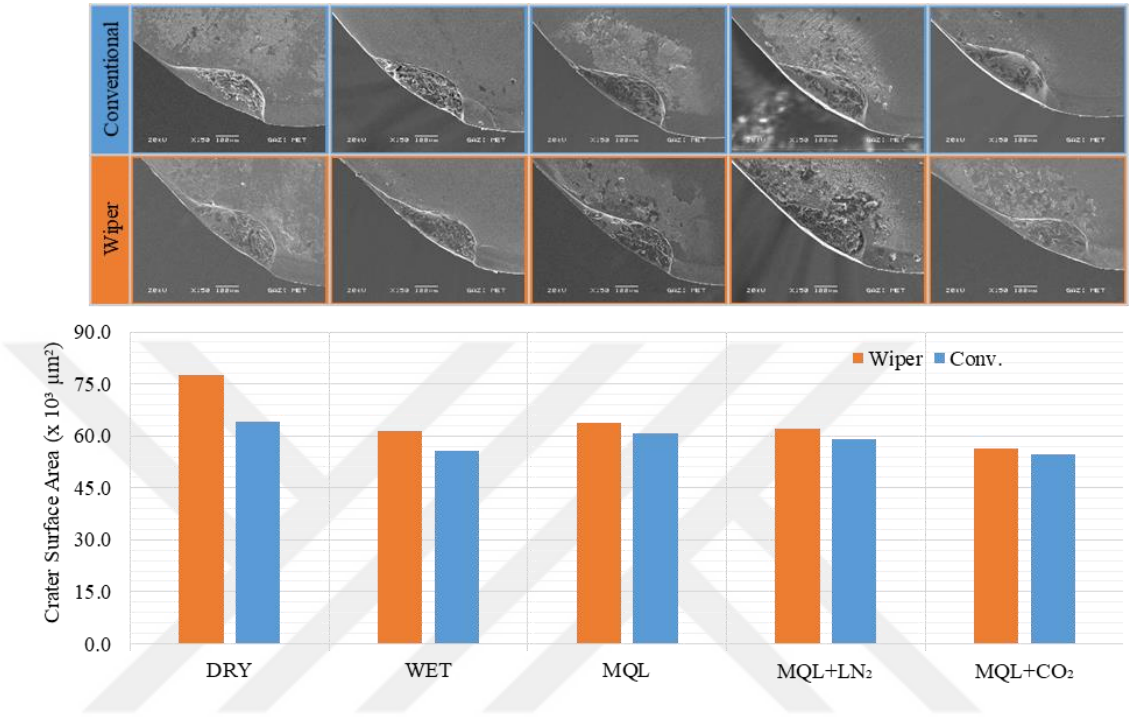

Figure 3.18 Crater wear values and SEM images of wiper and conventional CBN inserts under different cooling/lubrication conditions

As shown in Figure 3.18, crater surface area on rake face of the wiper inserts are larger than those of the conventional inserts. The enlargement in crater surface area is related to longer tool-chip contact length caused due to wiper insert geometry. As in the flank wear results, maximum crater surface area is observed under the dry conditions. Absence of any coolant and lubricant during cutting led to higher temperature in the cutting zone. The higher cutting temperatures caused to larger crater surface area on the rake face due to abrasion and diffusion wear mechanisms. It is well-known, high carbon amount in titanium carbide (TiC) content (50%) in CBN inserts employed in this study is responsible for the diffusion. The crater surface area on the conventional and wiper inserts under dry conditions was measured as 64.2 x 10^3 µm^2 and 77.7 x 10^3 µm^2 respectively that corresponds a reduction in crater wear by around 17.4% that of

the wiper insert. Under MQL conditions, crater wear amount significantly reduced when compared to dry conditions. Application of fine oil droplets in the pressurized air to the cutting zone prevented heat build-up by reducing frictions at the tool-chip interface. This case led to less crater wear by lowering diffusion rate. On the other hand, crater surface areas were measured as 63.8 x 10^3 μm^2 and 60.9 x 10^3 μm^2 for wiper and conventional inserts. These results indicate that the crater surface areas on the wiper and conventional inserts under MQL conditions are less by 17.9% and 5.1% in comparison to dry conditions respectively. When considered the hybrid conditions, the crater wear values under MQL+LN_2 conditions were measured as 62.1 x 103 μm^2 and 59.1 x 103 μm^2 for wiper and conventional inserts, respectively while they were 56.2 x 103 μm^2 and 54.6 x 103 μm^2 under MQL+CO_2 conditions. It is clear that the conventional and wiper inserts under MQL+CO_2 conditions exhibited better performance by 7.6% and 9.5% than ones under MQL+LN_2 conditions in terms of crater wear. Under MQL+LN_2 conditions, the amount of crater wear decreased on wiper cutting tools significantly when compared to dry conditions. In addition to the lubrication effect of MQL, proper precooling application onto work material using LN_2 resulted in lower crater wear than both dry and MQL conditions for wiper cutting tools. It can be said that due to effective cooling under hybrid conditions with cryogens, the oil droplets do not evaporate or burn at tool chip interface immediately. Therefore, higher penetration of oil into the cutting zone is achieved [116]. This condition leads to improvement of lubrication characteristics under hybrid conditions. The combined effect of lubrication and precooling not only reduced frictions at the tool-chip and tool-workpiece interfaces but also temperatures in the cutting zone. This case led to a reduction in diffusion rate and thus, crater wear amount decreased. As a result, the crater surface areas under MQL+LN_2 conditions were less by 20.1% and 7.9% for wiper and conventional inserts respectively when compared to dry conditions. As shown in Figure 3.18, under the wet conditions, although flank wear is higher than all cutting conditions except dry conditions, the crater surface area values also are lower than all cutting conditions excluding MQL+CO_2 conditions. This is because conventional cutting fluid was successful in reducing cutting temperatures due to its direct application to cutting zone (via internal passageways of the tool holder at 8 bars).

As shown in Figure 3.18, MQL+CO_2 conditions give the best crater wear results similar to the flank wear results. As mentioned earlier, CO_2 was applied to work material at a high pressure of 54 bars for precooling purposes and high pressure CO_2 showed a cooling effect on cutting zone as well as making precooling onto the work material. For these reasons, when considered efficient lubrication effect of MQL, the lowest crater surface was measured under MQL+CO_2 conditions. The crater surface areas reduced by 27.7% and 15.0% for the wiper and conventional inserts, respectively in comparison to dry conditions.

After main tool wear tests, some experimental studies were conducted to observe the effects of direct cryogenic cooling of cutting zone on tool wear (especially premature tool failure due to embrittlement of cutting inserts). To avoid excessive embrittlement of cutting inserts, CO_2 which can be cooled the cutting zone at higher temperatures than LN_2 was selected as a cryogen. The tests were performed at same cutting speed (200 m/min), feed (0.1 mm/rev) and depth of cut (0.1 mm) and cutting distance of 3474.35 m (cutting time of 17.5 min) using conventional inserts under dry and CO_2 conditions. After the tests, any fracture and chipping on the cutting insert depending on excessive mechanical loads were not observed under CO_2 conditions. As in the main wear tests, only flank wear and crater wear formed on the inserts under both dry and CO_2 conditions as shown in Figure 3.19.

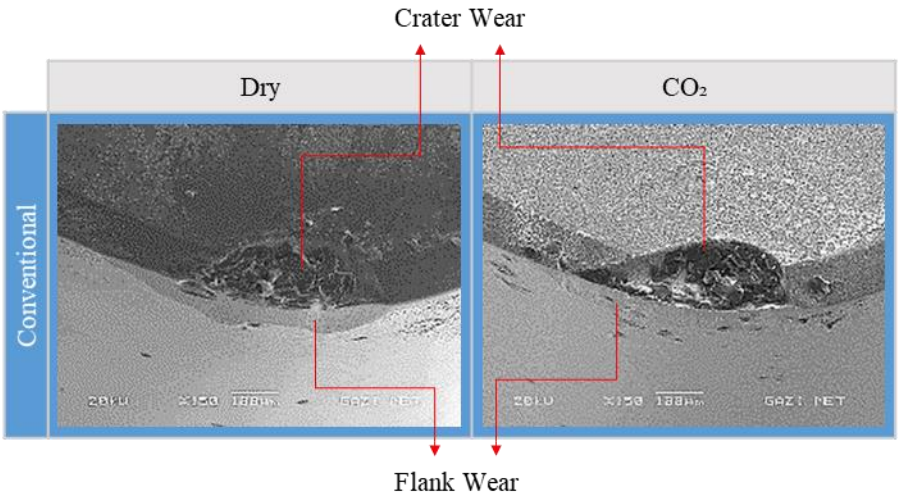

Figure 3.19 Tool wear types under dry and CO_2 conditions

The flank wear and crater wear results under both dry and CO_2 conditions are shown in Figure 3.20a and Figure 3.20b. As shown in Figure 3.20a, after wear tests, uniform flank wear occurs under CO_2 condition while non-uniform flank wear takes place under dry condition. Therefore, both average and maximum flank wear values are represented in Figure 3.20a. In both cases, flank wear values under CO_2 conditions are lower than ones under dry conditions. Average and maximum flank wear values were measured as 0.140 mm and 0.218 mm respectively under dry conditions whereas they determined as 0.118 mm and 0.156 mm under CO_2 conditions. Average and maximum flank wear values under CO_2 conditions are lower by 16.0% and 28.7% respectively than ones under dry conditions. This case can be attributed to effective cooling and lubrication effects of CO_2. It is well-known that flank wear widely occurs on flank face of the cutting insert as a result of abrasion wear mechanisms. Thermal softening effect at higher temperatures at the tool-workpiece interface make cutting insert more vulnerable to abrasion. Since CO_2 has a good cooling (-78.5 °C) and a slight lubrication effects, it reduces cutting temperatures efficiently when directly applied to cutting zone. Therefore, it is thought that due to this mechanism, the obtained flank wear bandwidth under CO_2 condition is lower than one under dry condition.

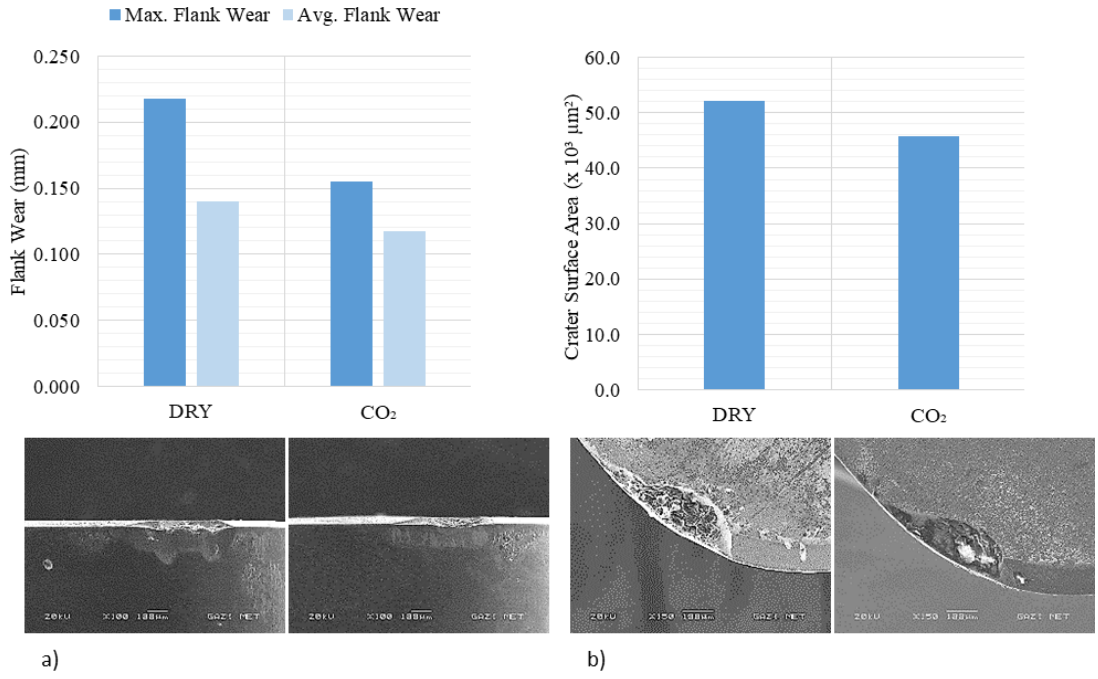

Figure 3.20 (a) Flank wear and (b) crater wear values under dry and CO_2 conditions

As can be seen in Figure 3.20b, crater surface area under CO_2 condition is smaller than one under dry condition. Crater surface area is measured as 45.8 x 10^3 μm^2 under CO_2 conditions while it is determined as 52.1 x 10^3 μm^2 under dry conditions. The use of CO_2 as a cryogen in the hard turning operation reduces crater wear by 12.1%. It is well-known that crater wear forms on rake face of the cutting insert in consequence of abrasion and diffusion wear mechanisms. These wear mechanisms are related to temperatures and frictions at the tool-chip interface directly. Therefore, for the smaller crater surface area, frictions and temperatures at the tool-chip interface should be minimized. It is believed that good cooling and slight lubrication properties of CO_2 reduces crater surface area.

CHAPTER 4

CONCLUSION AND FUTURE WORK

In this chapter, conclusions and the future works of the experimental study conducted under different cooling/lubrication conditions are presented. In this context, performance of these cooling techniques (wet, MQL, cryogenic and hybrid) and the effect of cutting edge geometry (wiper and conventional) are evaluated according to tool wear, surface roughness and residual stresses.

4.1 Summary of the Present Study

As given the literature review, it is observed that the effects of different cooling/lubrication conditions and tool geometry (conventional and wiper inserts) on tool wear and surface integrity are frequently investigated in turning of hardened steels. However, comprehensive comparisons of especially the precooling based hybrid conditions (MQL+LN_2 and MQL+CO_2) to conventional cooling/lubrication methods in terms of tool wear and surface integrity for machining hardened steels have not been performed yet. Additionally, the performance of the conventional and wiper inserts under hybrid conditions in which efficient cooling and lubrication are employed is an interesting topic. Therefore, the effects of different cooling/lubrication conditions and tool geometry on tool wear and surface integrity are the main focal point of this experimental study. The findings of this study are as follows;

- It is observed that passive force is measured higher than main cutting force due to being smaller depth of cut than nose radius of cutting inserts.
- The wiper inserts lead to higher main cutting and passive force components due to their larger tool-workpiece and tool-chip contact areas.
- The wiper inserts produce better surface roughness values than the conventional inserts owing to their longer tool-workpiece contact distance and additional radii.

- In case of the conventional inserts, the lowest Ra values are measured under dry conditions. This case is associated with flattening of the minor cutting edge with the effect of the excessive end flank wear.
- In case of the wiper inserts, the lowest Ra values are measured in the range of 0.076 to 0.078 μm under hybrid and MQL conditions. This case shows the importance of efficient lubrication for better Ra values.
- High compressive stresses produced in both hoop and axial directions are attributed to larger effective rake angle ($\gamma eff = -26°$)
- Residual stress trend lines depending on the depth for the conventional and wiper inserts are different from one another thanks to phase transformation and plastic deformation conditions occurred with the effect of different thermo-mechanical loads.
- The compressive residual stresses at the surface of the workpiece material produced by the wiper inserts are higher than ones of the conventional inserts. This case is explained by the fact that the wiper inserts lead to larger BUE formation and tool wear on the minor cutting edge and thus, cause to higher frictions and forces.
- Mean value of the maximum stresses in hoop direction is 32.7% more than ones of the residual stresses in the axial direction. This increase in the residual stresses is associated with the force components in cutting speed and feed directions.
- In case of the conventional inserts, wet conditions also increased the maximum compressive residual stresses at depth of 10 μm. Under wet conditions in which conventional cutting fluid is directly applied to cutting zone at 8 bars thermal effect reduces, and plastic deformation is made more dominant due to its moderate cooling and lubrication effect of the conventional cutting fluid.
- In case of the wiper inserts, the highest compressive stresses were measured under MQL conditions. This case shows the importance of effective lubrication for better plastic deformation with wiper inserts in the hard turning processes in which frictions are more dominant.

- Significant crater wear and flank wear formed on the rake face and flank face of both conventional and wiper inserts in consequence of abrasion and diffusion wear mechanisms.
- The lengths of flank wear on the wiper inserts are longer than ones on the conventional inserts. This case is associated with longer tool-workpiece contact distance of the wiper inserts due to their special geometries.
- Larger flank wear formations were observed on end flank face rather than side flank face. This is explained with longer tool-workpiece contact distance on minor cutting edge than tool-workpiece contact distance on major cutting edge due to lower depth of cut value (0.1 mm) than the tool tip radius (0.8 mm).
- Hybrid conditions (MQL+LN_2 and MQL+CO_2) exhibit different performance from other cooling/lubrication conditions in terms of wear performance of the wiper and conventional inserts. Under hybrid conditions, the wiper inserts show better performance than conventional inserts in terms of flank wear. This case shows that efficient cooling and lubrication conditions (hybrid) are more effective on cutting conditions in which frictions and temperatures are more dominant.
- The minimum bandwidth of flank wear is measured by the use of wiper inserts under MQL+CO_2 conditions. MQL+CO_2 provides a combined effect in terms of efficient cooling and lubrication at tool-chip and tool-workpiece interfaces.
- The minimum flank wear value for conventional inserts was achieved under MQL conditions due to their good lubrication properties.
- The crater surface area on rake face of the wiper inserts are larger than those of the conventional inserts. The enlargement in crater surface area is related to longer tool-chip contact distance caused due to wiper insert geometry.
- MQL+CO_2 conditions give the best crater wear results similar to the flank wear results. CO_2 is applied to work material at a high pressure of 54 bars for precooling purposes and high pressure CO_2 shows a cooling effect on cutting zone as well as making precooling onto the work material.

4.2 Future Work

The experimental study shows that it is possible to achieve lesser tool wear and better surface integrity using conventional or wiper cutting tools under several cooling/lubrication conditions. Even though better surface roughness and more compressive residual stress formations are obtained using wiper cutting tools, rapid tool wear emerges as a major disadvantage of these cutting tools. However, this study shows that it is possible to obtain better surface roughness, tool wear and residual stress values for the wiper inserts under hybrid conditions, especially MQL+CO_2 conditions. Nevertheless, following suggestions can be given for further investigations in turning of hardened steels:

- Different nozzle positions for MQL oil and cryogens under hybrid conditions at different pressures and flow rates can be proposed to literature.
- Cutting temperatures can be measured at cryogenic and hybrid conditions and their effects on surface integrity and tool wear can be discussed.
- The performance evaluations of different cutting edge geometries (such as honed and land edge geometries) and different rake angles can be performed under hybrid cooling conditions.
- Precooling based hybrid conditions can be applied to other difficult-to-cut materials such as titanium and super alloys.

REFERENCES

[1] Umbrello, D., Micari, F., & Jawahir, I. S. The effects of cryogenic cooling on surface integrity in hard machining: A comparison with dry machining, CIRP Annals - Manufacturing Technology, 61 (1), 103-106, 2012.

[2] Dhar, N. R. & Kamruzzaman, M. Cutting temperature, tool wear, surface roughness and dimensional deviation in turning AISI-4037 steel under cryogenic condition, International Journal of Machine Tools and Manufacture, 47, 754-759, 2007.

[3] Groover, M. P. *Fundamentals of Modern Manufacturing, Materials, Processing, and Systems* (4th ed.) JOHN WILEY & SONS, INC., 2010.

[4] Xavior, M. A. & Adithan, M. Determining the influence of cutting fluids on tool wear and surface roughness during turning of AISI 304 austenitic stainless steel, Journal of Materials Processing Technology, 209 (2), 900-909, 2009.

[5] Bartarya, G. & Choudhury, S. K. State of the art in hard turning, International Journal of Machine Tools and Manufacture, 53 (1), 1-14, 2012.

[6] Liu, C. R. & Mittal, S. Single-step superfinish hard machining: Feasibility and feasible cutting conditions, Robotics and Computer-Integrated Manufacturing, 12 (1), 15-27, 1996.

[7] Matsumoto, Y., Hashimoto, F., & Lahoti, G. Surface integrity generated by precision hard turning, CIRP Annals - Manufacturing Technology, 48 (1), 59-62, 1999.

[8] Klocke, F., Brinksmeier, E., & Weinert, K. Capability Profile of Hard Cutting and Grinding Processes, CIRP Annals - Manufacturing Technology, 54 (2), 22-45, 2005.

[9] Poulachon, G., Moisan, A., & Jawahir, I. S. Tool-wear mechanisms in hard turning with polycrystalline cubic boron nitride tools, Wear, 250-251 (1-12), 576-586, 2001.

[10] Agha, S. R. & Liu, C. R. Experimental study on the performance of superfinish hard turned surfaces in rolling contact, Wear, 244 (1-2), 52-59, 2000.

[11] Pal, A., Choudhury, S. K. & Chinchanikar, S. Machinability Assessment through Experimental Investigation during Hard and Soft Turning of Hardened Steel, Procedia Materials Science, 6, 80-91, 2014.

[12] Umbrello, D., Jayal, A. D., Caruso, S., Dillon, O. W. & Jawahir, I. S. Modeling of white and dark layer formation in hard machining of AISI 52100 bearing steel, Machining Science and Technology, 14 (1), 128-147, 2010.

[13] Ghosh, R., Zurecki, Z. & Frey, J. H. Cryogenic Machining With Brittle Tools and Effects on Tool Life, International Mechanical Engineering Congress and Exposition, 201-209, Washington, USA 2003.

[14] Barry, J. & Byrne G. Cutting tool wear in the machining of hardened steels Part II: cubic boron nitride cutting tool wear, Wear, 247 (2), 152-160, 2001.

[15] Turkish Standards Institution, Tool-life testing with single-point turning tools (TS ISO 3685:2015-04). Ankara, Turkey. 2016.

[16] Khan, A. A., Ali, M. Y. & Haque, M. M. A new approach of applying cryogenic coolant in turning AISI 304 stainless steel, International Journal of Mechanical and Materials Engineering,5 (2), 171-174, 2010.

[17] Kaynak, Y. Evaluation of machining performance in cryogenic machining of Inconel 718 and comparison with dry and MQL machining, International Journal of Advanced Manufacturing Technology, 72 (5-8), 919-933, 2014.

[18] Varadarajan, A. S., Philip, P. K. & Ramamoorthy, B. Investigations on hard turning with minimal cutting fluid application (HTMF) and its comparison with dry and wet turning, International Journal of Machine Tools and Manufacture, 42 (2), 193-200, 2002.

[19] Pereira, O., Rodríguez, A., Fernández-Valdivielso, A., Barreiro, J., Fernández-Abia, A. I. & López-De-Lacalle, L. N. Cryogenic Hard Turning of ASP23 Steel Using Carbon Dioxide, Procedia Engineering, 132, 486-491, 2015.

[20] Guo, Y. B. & Liu, C. R. Mechanical Properties of Hardened AISI 52100 Steel in Hard Machining Processes, Journal of Manufacturing Science and Engineering, 124 (1), 1-9, 2002.

[21] Tonshoff, H. K., Arendt, C. & Ben Amor, R. Cutting of hardened steel, CIRP Annals - Manufacturing Technology, 49 (2), 547-566, 2000.

[22] D'Addona, D. M. & Raykar, S. J. Analysis of Surface Roughness in Hard Turning Using Wiper Insert Geometry, Procedia CIRP, 41, 841-846, 2016.

[23] Zurecki, Z., Ghosh, R. & Frey, J. H. Investigation of White Layers Formed in Conventional and Cryogenic Hard Turning of Steels," Manufacturing, vol. 2003, pp. 211-220, 2003.

[24] Das, S. R., Surface Roughness Analysis for Economical Feasibility Study of Coated Ceramic Tool in Hard Turning Operation, Process Integr Optim Sustain, 4, 237-249, 2017.

[25] Grzesik, W., Żak, K. & Kiszka, P. Comparison of surface textures generated in hard turning and grinding operations, Procedia CIRP, 13, 84-89, 2014.

[26] Ramesh, A., Melkote, S. N., Allard, L. F., Riester, L. & Watkins, T. R. Analysis of white layers formed in hard turning of AISI 52100 steel, Materials Science and Engineering A, 390 (1-2), 88-97, 2005.

[27] Poulachon, G., Bandyopadhyay, B. P., Jawahir, I. S., Pheulpin, S. & Seguin, E. Wear behavior of CBN tools while turning various hardened steels, Wear, 256 (3-4), 302-310, 2004.

[28] Hosseini, S. B., Beno, T., Klement, U., Kaminski, J., & Ryttberg, K. Cutting temperatures during hard turning-Measurements and effects on white layer formation in AISI 52100, Journal of Materials Processing Tech, 214 (6), 1293-1300, 2014.

[29] Qian, L. & Hossan, M. R. Effect on cutting force in turning hardened tool steels with cubic boron nitride inserts, Journal of Materials Processing Technology, 191 (1-3), 274-278, 2007.

[30] Biček, M., Dumont, F., Courbon, C., Pušavec, F., Rech, J. & Kopač, J. Cryogenic machining as an alternative turning process of normalized and hardened AISI 52100 bearing steel, Journal of Materials Processing Technology, 212 (12), 2609-2618, 2012.

[31] König, W., Berktold, A. & Koch, K. F. Turning versus Grinding - A Comparison of Surface Integrity Aspects and Attainable Accuracies, CIRP Annals - Manufacturing Technology, 42 (1), 39-43, 1993.

[32] Cubic Boron Nitride (cBN), Retrieved 28 May 2019, from http://www.tomeidiamond.co.jp/en/tec/tec-10.html

[33] Panda, A., Sahoo, A. K., Rout, A. K., Kumar, R. & Das, R. K. Investigation of Flank Wear in Hard Turning of AISI 52100 Grade Steel Using Multilayer Coated Carbide and Mixed Ceramic Inserts, Procedia Manufacturing, 20, 365-371, 2018.

[34] Liu, X. L., Wen, D. H., Li, Z. J., Xiao, L. & Yan, F. G. Cutting temperature and tool wear of hard turning hardened bearing steel, Journal of Materials Processing Technology, 129 (1-3), 200-206, 2002.

[35] Caruso, S., Umbrello, D., Outeiro, J. C., Filice, L. & Micari, F. An experimental investigation of residual stresses in hard machining of AISI 52100 steel, Procedia Engineering, 19, 67-72, 2011.

[36] Umbrello, D., Yang, S., Dillon, O. W. & Jawahir, I. S. Effects of cryogenic cooling on surface layer alterations in machining of AISI 52100 steels, Materials Science and Technology, 28 (11), 1320-1331, 2012.

[37] Revel, P., Jouini, N., Thoquenne, G. & Lefebvre, F. High precision hard turning of AISI 52100 bearing steel, Precision Engineering, 43, 24-33, 2016.

[38] Grzesik, W. *Advanced Machining Processes of Metallic Materials* (1st ed.). Elsevier Science, 2008.

[39] Daoush, W. M., Park, H. S. & Hong, S. H. Fabrication of TiN/cBN and TiC/diamond coated particles by titanium deposition process, Transactions of Nonferrous Metals Society of China (English Edition), 24 (11), 3562-3570, 2014.

[40] Davies, M. A., Chou, Y. & Evans, C. J. On Chip Morphology, Tool Wear and Cutting Mechanics in Finish Hard Turning, CIRP Annals - Manufacturing Technology, 45(1), 77-82, 1996.

[41] Rewatkar, S. A., Deshbhratar, N. A., Kawale, A. P., Kardam, A. M. & Naik, A. D. Review of Influence of Different Cutting Angles of Single Point Cutting Tool on Turning Operation, International Research Journal of Engineering and Technology (IRJET), 4 (2), 1224-1228, 2017.

[42] Singh, D., Chadha, V. & Singari, R. M. Effect of Nose Radius on Surface Roughness During CNC Turning Using Response Surface Methodology, International Journal of Recent Advances in Mechanical Engineering, 5 (2), 31-45, 2016.

[43] Function of Tool Features for Turning (SCEA), Retrieved 02 Jun 2019, from http://www.mitsubishicarbide.com/en/technical_information/tec_turning_tools/tec_hsk-t/tec_hsk-t_technical/tec_turning_cutting_edge

[44] Function of Tool Features for Turning (H and L), Retrieved 02 Jun 2019, from http://www.mitsubishicarbide.com/en/technical_information/tec_turning_tools/tec_hsk-t/tec_hsk-t_technical/tec_turning_honing_land

[45] Davoudinejad, A. & Yusof, N. M. Effect of cutting edge preparation on tool performance in hard-turning of DF-3 tool steel with ceramic tools, Journal of Mechanical Science and Technology, 28 (11), 4727-4736, 2014.

[46] Thiele, J. D. & Melkote, S. N. Effect of tool edge geometry on workpiece subsurface deformation and through-thickness residual stresses for hard turning of AISI 52100 steel, Journal of Manufacturing Processes, 2 (4), 270-276, 2000.

[47] Ahmad, M. A., Nazir, A., Mahmood, M., Bhutta, A. & Abdullah, A. Influence of Wiper and Conventional Inserts at Profile Geometry During Turning of D2 Tool Steel, Engineering Technology Open Access Journal, 1 (5), 2018.

[48] Kalpakjian, S. & Schmid, S. R. *Manufacturing Engieering & Technology* (6th ed.), Pearson Education, 2006.

[49] Bermingham, M. J., Palanisamy, S., Kent, D. & Dargusch, M. S. A comparison of cryogenic and high pressure emulsion cooling technologies on tool life and chip morphology in Ti-6Al-4V cutting, Journal of Materials Processing Technology, 212 (4), 752-765, 2012.

[50] Attanasio, A., Umbrello, D., Cappellini, C., Rotella, G. & M'Saoubi, R. Tool wear effects on white and dark layer formation in hard turning of AISI 52100 steel, Wear, 286-287, 98-107, 2012.

[51] Suresh, R., Basavarajappa, S. & Samuel, G. L. Some studies on hard turning of AISI 4340 steel using multilayer coated carbide tool, Measurement: Journal of the International Measurement Confederation, 45 (7), 1872-1884, 2012.

[52] Mook, W. K., Shahabi, H. H. & Ratnam, M. M. Measurement of nose radius wear in turning tools from a single 2D image using machine vision, International Journal of Advanced Manufacturing Technology, 43 (3), 217-225, 2009.

[53] Wang, W. H., Wong, Y. S. & Hong, G. S. 3D measurement of crater wear by phase shifting method, Wear, 45 (3), 217-225, 2006.

[54] Huang, Y., Chou, Y. K. & Liang, S. Y. CBN tool wear in hard turning: A survey on research progresses, International Journal of Advanced Manufacturing Technology, 35 (5), 443-453, 2007.

[55] Chou, Y.K., Evans, C.J. Tool wear mechanism in continuous cutting of hardened tool steels. Wear 212, 59–65, 1997

[56] Barbacki, A., Kawalec, M. & Hamrol, A. Turning and grinding as a source of microstructural changes in the surface layer of hardened steel, Journal of Materials Processing Technology, 133 (1-2), 21-25, 2003.

[57] Paul, S., Dhar, N. R. & Chattopadhyay, A. B. Beneficial effects of cryogenic cooling over dry and wet machining on tool wear and surface finish in turning AISI 1060 steel, Journal of Materials Processing Technology, 116 (1), 44-48, 2001.

[58] Kaynak, Y., Lu, T. & Jawahir, I. S. Cryogenic machining-induced surface integrity: A review and comparison with dry, mql, and flood-cooled machining, Machining Science and Technology, 18 (2), 149-198, 2014.

[59] Rantala J. Surface Flatness, Retrieved 30 Mar 2019, from https://www.electronics-cooling.com/2004/05/surface-flatness/, 2004

[60] Agrawal, A., Goel, S., Bin Rashid, W. & Price, M. Prediction of surface roughness during hard turning of AISI 4340 steel (69 HRC), Applied Soft Computing Journal, 30, 279-286, 2015.

[61] Dhar, N. R., Paul, S. & Chattopadhyay, A. B. The influence of cryogenic cooling on tool wear, dimensional accuracy and surface finish in turning AISI 1040 and E4340C steels, Wear, 249 (10-11), 932-942, 2001.

[62] Pereira O., Rodríguez A., Fernández-Abia A. I., Barreiro J. & López de Lacalle L. N. Cryogenic and minimum quantity lubrication for an eco-efficiency turning of AISI 304, Journal of Cleaner Production, 139, 440-449, 2016.

[63] Yüzey Ölçüm Parametreleri, Retrieved 06 Apr 2019, from http://yamasa.com.tr/242/1/4/yamasa/yuzeyolcumparametreleri.aspx

[64] Demir E., Investigation of the Effects of Holding Times At Cryogenic Temperatures on Residual Stress Distribution of AISI D2 Tool Steel, master's thesis, Yıldırım Beyazıt University Department of Mechanical Engineering, 2014.

[65] Davim, P. J. *Machining of Hard Materials* (1st ed.) Springer-Verlag London. 2011

[66] Callister, W. D. & Rethwisch, D. G. *Materials Science and Engineering an Introduction* (8th ed.) John Wiley and Sons, 2009.

[67] Chou, Y. K. & Evans, C. J. White layers and thermal modeling of hard turned surfaces, International Journal of Machine Tools & Manufacture, 39 (12), 1863-1881, 1999.

[68] Hosseini, S. B., Klement, U., Yao, Y. & Ryttberg, K. Formation mechanisms of white layers induced by hard turning of AISI 52100 steel, Acta Materialia, 89, 258-267, 2015.

[69] Hosseini, S. B., Ryttberg, K., Kaminski, J. & Klement, U. Characterization of the surface integrity induced by hard turning of bainitic and martensitic AISI 52100 steel, Procedia CIRP, 1, 494-499, 2012.

[70] Chaudhari, R. G. & Hashimoto, F. Process Controls for Surface Integrity Generated by Hard Turning, Procedia CIRP, 45, 15-18, 2016.

[71] Pawar, S., Salve, A., Chinchanikar, S., Kulkarni, A. & Lamdhade, G. Residual Stresses during Hard Turning of AISI 52100 Steel: Numerical Modelling with Experimental Validation, Materials Today: Proceedings, 4 (2), 2350-2359, 2017.

[72] Noyan, I. C. & Cohen, J. B. *Residual Stress Measurement by Diffraction and Interpretation* (1st ed.) Springer-Verlag London, 1987.

[73] Measurement of Bulk Residual Stress Distributions in Thick-section Components using the Contour Method, Retrieved 16 Apr 2019, from http://what-when-how.com/engineering-applications-of-residual-

stress/measurement-of-bulk-residual-stress-distributions-in-thick-section-components-using-the-contour-method/

[74] Liu, X. L., Wen, D. H., Li, Z. J., Xiao, L. & Yan, F. G. Experimental study on hard turning hardened GCr15 steel with PCBN tool, Journal of Materials Processing Technology, 129 (1-3), 217-221, 2002.

[75] Capello, E. E. Residual stresses in turning Part I : Influence of process parameters, Journal of Materials Processing Technology, 160, 221-228, 2005.

[76] Ezugwu, E. O. & Bonney, J. Effect of high-pressure coolant supply when machining nickel-base, Inconel 718, alloy with coated carbide tools, Journal of Materials Processing Technology, 153-154 (1-3), 1045-1050, 2004.

[77] Anand, A., Behera, A. K., & Das, S. R. An overview on economic machining of hardened steels by hard turning and its process variables, Manufacturing, 6, 1-9, 2019.

[78] Debnath, S., Reddy, M. M. & Yi, Q. S. Environmental friendly cutting fluids and cooling techniques in machining: A review, Journal of Cleaner Production, 83, 33-47, 2014.

[79] Liew, P. J., Shaaroni, A., Sidik, N. A. C. & Yan, J. An overview of current status of cutting fluids and cooling techniques of turning hard steel, International Journal of Heat and Mass Transfer, 114, 380-394, 2017.

[80] Jawahir, I. S., Attia, H., Biermann, D., Duflou, J., Klocke, F., Meyer, D. et al., “Cryogenic manufacturing processes,” CIRP Annals - Manufacturing Technology, 65 (2), 713-736, 2016.

[81] Tunable MQLTM - Spray Cooling Lubrication - Cleanlogix, Retrieved 15 Apr 2019, from https://cleanlogix.com/tunable-mql-spray-cooling-lubrication/

[82] Aslantas, K., Çicek, A., Ucun, I., Percin, M. & Hopa, H. E. Performance Evaluation of a Hybrid Cooling-lubrication System in Micro-milling of Ti6Al4V Alloy, Procedia CIRP, 46, 492-495, 2016.

[83] Gatade, V. T., Patil, V. T., Kuppan, P., Balan, A. S. S. & Oyyaravelu, R. Experimental investigation of machining parameter under MQL milling of SS304, IOP Conference Series: Materials Science and Engineering, 149 (1), 2016.

[84] Pereira, O., Rodríguez, A., Ayesta, I., García, J. B., Fernández-Abia, A. I. & de Lacalle L. N. L. A cryo lubri-coolant approach for finish milling of aeronautical hard-to-cut materials, Int. J. Mechatronics and Manufacturing Systems, 9 (4), 370-384, 2016.

[85] Ahmed, L. S. & Kumar, M. P. Cryogenic Drilling of Ti-6Al-4V Alloy Under Liquid Nitrogen Cooling, Materials and Manufacturing Processes, 31 (7), 951-959, 2015.

[86] Pusavec, F., Stoic, A. & Kopac, J. The role of cryogenics in machining processes, Technical Gazette, 4 (16), 3-10, 2009.

[87] Jalandhar, C., Alemayehu, H., Behera, B. C. & Ghosh, S. Machining of Nimonic 90 Alloy Under Dry and LN 2 Environment Using AlTiN Coated and Uncoated Tungsten Carbide Inserts, International Conference on Precision, Meso, Micro and Nano Engineering, India, 2017.

[88] Uçak, N. The Effects of cutting conditions on cutting temperature and hole quality in drilling of Inconel 718 using solid carbide drills, Published master's thesis, Ankara Yıldırım Beyazıt University, 2017.

[89] Dhar, N. R., Kishore, N. S. V., Paul, S. & Chattopadhyay, A. B. The effects of cryogenic cooling on chips and cutting forces in turning AISI 1040 and AISI 4320 steels, Proceedings of the Institution of Mechanical Engineers, Part B: Journal of Engineering Manufacture, 216 (5), 713-724, 2002.

[90] Kaynak, Y., Gharibi, A. & Ozkutuk, M. Experimental and numerical study of chip formation in orthogonal cutting of Ti-5553 alloy: the influence of cryogenic, MQL, and high pressure coolant supply, International Journal of Advanced Manufacturing Technology, 94 (1-4), 1411-1428, 2018.

[91] Natasha, A. R., Ghani, J. A., Che Haron, C. H., Syarif, J. & Musfirah A. H. Temperature at the tool-chip interface in cryogenic and dry turning of AISI 4340 using carbide tool, International Journal of Simulation Modelling, 15 (2), 201-212, 2016.

[92] Bermingham, M. J., Kirsch, J., Sun, S., Palanisamy, S. & Dargusch, M. S. New observations on tool life, cutting forces and chip morphology in cryogenic machining Ti-6Al-4V, International Journal of Machine Tools and Manufacture, 51 (6), 500-511, 2011.

[93] O. Pereira et al., "The Use of Hybrid CO2+MQL in Machining Operations," Procedia Engineering, vol. 132, pp. 492-499, 2015.

[94] S. Sartori, A. Ghiotti, & S. Bruschi, "Hybrid lubricating/cooling strategies to reduce the tool wear in finishing turning of difficult-to-cut alloys," Wear, vol. 376-377, pp. 107-114, 2017.

[95] Pusavec, F., Deshpande, A., Yang, S., M'Saoubi, R., Kopac, J., Dillion Jr., O. W. et al. Sustainable machining of high temperature Nickel alloy - Inconel 718: Part 1 - Predictive performance models, Journal of Cleaner Production, 81, 255-269, 2014.

[96] Kaynak, Y. & Gharibi, A. The influence of liquid nitrogen and carbon dioxide cryogenic coolants on machining performance of hardened steel, 7th International Symposium On Machining, 177-191, Istanbul, Turkey, 2016.

[97] Aramcharoen, A. & Mativenga, P. T. White layer formation and hardening effects in hard turning of H13 tool steel with CrTiAlN and CrTiAlN/MoST-coated carbide tools, International Journal of Advanced Manufacturing Technology, 36 (7-8), 650-657, 2008.

[98] Jerold, B. D. & Kumar, M. P. Experimental investigation of turning AISI 1045 steel using cryogenic carbon dioxide as the cutting fluid, Journal of Manufacturing Processes, 13 (2), 113-119, 2011.

[99] Jerold, B. D. & Kumar, M. P. Experimental comparison of carbon-dioxide and liquid nitrogen cryogenic coolants in turning of AISI 1045 steel, Cryogenics, 52 (10), 569-574, 2012.

[100] Hong, S. Y. & Ding, Y. Cooling approaches and cutting temperatures in cryogenic machining of Ti-6Al-4V, International Journal of Machine Tools and Manufacture, 41 (10), 1417-1437, 2001.

[101] Srithar, A., Palanikumar, K. & Durgaprasad, B. Experimental investigation and surface roughness analysis on hard turning of AISI D2 steel using coated Carbide insert, Procedia Engineering, 97, 72-77, 2014.

[102] Elmunafi, M. H. S., Kurniawan, D. & Noordin, M. Y. Use of castor oil as cutting fluid in machining of hardened stainless steel with minimum quantity of lubricant, Procedia CIRP, 26, 408-411, 2015.

[103] Das, R. K., Sahoo, A. K., Mishra, P. C., Kumar, R. & Panda, A. Comparative machinability performance of heat treated 4340 Steel under dry and minimum quantity lubrication surroundings, Procedia Manufacturing, 20, 377-385, 2018.

[104] Magadum, S., Kumar, S. A., Yoganath, V. G., Srinivasa, C. K. & GuruMurthy, T. Evaluation of Tool Life and Cutting Forces in Cryogenic Machining of Hardened Steel, Procedia Materials Science, 5, 2542-2549, 2014.

[105] Navas, V. G., Fernández, D., Sandá, A., Sanz, C., Suzon, S. & De Mendiola, T. F. Surface integrity of AISI 4150 (50CrMo4) steel turned with different types of cooling-lubrication, Procedia CIRP, 13, 97-102, 2014.

[106] Khan, A. A. & Ahmed, M. I. Improving tool life using cryogenic cooling, Journal of Materials Processing Technology, 196 (1-3), 149-154, 2008.

[107] Guddata, J., M'Saoubi, R., Alma, P. & Meyer, D. Hard turning of aisi 52100 using pcbn wiper geometry inserts and the resulting surface integrity, Procedia Engineering, 19, 118-124, 2011.

[108] Gaitonde, V. N., Karnik, S. R., Figueira, L. & Davim, J. P. Machinability investigations in hard turning of AISI D2 cold work tool steel with conventional and wiper ceramic inserts, International Journal of Refractory Metals and Hard Materials, 27 (4), 754-763, 2009.

[109] Sivaiah, P. & Chakradhar, D. Influence of cryogenic coolant on turning performance characteristics: A comparison with wet machining, Materials and Manufacturing Processes, 32 (13), 626-631, 2017.

[110] Carnegie Illinois-Steel Corp. U.S.S Carilloy Steels, Chicago: Carnegie-Illinois Steel Corp., 1938.

[111] ASTM 52100 Bearing Steel | 1.3505 | 100Cr6 | SUJ2 | EN31, Retrieved 02 Jun 2019, from http://www.astmsteel.com/product/52100-bearing-steel-aisi/

[112] Askeland, D. R. & Fulay, P. P. *Essentials of Materials Science and Engineering* (2nd ed.), Toronto: Cengage Learning, 2009.

[113] Smith, S., Melkote, S. N., Lara-Curzio, E., Watkins, T. R., Allard, L. & Riester, L. Effect of surface integrity of hard turned AISI 52100 steel on fatigue performance, Materials Science and Engineering A, 459 (1-2), 337-346, 2007.

[114] Zhou, J. M., Walter, H., Andersson, M. & Stahl, J. E. Effect of chamfer angle on wear of PCBN cutting tool, International Journal of Machine Tools and Manufacture, 43 (3), 301-305, 2003.

[115] Davim, J. P. *Machinability of Advanced Materials*. London: Wiley, 2014.

[116] Bagherzadeh, A. & Budak, E. Investigation of machinability in turning of difficult-to-cut materials using a new cryogenic cooling approach, Tribology International, 119, 510-520, 2018.

[117] Yap, T. C., Sivaraos, A., Lim, C. S. & Leau, J. W. Surface roughness and cutting forces in cryogenic turning of carbon steel, Journal of Engineering Science and Technology, 10 (7), 911-920, 2015.

[118] M'Saoubi, R., Outeiro, J. C., Chandrasekaran, H., Dillon Jr, O.W. & Jawahir, I. S. A review of surface integrity in machining and its impact on functional performance and life of machined products, International Journal of Sustainable Manufacturing, 1 (1/2), 203-236, 2008.

[119] Bosheh, S. S. & Mativenga, P. T. White layer formation in hard turning of H13 tool steel at high cutting speeds using CBN tooling, International Journal of Machine Tools and Manufacture, 46 (2), 225-233, 2006.

[120] Zhang, P. R., Liu, Z. Q. & Guo, Y. B. Machinability for dry turning of laser cladded parts with conventional vs. wiper insert, Journal of Manufacturing Processes, 28 (3), 494-499, 2017.

[121] Neslusan, M., Faktor, M. & Cillikova, M. Analysis of Surface Integrity After Hard Turning With Wiper Inserts, MM Science Journal, 03, 481-484, 2014.

[122] Guo, Y. B., Warren, A. W. & Hashimoto, F. The basic relationships between residual stress, white layer, and fatigue life of hard turned and ground surfaces in rolling contact, CIRP Journal of Manufacturing Science and Technology, 2 (2), 129-134, 2010.

[123] Zhang, F., Duan, C., Sun, W. & Ju, K. Effects of cutting conditions on the microstructure and residual stress of white and dark layers in cutting hardened steel, Journal of Materials Processing Technology, 266, 599-611, 2019.

[124] Griffiths, B. Manufacturing Surface Technology Surface Integrity & Functional Performance (1st ed.), Penton Press, London, 2001.

[125] Elbah, M., Yallese, M. A., Aouici, H., Mabrouki, T. & Rigal, J. F. Comparative assessment of wiper and conventional ceramic tools on surface roughness in hard turning AISI 4140 steel, Measurement: Journal of the International Measurement Confederation, 46 (9), 3041-3056, 2013.

[126] Sampaio, M. A., Machado, Á. R., Laurindo, C. A. H., Torres, R. D. & Amorim, F. L. Influence of minimum quantity of lubrication (MQL) when turning hardened SAE 1045 steel: a comparison with dry machining, International Journal of Advanced Manufacturing Technology, 98 (1-4), 959-968, 2018.

[127] Özel, T., Karpat, Y. & Srivastava, A. Hard turning with variable micro-geometry PcBN tools, CIRP Annals - Manufacturing Technology, 57, 73-76, 2008.

[128] MacHai, C. & Biermann, D. Machining of β-titanium-alloy Ti-10V-2Fe-3Al under cryogenic conditions: Cooling with carbon dioxide snow, Journal of Materials Processing Technology, 211 (6), 1175-1183, 2011.

CURRICULUM VITAE

PERSONAL INFORMATION



Name Surname	**:**	Hüseyin Alp Çetindağ
Date of Birth	**:**	26.04.1993
Phone	**:**	+90 554 262 7014
E-mail	**:**	h.a.cetindag@outlook.com

EDUCATION

High School	**:**	Aydınlıkevler Anadolu High School / Ankara
Bachelor	**:**	Ankara Yıldırım Beyazıt University / Ankara
Master Degree	**:**	Ankara Yıldırım Beyazıt University / Ankara

WORK EXPERIENCE

Project Engineer	**:**	Undersecretariat for Defence Industries / Ankara (2018 – Cont.)
R&D/Design Engineer	**:**	ProMec Engineering Co.,Ltd./Ankara (2018)
Head of Production	**:**	Konak Rakor Co. Ltd / Ankara (2016 – 2018)

RESEARCHES

- Çetindağ H., Çiçek A., Uçak N., Performance of CBN Inserts in CO_2 Assisted Hard Turning of AISI 52100 Bearing Steel. 4th International Mediterranean Science and Engineering Congress (IMSEC), 25-27 April 2019, Antalya, Turkey.

- H A Çetindağ, M T Özkan, İ Toktaş, A E Kılıçarslan, H N Ünver, ANN Analysis Of Titanium Alloy Beams According To Bending For Medical Applications, 5th International Symposium on Engineering, Artificial Intelligence & Applications, 1-3 Nov. 2017, Kyrenia/Northern Cyprus

- İ. Toktaş, H. A. Çetindağ, M. T. Özkan, H. N. Ünver, A. E. Kılıçarslan, ANN Model Of The Medical Ceramic Beams Which Were Subjected To Tension/Compression Stress, 5th International Symposium on Engineering, Artificial Intelligence & Applications, 1-3 Nov. 2017, Kyrenia/Northern Cyprus

- M T Özkan, İ Toktaş, H A Çetindağ, A E Kılıçarslan, H N Ünver, ANN Modelling For The Buckling Analysis Of Medical Titanium Alloys, 5th International Symposium on Engineering, Artificial Intelligence & Applications, 1-3 Nov. 2017, Kyrenia/Northern Cyprus